

論文 / 著書情報
Article / Book Information

題目(和文)	
Title(English)	Fundamental Study on Critical Heat Flux in Tight Lattice Core for High Conversion Boiling Water Reactor
著者(和文)	Le Tri Dan
Author(English)	Dan Tri Le
出典(和文)	学位:博士(工学), 学位授与機関:東京工業大学, 報告番号:甲第10173号, 授与年月日:2016年3月26日, 学位の種別:課程博士, 審査員:高橋 実,加藤 之貴,赤塚 洋,木倉 宏成,古谷 正裕
Citation(English)	Degree:Doctor (Engineering), Conferring organization: Tokyo Institute of Technology, Report number:甲第10173号, Conferred date:2016/3/26, Degree Type:Course doctor, Examiner:,,,,
学位種別(和文)	博士論文
Type(English)	Doctoral Thesis

Fundamental Study on Critical Heat Flux in Tight Lattice Core for High Conversion Boiling Water Reactor

Dissertation

Submitted to Tokyo Institute of Technology

In Partial Fulfillment of the Requirements for the Degree of
Doctor of Engineering

by:

Le Tri Dan

13D19080

supervised by:

Professor Dr. Minoru Takahashi



Department of Nuclear Engineering
Graduated School of Science and Engineering
Tokyo Institute of Technology

March 2016

Acknowledgements

At first I would like to express my deepest gratitude to my academic advisor, Professor Minoru Takahashi for giving me priceless opportunity to work and study about thermal-hydraulic in nuclear reactor under his supervision in his laboratories. I would like to thank him for his nicely and kindly guidance and supports during my doctoral project. By working under his supervision, I could get a huge amount of knowledge not only about my field of research but also many other field of study. I also would like to give a special thanks to him for his encouragements whenever I faced with the difficulty during my research progress. Finally, I would like to thank him for always on my side and give me a strong power to finish my doctoral dissertation.

I wish to thank Professor Masahiro Furuya and Dr. Masatoshi Kondo for their kindly supports and comments during the writing and finishing of dissertation. Following their comments and advices, I could finish my Ph.D project quickly and smoothly.

My special thanks go to all members of my Ph.D committee, Prof. Masahiro Furuya, Prof. Yukikata Kato, Assoc.Prof Hiroshi Akatsuka, and Assoc.Prof Hiroshige Kikura for their valuable comments and suggestions for improvement of my study and doctoral dissertation.

I would like to express my sincere gratitude to Hitachi Nuclear Scholarship for their financial support during my Ph.D project. I thank also to Hitachi's members, Prof. Ujita, Prof. Futami, Prof. Himeno, Prof Fukuzaki, Mr. Murata, Ms. Shimizu, Ms. Ikeda, Ms. Miyazaki, Ms Sakai for their kindly supports. Their support is deeply acknowledged.

My thanks go to Mr. Naoyuki Tsuruoka and Mr. Shoji Matsui for their assistance in the technical work.

I would like to thank my lab mates in Takahashi laboratory, Gao, Adhi, Maeahara, Tanabe, Dr. Inaba, Marion, Mihalache, Radu and Gregu; for their nice discussions, good friendship and sharing all the good things to me. It would be unforgettable memories for me. I thank also all of my friends in my home country, Vietnam for their support and encouragements.

Finally I would like to give the biggest thanks to my family, my father Le Van Han, my mother Le Thi Dong Phuong, my small brother Le Phuc Duc, especially my wife Tran Thuy Nga and my daughter Le Ngan Hanh for their special supports, encouragements and always on my side in my whole life.

Contents

Chapter 1. Introduction.....	1
1.1. Background	2
1.2. High conversion light water reactor.....	3
1.3. Tight lattice fuel assembly and wire spacer	6
1.4. Critical heat flux phenomena	11
1.5. Review of previous studies	15
1.5.1 CHF behavior in tight lattice core with grid spacer.....	15
1.5.2 CHF behavior in tight lattice core with wire spacers	23
1.5.3. Summary of previous studies.....	26
1.6. Motivations of the study	27
1.7. Purpose of present study	28
1.8. Outline of thesis	29
Chapter 2. Design and setup forced convection type water loop and CHF test section	32
2.1. Introduction	33
2.2. Experimental apparatus	33

2.3. Single pin test Section	37
2.3.1. Heater pin.....	40
2.3.2. Wire spacer	41
2.3.3. Glass flow channel.....	43
2.3.4. Thermocouples	43
2.4. Three-pin bundle test section	45
2.4.1 Bundle heater pin	46
2.4.2 Triangular glass flow channel.....	50
2.4.3 Wire spacers.....	55
2.4.4 Thermocouples	55
2.5. Experimental Procedure and Measurement Items	56
2.6. Conclusion.....	60
Chapter 3. Experimental study on CHF behavior in single pin with and without wire spacer	62
3.1. Introduction	63
3.2 Experimental Conditions.....	64
3.3. Results and Discussion.....	66
3.3.1. Effect of mass flux.....	66

3.3.2 Effect of Wire Spacer	68
3.3.3 Effect of gap size and wire pitch	72
3.3.4 Axial Position of CHF	75
3.4. Comparison with previous study and prediction methods	79
3.5. Conclusion.....	87
Chapter 4. Experimental study on CHF behavior in bundle pin with and without	
wire spacer	90
4.1. Introduction	91
4.2 Experimental Conditions.....	92
4.3. Results and discussion	94
4.3.1. Effect of mass flux.....	94
4.3.2 Effect of wire spacer.....	96
4.3.3 Effect of pitch to diameter ratio.....	101
4.3.4 Effect of wire pitch	108
4.3.5 Axial CHF position.....	109
4.4. Comparison with previous study and prediction methods	111
4.5. New CHF empirical correlation	118
4.5. Conclusions	125

Chapter 5. Analytical study on CHF behavior in tight rod bundle using CHF simulation method	128
5.1. Introduction	129
5.2. Dryout simulation method and boundary condition	129
5.3. Dryout simulation for annulus channel	132
5.3.1. Three fluid model in annulus channel	132
5.3.2. Dryout simulation model and constitutive equation	136
5.3.3. Analyzing the enhancement of CHF in single pin experiment.....	140
5.4. Dryout simulation for three-pin bundle experiment	141
5.4.1. Three fluid model in three-pin bundle channel	141
5.4.2. Analyzing the enhancement of CHF in three-pin experiment.....	143
5.5. Results and discussion	144
5.5.1. Calculation results for single pin channel.....	144
5.5.2. Calculation results for three-pin channel.....	150
5.6. Conclusion.....	155
Chapter 6. Conclusion	156
References	164

List of Figures

Fig.1.1 Reactor vessel and the internal of RMWR [Ref]	5
Fig.1.2 Schematic of typical tight lattice core.....	7
Fig. 1.3. Comparison of neutron flux between RMWR with conventional LWR and SFR	8
Fig.1.4 Conversion ratio as a function of volume ratio.....	8
Fig.1.5 MONJU core design	10
Fig.1.6 Schematic of spacer	11
Fig.1.7 Burnout phenomenon.....	12
Fig.1.8 Dryout phenomenon.....	14
Fig.1.9 DNB phenomenon	14
Fig.1.10 Design of core and fuel assembly in RMWR	19
Fig.1.11 Effect of mass flux on critical power in RMWR.....	20
Fig.1.12 Effect of inlet temperature on CHF in RMWR.....	20
Fig.1.13 NASCA nodding for RMWR core simulation.....	21
Fig.1.14 Effect of inlet temperature on critical power in RMWR with two difference gap size.....	22

Fig.2.1 Schematic of the experimental apparatus	35
Fig.2.2 Experimental apparatus.....	36
Fig.2.3. Calibration curve of the orifice	37
Fig. 2.4 Single pin test section.	39
Fig. 2.5 Cross-section of the test section.....	40
Fig.2.6. Three point junctions	45
Fig.2.7 Three-pins bundle test section	47
Fig.2.8 Cross section of flow channel	48
Fig.2.9 Schematic of the upper and lower part of the test section	48
Fig.2.10 Copper electrode	49
Fig.2.11 Structure of flow channel.....	52
Fig.2.12 Cross section of the test section.....	53
Fig.2.13 Thermocouple position	56
Fig.2.14 Temperature behavior during the CHF experiment in single pin test section.....	58
Fig.3.1 Effect of mass flux on CHF (gap size, $\delta = 1.5$ mm)	67
Fig.3.2 Effect of mass flux on CHF (gap size, $\delta = 2.0$ mm)	68
Fig. 3.2 Critical heat flux base on inlet condition.	70

Fig.3.3 Effect of wire on the entrainment and deposition rate	71
Fig. 3.4 Critical heat flux base on inlet condition	72
Fig. 3.5 Critical heat flux of three different values of gap size.....	74
Fig. 3.6 Critical heat flux of two different values of wire pitch, H	75
Fig. 3.7 Critical heat flux base on the heated length	77
Fig.3.8. CHF position for heater pin with and without wire spacer.....	79
Fig.3.9 Comparison between CHF experimental data without wire spacer with Haas's results.....	80
Fig.3.10 Comparison of experimental results of wire type with the calculated results of non-wire type using concentric annuli correlation of Doerffer et al.(1994) for the 2006 CHF look-up table of Groeneveld et al.(2007)	82
Fig.3.11 CHF ratio of experimental results to calculated results obtained from Eq.3.1.....	84
Fig.3.12 Concentric and eccentric annuli.....	85
Fig.3.13. Comparison of experimental results with the calculated results using CHF correlation for the rod-centered approach of Doerffer et al.(1994) for the 2006 CHF look-up table of Groeneveld et al.(2007)	87
Fig.4.1 Effect of mass flux on CHF in tight lattice bundle	95

Fig.4.2 CHF in three-pin bundle with two difference mass flux values as a function of inlet enthalpy	96
Fig. 4.3 Critical heat flux in bundle with and without wire spacer.....	99
Fig.4.4 Enhancement of deposition rate by centrifugal force	100
Fig. 4.5 Critical heat flux in bundle with and without wire spacer as a function of inlet subcooling temperature.....	101
Fig. 4.6 CHF of difference values of p/d under the same mass flux condition.	103
Fig. 4.7 CHF of difference values of p/d under the same mass flux and inlet enthalpy condition.	104
Fig. 4.8 CHF of difference values of p/d with the same flow rate condition.	106
Fig. 4.9 CHF of difference values of p/d with the same flow rate and inlet enthalpy condition.	107
Fig.4.10 Effect of wire pitch on CHF in tight rod bundle.....	109
Fig.4.11 CHF position along the heated length with the effect of mass flux.	110
Fig.4.12 CHF position along the heated length with the effect of p/d	111

Fig. 4.13 Comparison of CHF experimental data in three-pin bundle without wire spacer with JAEA data in 37-pin bundle.....	113
Fig.4.14 Comparison between CHF experimental data in three-pin bundle without wire spacer and the calculation results [Eq.4.2]	116
Fig.4.15 Critical heat flux in heated annuli [18]	117
Fig.4.16 CHF ratio of experimental data to calculated results.....	118
Fig.4.17. CHF in three-pin bundle with wire spacer as a function of local quality	121
Fig.4.18 CHF to quality factor ratio as a function of mass flux.....	122
Fig.4.19 CHF to quality and mass flux factor ratio as a function of gap size.	122
Fig.4.20 Experimental data and calculation results at $G=280 \text{ kg/m}^2\text{s}$	124
Fig.4.21 Experimental data and calculation results at $\delta=0.43 \text{ mm}$	124
Fig.4.22 Experimental data and calculation results at $G=435 \text{ kg/m}^2\text{s}$	125
Fig.5.1 Flow behavior in annulus channel	133
Fig.5.2. Cross section at the center of three-pin rod bundle	141
Fig.5.3 Comparison between experimental data and calculation results in case of flow channel without wire spacer	146

Fig.5.4 CHF postion in single pin channel with wire spacer ($\Delta h_{\text{sub}} = 51.66$ kJ/kg)	147
Fig.5.5 CHF postion in single pin channel with wire spacer ($\Delta h_{\text{sub}} = 68.04$ kJ/kg)	147
Fig.5.6 CHF postion in single pin channel with wire spacer ($\Delta h_{\text{sub}} = 77.7$ kJ/kg)	148
Fig.5.7 CHF postion in single pin channel with wire spacer ($\Delta h_{\text{sub}} = 112.98$ kJ/kg)	148
Fig.5.8 CHF postion in single pin channel with wire spacer ($\Delta h_{\text{sub}} = 121.8$ kJ/kg)	149
Fig.5.9 CHF postion in single pin channel with wire spacer ($\Delta h_{\text{sub}} = 161$ kJ/kg)	149
Fig.5.10 Comparison between experimental data and calculation results in case of three-pin bundle without wire spacer	151
Fig.5.11 CHF postion in bundle pin channel with wire spacer	152
($\Delta h_{\text{sub}} = 92.4$ kJ/kg)	152
Fig.5.12 CHF postion in bundle pin channel with wire spacer ($\Delta h_{\text{sub}} = 97.02$ kJ/kg)	152

Fig.5.14 CHF postion in bundle pin channel with wire spacer ($\Delta h_{\text{sub}} = 118.86$ kJ/kg)	153
Fig.5.16 CHF postion in bundle pin channel with wire spacer ($\Delta h_{\text{sub}} = 161.28$ kJ/kg)	154

List of Tables

Table 2.1 Flow channel geometric parameter	54
Table 3.1 Experimental condition.....	65
Table 4.1 Experimental condition.....	93
Table.5.1. Single pin experiment calculation	131
Table.5.2 Three-pin experiment calculation	132

Chapter 1. Introduction

1.1. Background

Nowadays, energy is the most important key factor not only for the development of science and technology but also for the improvement of life quality. However, social developments as well as explosive growth of industries have resulted in rapid exhaustion of energy resources. On the other hand, exploitation of energy sources has also come along with large amount of CO₂ emission that leads to global warming. Thus, there's an urgent need for the use of clean and renewable energies. Nuclear power, with no doubt, has emerged as one of the optimal solutions.

Recently, almost the nuclear reactors in over the world are Light water reactors (LWRs). Nevertheless, for the sustainability of the nuclear energy and transmutation, fast breeder reactors which named generation IV reactors is one of the best solutions. There are many types of fast breeder reactor such as Sodium-cooled fast reactor, Lead cooled fast reactor, Gas-cooled fast reactor and Supercritical water reactor. However, most of the generation IV fast reactors will not be commercialized in near future because it faced with some unique design and operation problems.

On the other hand, the commercial LWRs can be transferred to fast breeder reactor by using the tight lattice core, which named High conversion light water reactor (HCLWR). However, due to the small flow area in tight lattice core, the

study on coolability is necessary. Hence, the study on thermal hydraulic behavior to evaluate the coolability for such kind of fuel arrangement is needed.

1.2. High conversion light water reactor

The high conversion light water reactor (HCLWR) is the fast breeder reactor with the coolant is the light water. There are two type of HCLWR which named high conversion boiling water reactor (HCBWR) and high conversion pressurized light water reactor (HCPWR). However, it is better to design the HCLWR with the boiling type because the HCLWR with the pressurized type may have a difficulty to have a harder neutron spectrum. In the case of PWR, the moderator density is much higher than that in BWR due to the higher pressure condition. On the other hand, in the PWR, there is very small local boiling so that the void fraction is much lower in comparison with BWR. Therefore, the moderator to fuel ratio in PWR is much smaller than that in BWR. Thus, in the BWR, it is easier to have a harder neutron spectrum which is the most important point to design the High conversion reactor.

Since 1984, the research and develop work had been made for high conversion light water reactor (HCLWR) by JAEA [27]. Various HCLWR core design concepts were investigated such as homogeneous core with tight lattice, homogeneous semi-tight lattice, flat core, double flat core, etc. In the first design of HCBWR, the tight lattice fuel assembly with grid spacers, which have the rod

diameter of 9.5 mm and pitch of 11.1 mm, at which the pitch to diameter ratio, p/d , nearly equal to 1.17 was chosen.

Since 2000, other research and develop work had been started for Reduced moderation water reactor (RMWR) by JAEA [39]. The schematic design of the RMWR reactor is shown in fig.1.1. It can be seen that the design concept of the RMWR reactor is nearly the same with the conventional BWR. However, the double-flat core type was chosen for the design concept of the RMWR. Again once more, the tight lattice core with grid spacers was used for such kind of reactor. The rod diameter was 13.0 mm and the gap width was 1.3 mm at which the pitch to diameter ratio was nearly equal to 1.1.

Beside, in order to design the new type of HCBWR, the safety analysis should be considered. The safety features of the nuclear reactor are related with three main parts which are thermal-hydraulic and reactor physic.

From the reactor physic point of view, due to the characteristic of tight lattice core with wire spacer, the coolant to fuel volume ratio is small, which related to the issue of re-criticality in the reactor core. Therefore, for the safety purpose, it is necessary to consider about such kind of issue when design the new BWR with tight lattice core and wire spacer. On the other hand, if we try to increase the conversion ratio the void reactivity coefficients also increase. However, in the design concept of

RMWR, JAEA proposed two ways to solve for such kind of issue: design a shorter core height (increasing the neutron leakage in the axial direction) and utilize axial and radial blanket effect.

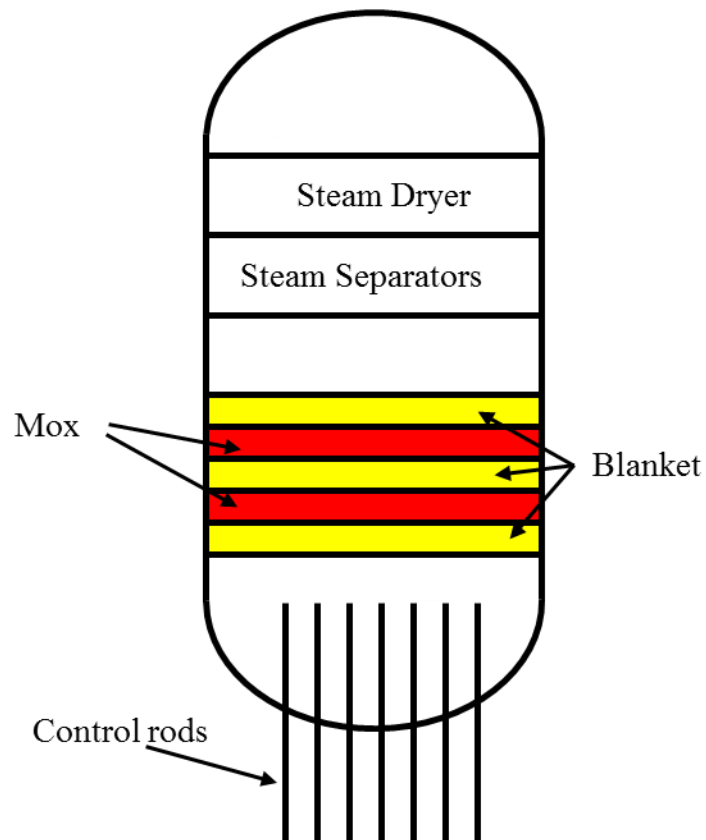


Fig.1.1 Schematic design: Reactor vessel and the internal of RMWR

From the thermal-hydraulic point of view, in the light water reactor type, one of the most important accidents named loss of coolant accident (LOCA). The LOCA occurs when the coolant of the nuclear reactor leak from the system to the outside. In this case, the emergency core cooling system (ECCS) will inject the coolant into the reactor core, which named as re-flooding and re-wetting process. In the case of

commercial BWR with square type and larger gap size, the coolant will easy to re-flood and re-wetting the reactor core. However, in the case of tight lattice with small gap width, the coolant may have a difficulty in re-flooding and rewetting process. In other words, the heat removal during the LOCA becomes worst in the case of tight lattice core.

On the other hand, the coolability or heat removability is also one of key issues for the feasibility of the tight lattice core because of the small flow area which is related with the small value of rod-to-rod gap.

1.3. Tight lattice fuel assembly and wire spacer

As mentioned in above subsection, the tight lattice core was used in the the design concept of the HCBWR. The tight lattice core was defined as a fuel assembly which has a pitch to diameter ratio, p/d , is smaller than that of conventional light water reactors (LWRs) of 1.3 to 1.4 [2]. And most of the tight lattice core has a triangular arrangement. The schematic of the typical tight lattice core is shown in Fig.1.2.

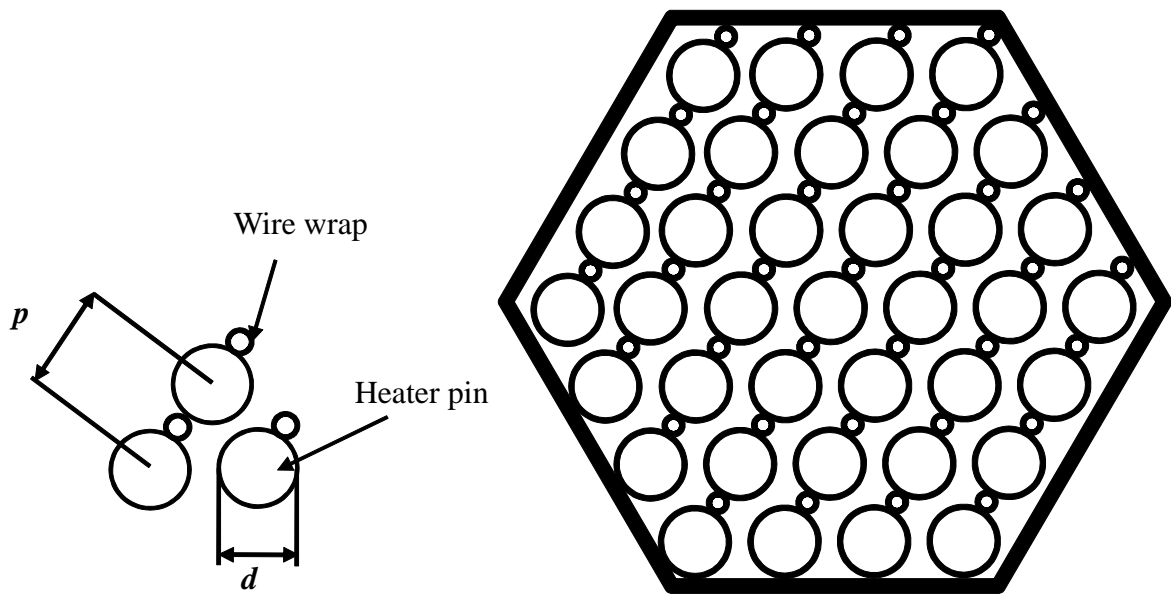


Fig.1.2 Schematic of typical tight lattice core

The tight lattice core was well known can be applied for the design concept of the fast reactor because the tight lattice core has a small value of moderator-fuel ratio, which has a harder neutron spectrum and high conversion ratio. These advantages of the tight lattice core were found in previous studies [21][27][43]. Details, fig.1.3 shows the comparison in neutron flux between the RMWR with the conventional LWR and Sodium-cooled fast breeder reactor (SFR) [21]. It can be seen that the RMWR with the tight lattice core could have a harder neutron spectrum in comparison with SFR the even with the coolant is the light water. On the other hand, fig. 1.4 shows the conversion ratio as a function of the moderator to fuel pellet volume ratio [27]. It can be seen that the conversion ratio increase with the decrease of moderator to fuel pellet volume ratio, which is one of the tight lattice core

advantages.

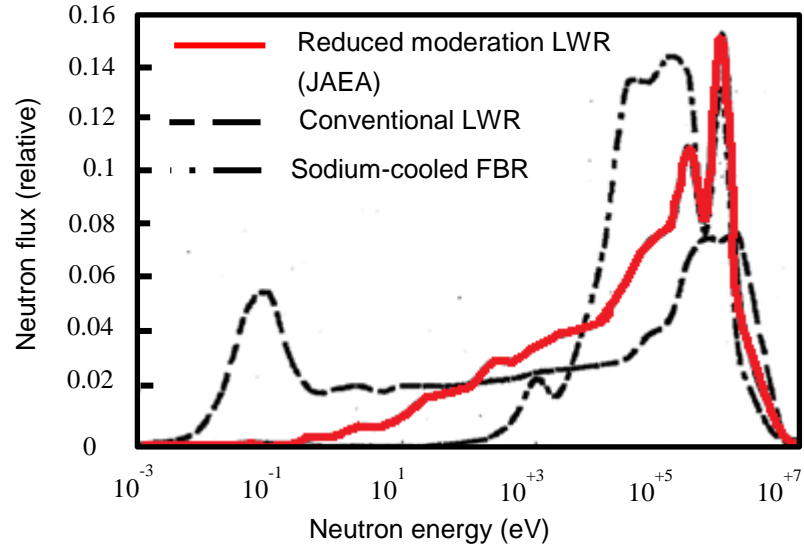


Fig. 1.3. Comparison of neutron flux between RMWR with conventional LWR and SFR [21]

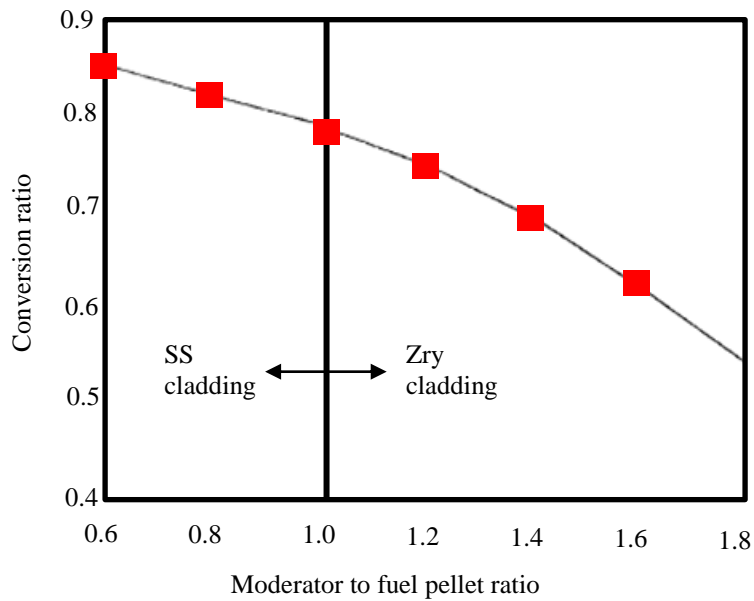


Fig.1.4 Conversion ratio as a function of volume ratio [27]

For the practical reactor, the tight lattice core was used in MONJU reactor [20]. MONJU is a Japanese sodium-cooled fast reactor with the breeding ratio is nearly 1.2 [20]. Figure 1.5 shows the schematic reactor core design and the fuel rod of MONJU reactor. Moreover, due to the small values of moderator-fuel ratio, the tight lattice core allow us to have a higher conversion ratio nearly equal unity even in the LWRs, particularly boiling water reactors (BWRs). In order to have a harder neutron spectrum even in the LWR, it is well known that, the tight lattice core with the pitch to diameter ratio of nearly 1.09 [51] and 1.06 [42], which has the gap size distance of 1.3 mm and 0.9 mm, respectively, can be used.

There are two type of spacer can be apply for the tight lattice core, which are wire spacer and grid spacer [Fig.1.6]. However, the use of wire spacers is more suitable for the tight lattice core than the use of grid spacers. On the other hand, the circular shape wire was reported as a wire spacer shape which has a best thermal hydraulic performance [53].

Nevertheless, from the thermal-hydraulic point of view the coolability or heat removability is one of key issues for the feasibility of the tight lattice core with the wire spacer because of the small flow area which is related with the small value of rod-to-rod gap. Besides, the most important feature of coolability of tight lattice core is the critical heat flux.

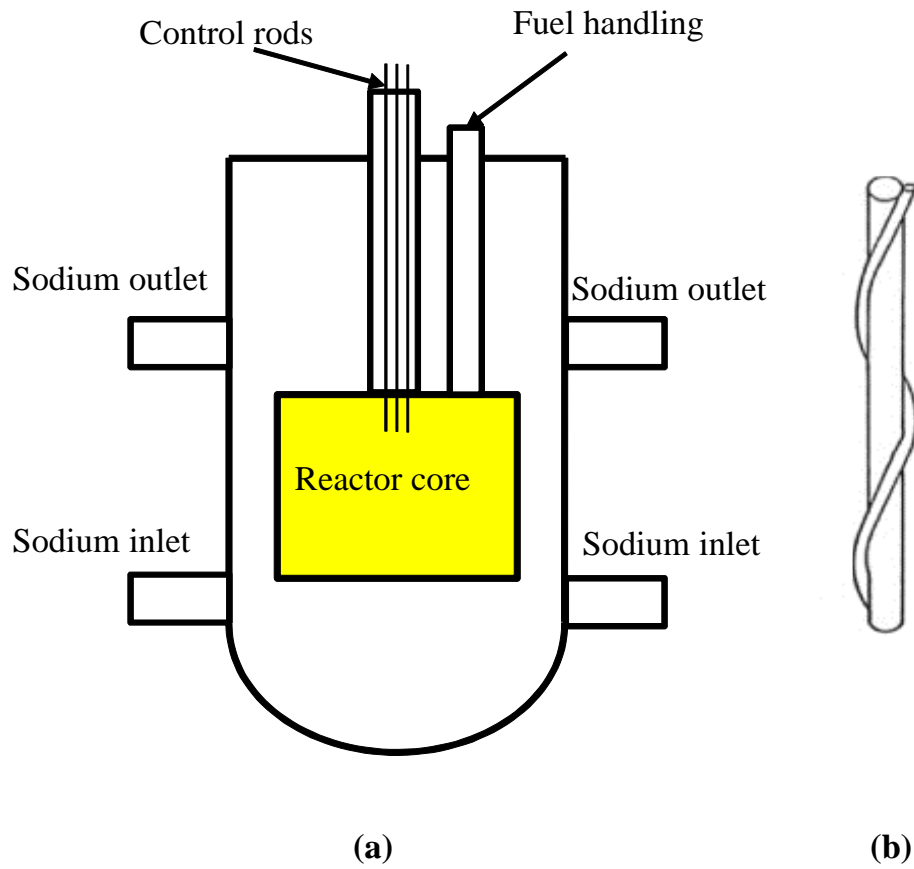


Fig.1.5 MONJU core design[19]:

a. Reactor core ; b. Fuel rod

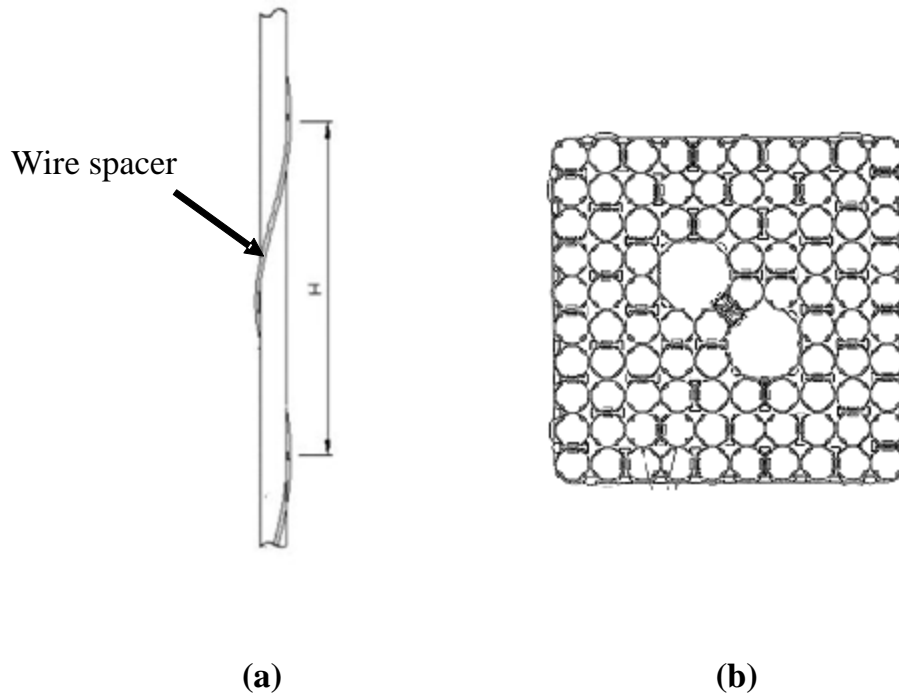


Fig.1.6 Schematic of spacer:

a. Wire spacer; b. Grid spacer

1.4. Critical heat flux phenomena

Critical heat flux (CHF) is defined as a heat flux at which the boiling crisis occurred lead to the suddenly decline of heat transfer ability. The phenomenon named burnout phenomenon. When the burnout occur, the heated surface will be burned and deform [Fig.1.7]. The CHF can be occurred due to two differences mechanism.



Fig.1.7 Burnout phenomenon.

The first mechanism named a liquid film dry out phenomenon which is occurred by the breakdown of the coolant liquid film flow along the heated surface in the annular flow base on the entrainment and deposition of the droplets [Fig.1.8]. Details, in annular flow, the liquid droplets are entrained from the liquid film surface to the gas core and make the liquid film become thinner. At the same time, the liquid droplets from the gas core is come back to the heated surface and formed with the liquid film which called deposition phenomena. Due to the high boiling rate and high heat flux, the entrainment rate become higher which mean the increase in number of liquid droplets entrained from the liquid film to gas core. This phenomenon will continue until the liquid film breakdown then the CHF occurred.

The Dryout phenomenon is mostly appeared in the BWRs. If the Dryout is well known as an issue in BWRs, the typical CHF mechanism in PWRs is called departure from nucleate boiling (DNB) phenomenon. The mechanism of this phenomenon is due to the generation and collapsed of the bubbles on the heated surface. In detail, due to the heating, the bubbles are generated on the heated surface and tend to become bigger by continue heating. Those bubbles will be collapsed and formed with each other as a shape of mushroom. When the bubbles are big enough, it will cover the heated surface and decrease the heat transfer rate then CHF will be occurred [Fig.1.9].

In nuclear reactor, CHF can be occurred in non-flow system such as in the spent fuel pool, which named CHF in pool boiling. There were many studies were obtained for such kind of phenomena [4][17][40] with various differences geometric parameter. Besides, CHF also can be appeared in the flowing system such as in the reactor core, which named CHF in flow boiling. The CHF in flow boiling condition is one the most important phenomena in nuclear reactor. Therefore, a lot of experimental studies on CHF in flow boiling condition were obtained to investigate the CHF behavior with various geometry designs under the effect of quality, mass flux and pressure [17][22][26][34][36][54]. On the other hand, various correlations or prediction methods for CHF with a lot of different condition such as pressure, mass flux, quality and geometric parameter were created [23-25].

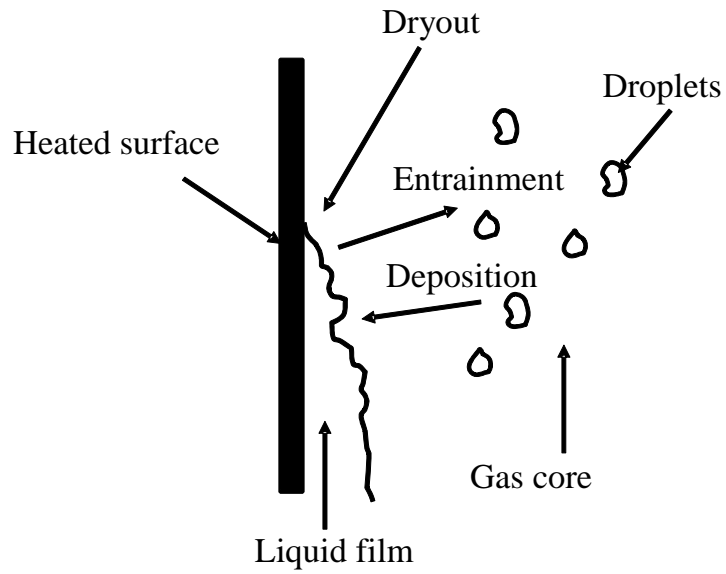


Fig.1.8 Dryout phenomenon

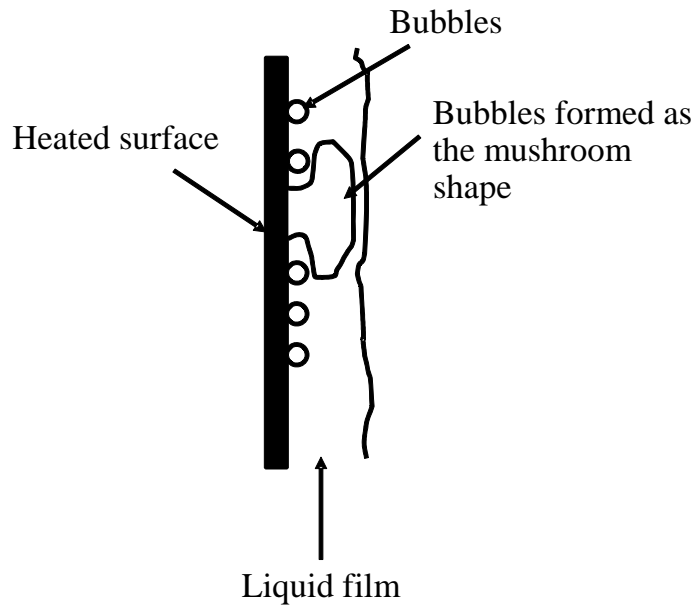


Fig.1.9 DNB phenomenon

Base on the characteristic and mechanism, it can be concluded that the CHF shows the upper limit of the heat transfer ability of the heating system. In the nuclear reactor point of view, the CHF phenomenon is the most important feature of coolability, in other word is the safety margin of the nuclear reactor. Therefore, in order to design any new nuclear reactor, the study on CHF behavior with the effect of flow parameter and geometry is always needed.

1.5. Review of previous studies

As mentioned above, in order to design the new type of nuclear reactor using tight lattice fuel assembly, the study on coolability is needed. On the other hand, the CHF is the most important feature of coolability, thus the study on CHF behavior in tight lattice core is necessary. Therefore, various studies in this field were obtained by many researchers. The previous study on CHF in tight lattice core can be divided into two parts which are related with two types of spacer: grid spacer and wire spacer.

1.5.1 CHF behavior in tight lattice core with grid spacer

Reduced-Moderation Water Reactor (RMWR) is the advanced light water reactor which was developed by Japan Atomic Energy Research Institute (JAERI) and their collaboration [39]. Since 2002, Japan Atomic Energy Research Institute and their partners started the R&D project [38] in order to investigate the thermal-

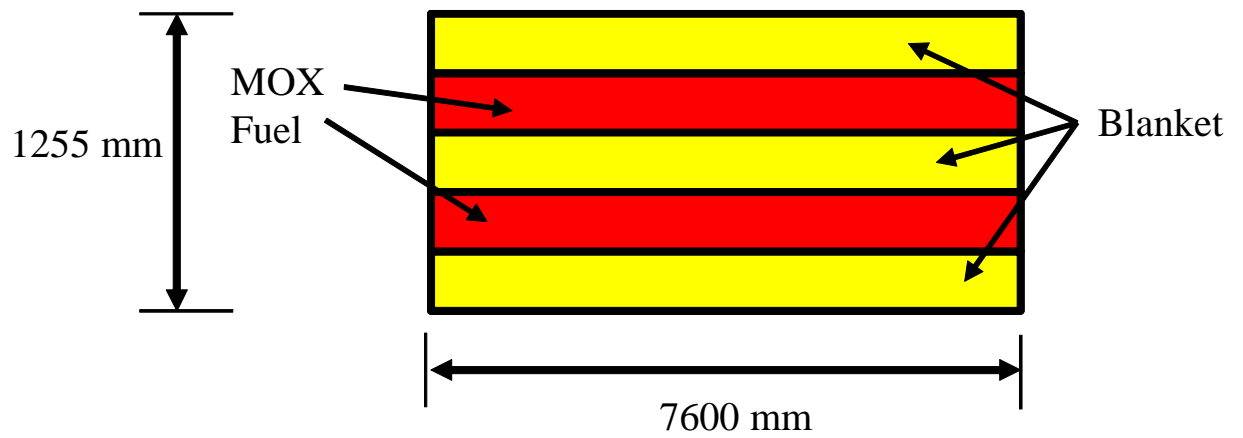
hydraulic performance in tight rod bundle for RMWR and the critical power for such kind of reactor was also well investigated [28][33][55]. The design of core and fuel assembly is shown in Fig.1.10. In this project, the experimental study and analytical study were obtained as well. The large-scale of 37-rod bundle test loop was the main test facility used the experiment. Besides, the experiment study using the tight lattice 7 rod bundle test section was also performed [32]. The effect of other parameters on critical power was obtained such as mass flux, inlet temperature, pressure drop [49][50] and gap width [48].

The critical power experiment was obtained using a tight lattice 37-rod bundle with grid pacer [28], rod diameter of 13.0 mm and gap width (between two adjacent rod) of 1.3 mm, resulting the pitch to diameter ratio of 1.1. The test section has the hydraulic diameter of 4.4 mm and the heated length of 1.26 m. There were two hundred and fifty thermocouples (outer diameter of 0.5 mm) used to detect the temperature of the heated surface. The spacers are of hexagonal honeycomb shape with the thickness of 0.3 mm and height of 20 mm. The experiment was performed at the pressure from 2 to 9 MPa and the mass flux from 150 to 1000 kg/m²s. The results showed the critical power behavior with the effect of mass flux and the water inlet temperature. In tight lattice with grid spacer, the critical power increase with the increase of mass flux. Details the critical power linearly went up from around 500 kW to nearly 1500 kW while the mass flux increased from 200 to 1000 kg/m²s

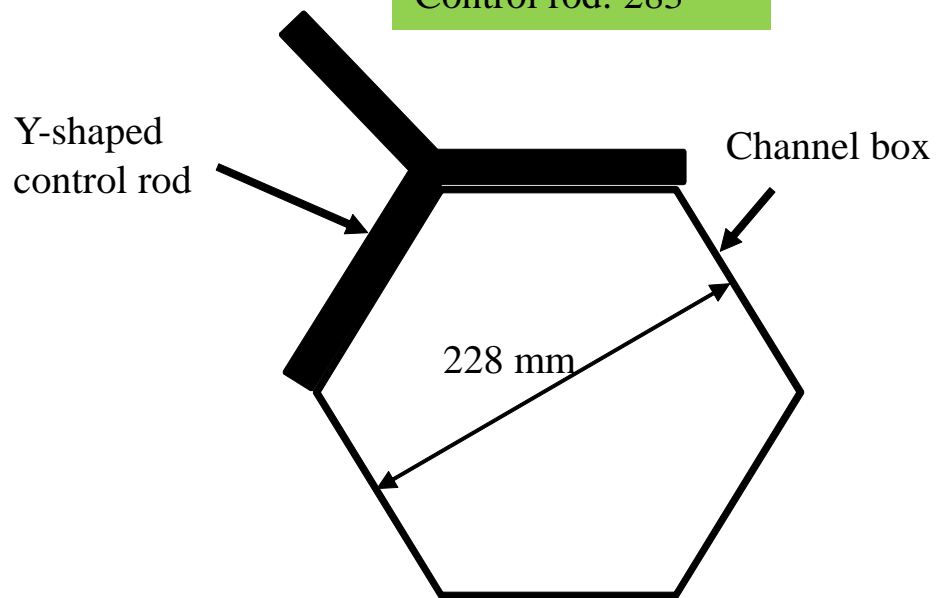
[Fig.1.11]. At the same time, the critical power was increase by about 200 kW while the inlet temperature declined from 559K to 511K [Fig.1.12], in other words the critical power increase with the decrease of inlet temperature. This result trend was nearly the same with that in case of 7 rod bundle experiment [31]. From the experimental results, it can be seen that the effect of flow parameter on the critical power in tight lattice rod bundle was well investigated. The analytical work for this experiment was also conducted by using the subchannel analysis method [35]. The subchannel analysis code NASCA [37] was used in this study. This code was constructed base on the two-phase flow three-fluid models: liquid film, entrainment droplets and the vapor core. In this study, the interface movement was simulated based on an advanced interface-tracking method [56]. The boiling transition was determined while the liquid film volumetric fraction nearly equal zero. Only 1/6 of symmetry of the bundle which contains 10 of total 37 rods was taken into account in order to reduce the calculation time. The total number of subchannel is 14 and 52 nodes along the vertical direction of the subchannel [Fig.1.13]. The boundary conditions consist of inlet temperature, inlet velocity and the outlet pressure. The results of boiling transition obtained from NASCA were agreed with the experimental data. However, the prediction values of critical power for the gap width of 1.3 mm were better than that for the gap width of 1.0 mm. The difference value between experiment and analytical is around 10% in the case of gap with of

1.3 mm. In the case of gap width of 1.0 mm, the difference value becomes nearly 20%.

Under the same project (R&D), the effect of gap width on critical power was taken into account via experiment for tight lattice 37 rod bundle with grid spacer. Most of the parameters were the same with the previous study [48] such as rod diameter and pressure. The mass flux ranged from 150 to 1200 kg/m²s . There were two different values of gap width: 1.0 and 1.3 mm were investigated. The p/d was nearly 1.08 and 1.1, respectively. Considering the experimental results, it is clear that the critical power was higher with the gap width of 1.3 mm than that with the gap width of 1.0 mm under the same mass flux and inlet temperature condition. For example, at the inlet temperature of 511 K and mass flux of 800 kg/m²s, the critical power in the case gap width of 1.3 mm can reach nearly 1500 kW while it only stays around 1200 kW in the case of gap width of 1.0 mm [Fig.1.14]. The effect of gap width on critical power was made clear through this study. Nevertheless, from the reactor design point of view, the experiment with the same mass flow rate for different values of gap width is necessary, in order to keep the best cooling capability performance.



Fuel assembly: 900
Control rod: 283



Number of fuel rods: 217
Outer diameter of fuel rods: 13.7 mm
Fuel rod gap clearance: 1.3 mm

Fig.1.10 Design of core and fuel assembly in RMWR.[28]

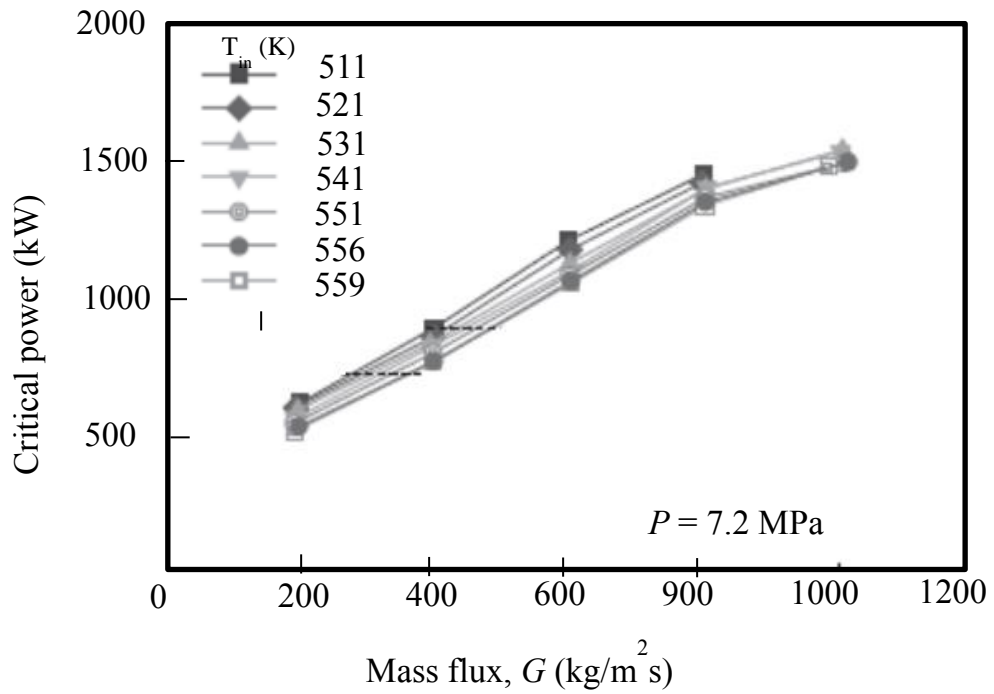


Fig.1.11 Effect of mass flux on critical power in RMWR[28]

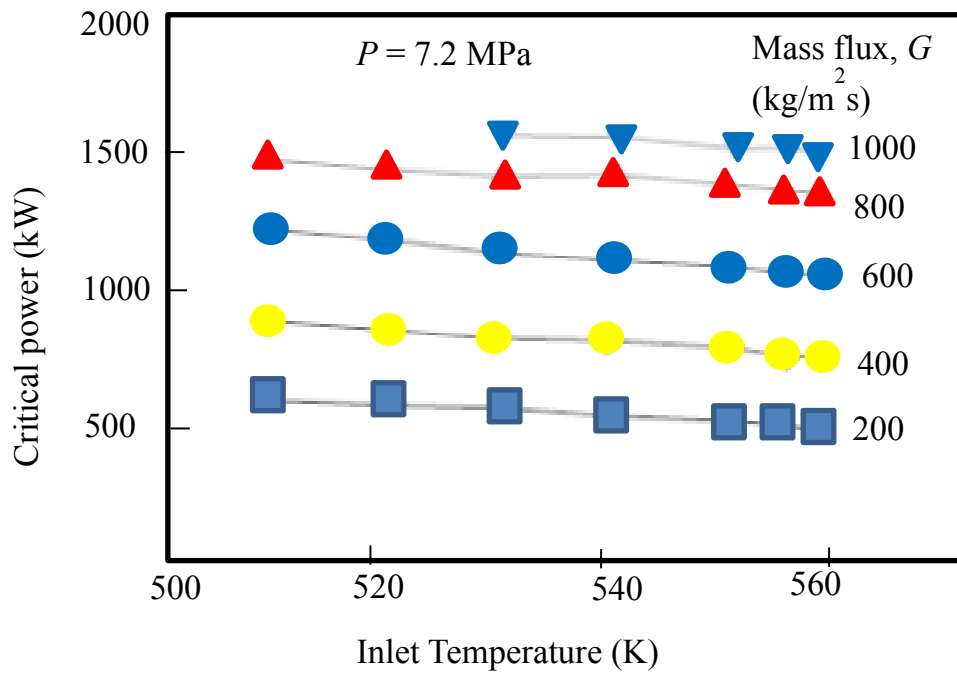


Fig.1.12 Effect of inlet temperature on CHF in RMWR[28]

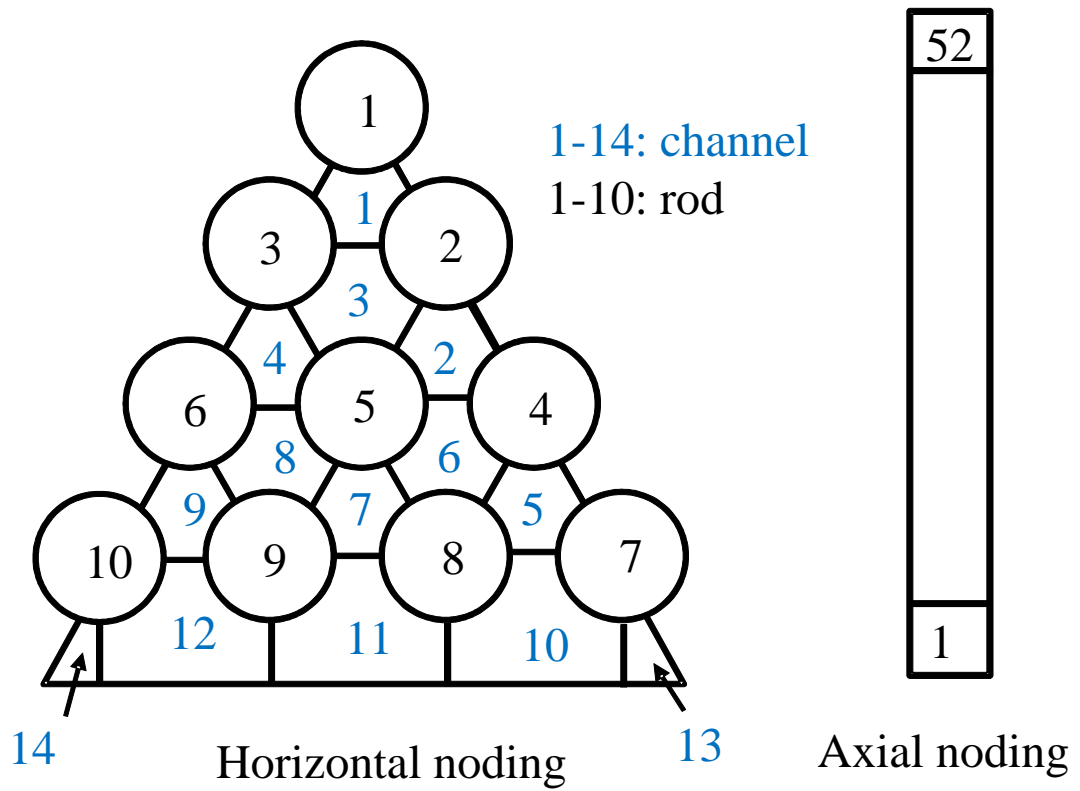
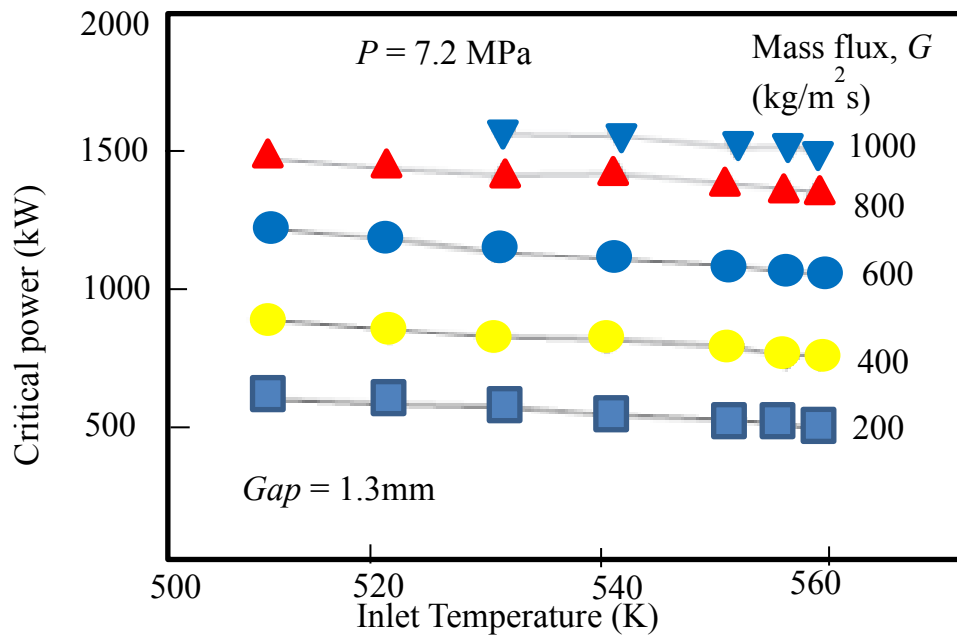
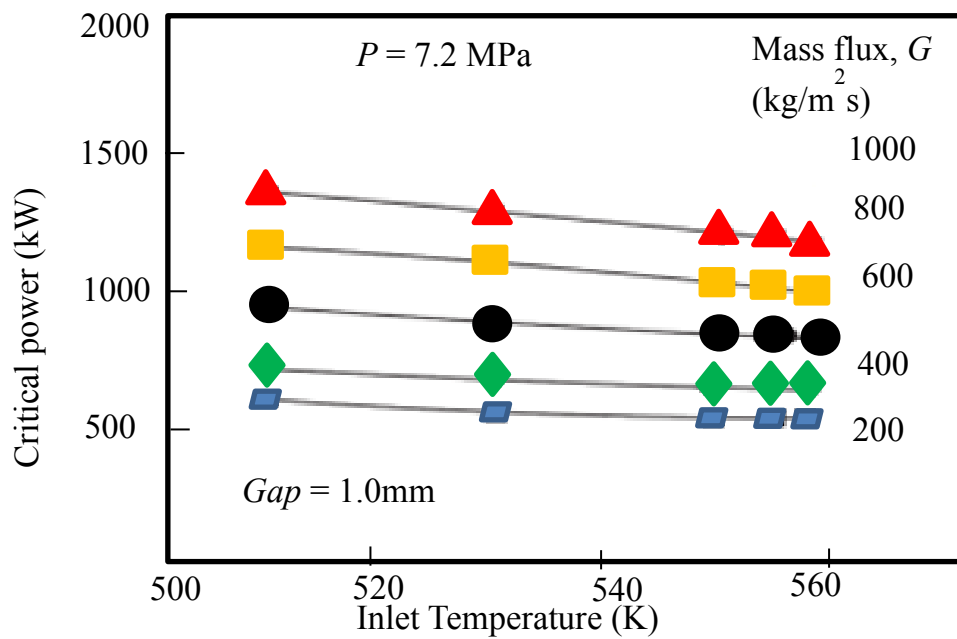


Fig.1.13 NASCA nodding for RMWR core simulation[35]



(a)



(b)

Fig.1.14 Effect of inlet temperature on critical power in RMWR with two difference gap size [48]

1.5.2 CHF behavior in tight lattice core with wire spacers

The experimental study in tight 7-rods bundle [7] was performed with both types of grid spacer and wire spacer. In this study, as the Freon-12 was used as a coolant because of low latent heat and low critical pressure, the experiment could be obtained at high temperature and high pressure condition. Since the fluid-to-fluid scaling law [8] was used, the results can be transferred from Freon-12 to water condition. The test results in the case of grid spacer were compared and had a good agreement with difference prediction method [9][13]. The experiments were performed at the pressure ranging from 1.0 to 3.0 MPa and mass flux from 1.0 to 6.0 Mg/m²s. The total length of rod bundle is 1.24 m and the heated length of 0.6 m. The cross section of the test section was as shown in Fig.1.15. Each heater pin has a rod diameter of 9.5 mm and the rod-to-rod pitch of 10.9 mm. Therefore, the pitch to diameter ratio, p/d , is nearly equal 1.15. By gradually increasing the electric power of the heated rod, CHF was detected by the rapid rise of surface temperature which was measured using thermocouples. As revealed from the test results, the critical heat flux in the hexagonal 7 rod bundle with wire spacers was higher than that with grid spacer at the inlet vapor quality from -1.2 to -0.9 under the pressure condition of 2.7 MPa and mass flux of 2.0 Mg/m²s. It can be seen that the improvement of CHF with wire spacer was indicated. However, the high quality region witnessed unclear improvement of CHF with wire spacer. On the other hand, only one value of

p/d was taken into account in this study, thus, the test results cannot be used for various core design models. Moreover, the wire diameter was not made clear in this study, and hence, it was difficult to clarify the effect of wire spacer on CHF.

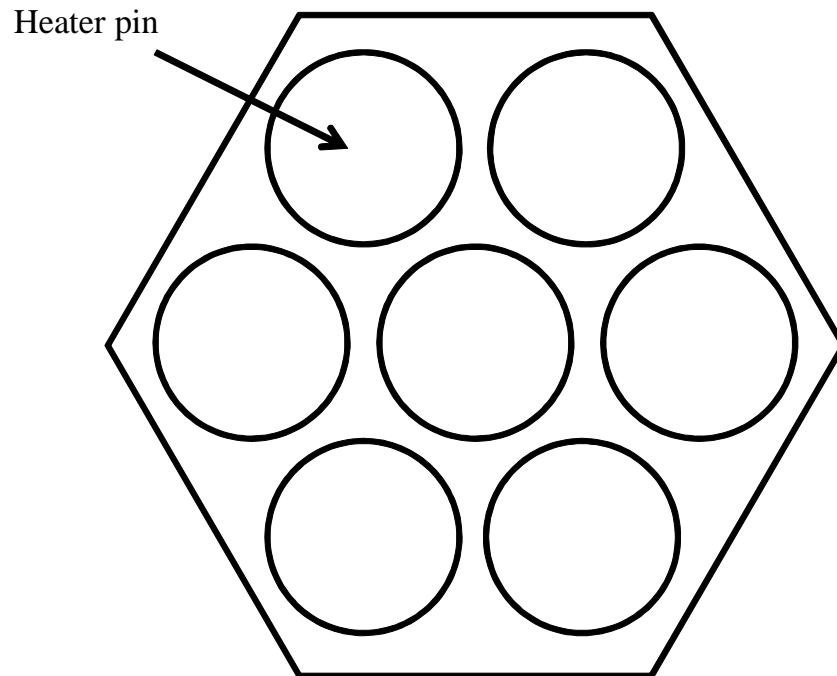


Fig.1.15 Cross section of CHF test section for tight 7-rods bundle [7]

In 2005, the experimental study on critical heat flux in tight lattice 37 rod bundles was also performed using Freon-12[5] with the pressure from 1.0 to 2.7 MPa, mass flux from 1.4 to 4.5 Mg/m²s and the exit steam quality from -0.4 to 0.2. The experiment used grid spacer to assemble all the heater pins. Since the fluid-to-fluid scaling law [1] was used, the results can be transferred from Freon-12 to water condition. The heater pin has a diameter of 9.0 mm and pitch of 10.6 mm, meaning

the pitch to diameter ratio is nearly 1.18. The heated length is only 600 mm over 1240 mm of length in total. The power distribution was similar to that of water cooled bundle [3]. In details, the power supply for seven rods located at the central of bundle is 20% higher than that of other twenty-four ones. According the test results, the effect of steam quality, mass flux and pressure on CHF was well investigated. The CHF values went down with the increase of steam quality under the same mass flux and pressure condition in all the test cases. The enhancement of CHF with the rise of mass flux values at the same pressure and steam quality condition was recorded. However, the difference of CHF for dissimilar mass flux condition is larger in the inlet quality region compared with it in high inlet quality region. For example, at the pressure of 2.3 MPa and the inlet steam quality from -1.0 to -0.6, the CHF values with the mass flux of $4.2 \text{ Mg/m}^2\text{s}$ are twice as high as that with the mass flux of $2.1 \text{ Mg/m}^2\text{s}$. Nevertheless, the difference in CHF values decrease by 50% while the inlet steam quality is increased to -0.2. Regarding the effect of pressure on CHF, at the same steam quality and mass flux, the CHF becomes lower if the pressure value is increased. Besides, at high mass flux condition of $4.2 \text{ Mg/m}^2\text{s}$, the CHF value was nearly the same despite different pressure values or it might be seen that the effect of pressure on CHF at high mass flux condition can be neglected. From the comparison between the experiment data with the CHF data obtained for the tube channel [6], it was found that the effect of

pressure, mass flux and steam quality on CHF is nearly the same between 37 rod bundles and the tube channel. In summary, the CHF behavior in tight rod bundle with grid spacer under the effect of pressure, mass flux and steam quality was deeply considered. Unfortunately, the effect of gap width was not taken into account. Moreover, for the tight lattice core, the use of wire spacers is more suitable compared with grid spacers.

1.5.3. Summary of previous studies

As mentioned above, grid spacer and wire spacer can be applied in tight lattice core. Nevertheless, the used of wire spacer is more suitable for tight lattice arrangement.

Most of studies on CHF behavior in tight lattice core which were reviewed above were well developed for the case of grid spacer. The effects of quality, mass flux and pressure on CHF were well investigated for tight lattice core with grid spacer as well. However, in the case of tight lattice core with wire spacer, the study on CHF behavior is still limited. Especially, the effect of wire spacer on CHF was not investigated well. On the other hand, from the nuclear reactor design point of view, the effects of gap size or pitch to diameter ratio on CHF in tight lattice core with wire spacer are very important. However, very few studies were created to investigate for such kind of effect on CHF. Only the study of Tamai et al. [48] was

constructed to investigate the effect of gap width on CHF in tight rod bundle with grid spacer but in the case of wire spacer, the study on such kind of effect was not existed.

1.6. Motivations of the study

By reviewing the previous study, the motivations for creating the present study are as follow

- In order to design the new type of boiling water reactor (BWR) with tight lattice core, it is necessary to create the study to investigate the thermal hydraulic performance in the nuclear reactor core.
- The tight lattice fuel assembly could have a high conversion ratio even in BWR. However, the tight lattice core have a small flow area, thus the coolability is one of the most important issue. Beside, critical heat flux is the most important feature of coolability. Therefore, it is necessary to investigate the CHF behavior in a tight lattice core to consider about the coolability for such kind of fuel assembly.
- It is important to investigate the effect of flow parameter on CHF in tight lattice core with wire spacer.
- Wire spacer is more suitable for the tight lattice core. Nevertheless, the studies on the effect of wire spacer on the coolability, particularly on CHF in

tight lattice core are limited. Thus the study on the effect of wire spacer on CHF is needed.

- In order to have a conversion ratio nearly equal unity, the pitch to diameter ratio or the gap size between the adjacent fuel rod should be change to a small value and will have a difference value base on the core design. The CHF behavior also changed with the change of p/d value. Thus, it is needed to consider the effect of p/d on CHF.

The present study can be considered as a fundamental study of CHF behavior in tight lattice core with wire spacer.

1.7. Purpose of present study

After reviewing the previous study and considering the motivation, the main purpose of present study is to investigate the CHF behavior in tight lattice core with wire spacer in boiling two phase flow. In more details, the purposes of the present study are listed as follow

- (1) To investigate the effect of flow parameter on CHF in tight lattice core with wire spacer by means of CHF experiment in single pin and three-pin bundle test section with wire spacer.

- (2) To clarify the effect of wire spacer on CHF in tight lattice core by means of CHF experiment in single pin and three-pin bundle test section with wire spacer.
- (3) To evaluate the effect of gap size on CHF in tight lattice core by means of experiment in single pin test section with wire spacer. Three difference values of gap size are taken into account: 1.1, 1.5 and 2.0 mm
- (4) To investigate the effect of pitch to diameter ratio on CHF in tight lattice bundle by mean of experiment in three-pin bundle test section with wire spacer. Two difference values of pitch to diameter ratio are chosen: 1.10 and 1.18.
- (5) To clarify the main mechanism of CHF occurrence in tight lattice core with wire spacer.
- (6) To clarify the main mechanism which is related to the enhancement of CHF with wire spacer in single pin and bundle pin channel by mean of dryout simulation method and parametric studies.

1.8. Outline of thesis

The outline of the dissertation is shown as follow

Chapter 1 Introduction – This chapter presents the overview of the dissertation. The first part of this chapter mentions about the background of nuclear

energy status and also gives the definition of tight lattice core and CHF. The related studies are reviewed in details in this chapter. The motivation to create this study is also given in this chapter. Finally, the purpose of present study is also listed.

Chapter 2 Design and setup of forced convection type water loop and CHF test section – In this chapter, the detail information of the experimental apparatus is given. Besides, the originally design and setup technique of the single pin and three-pin bundle CHF test section are presented in details. The experimental procedure and measurement items are also given in this chapter.

Chapter 3 Experimental study on CHF behavior in single pin with and without wire spacer – This chapter presents the experimental study on CHF behavior in single pin with and without wire spacer to investigate the effect of flow parameter and wire spacer on CHF. The results show the CHF value was higher in the heater pin channel with the wire spacer than in that without the wire spacer at the same mass flux condition. On the other hand, the CHF was increase with the decrease of gap size values under the same flow rate condition. The results were also compared with the CHF correlation.

Chapter 4 Experimental study on CHF behavior in Bundle pin with and without wire spacer – In this chapter, the CHF behavior in bundle pin with and without wire spacer was investigated by means of experiment in three-pins tight rod

bundle test section. According to the results, the CHF was enhanced by wire spacers in comparison with the results of CHF without wire spacers. The CHF was enhanced by reducing the pitch to diameter ratio value under the same flow rate condition, although it did not change appreciably with the change of pitch to diameter ratio under the same mass flux condition.

Chapter 5 Analytical study on CHF behavior in tight rod bundle using CHF simulation method – This chapter presents the analytical study on CHF behavior in tight lattice core by using dryout simulation method. The calculation method was obtained for both of single pin and bundle pin channel. The parametric studies on the droplet entrainment and deposition rate were obtained to clarify the enhancement mechanism of CHF in annulus channel and bundle pin channel, respectively.

Chapter 6 Conclusions – This chapter summarizes the overall conclusions obtained from this study.

Chapter 2. Design and setup of forced convection type water loop and CHF test section

2.1. Introduction

CHF behavior in tight lattice core will be simulated by means of design and setup of water test loop and CHF test sections. Two types of simulation test were created, which were single pin test section and three-pin bundle test section. The single pin with wire spacer test sections were design to investigate the effect of wire spacer on the CHF behavior in tight lattice channel. On the other hand, the three-pin bundle test sections were designed to investigate the effect of multiple wire spacers on the CHF behavior in tight lattice core, which was close to the practical case.

The two water coolant types of test sections were designed to work at the atmospheric pressure. The heater pins were heated up by the directly Joule-heating and the burnout phenomena would be detected by the thermocouples.

2.2. Experimental apparatus

The experimental apparatus of a water circulation loop named T-PBBOIL is shown in Fig.2.1 and Fig.2.2. The experiment apparatus consists of the water storage tank, the circulation pump, the pre-heater, the orifice flow meter and the CHF test section. The water storage tank has a capacity of 0.06 m^3 . The pre-heater is an electrically type which has a maximum power up to 50 kW. All the main parts of the experimental apparatus are connected with each other by stainless steel pipe and tube. Besides, all the parts of the experimental apparatus were insulated to minimize

heat loss.

The orifice flow meter is located at the upstream of the pre-heater to prevent the bubble flow into the orifice during the heating process. The orifice used in this experiment has a orifice hole diameter of 3 mm. The calibration curve of the orifice is shown in Fig.2.3. The inlet of the test section was located at 4200 mm far from the outlet of the pre-heater. Therefore, the water temperature is constant prior to supply to the test section. The water was circulated from the water tank to the pre-heater before coming to the test section.

The valve was setup at location of 200 mm far from the downstream of the test section to control the flow resistance prior to flow into the test section. The flow resistance should be kept high enough to prevent the instability of flow in the test section which may influence on the experimental data.

The pressure gauge was setup at the outlet of the test section to measure the outlet pressure of the experiment. In order to keep the system pressure equal the atmospheric pressure, the valve which is located at the top of the apparatus was kept open to the air. There are two type of the CHF test section: single pin test section and three-pin bundle test section.

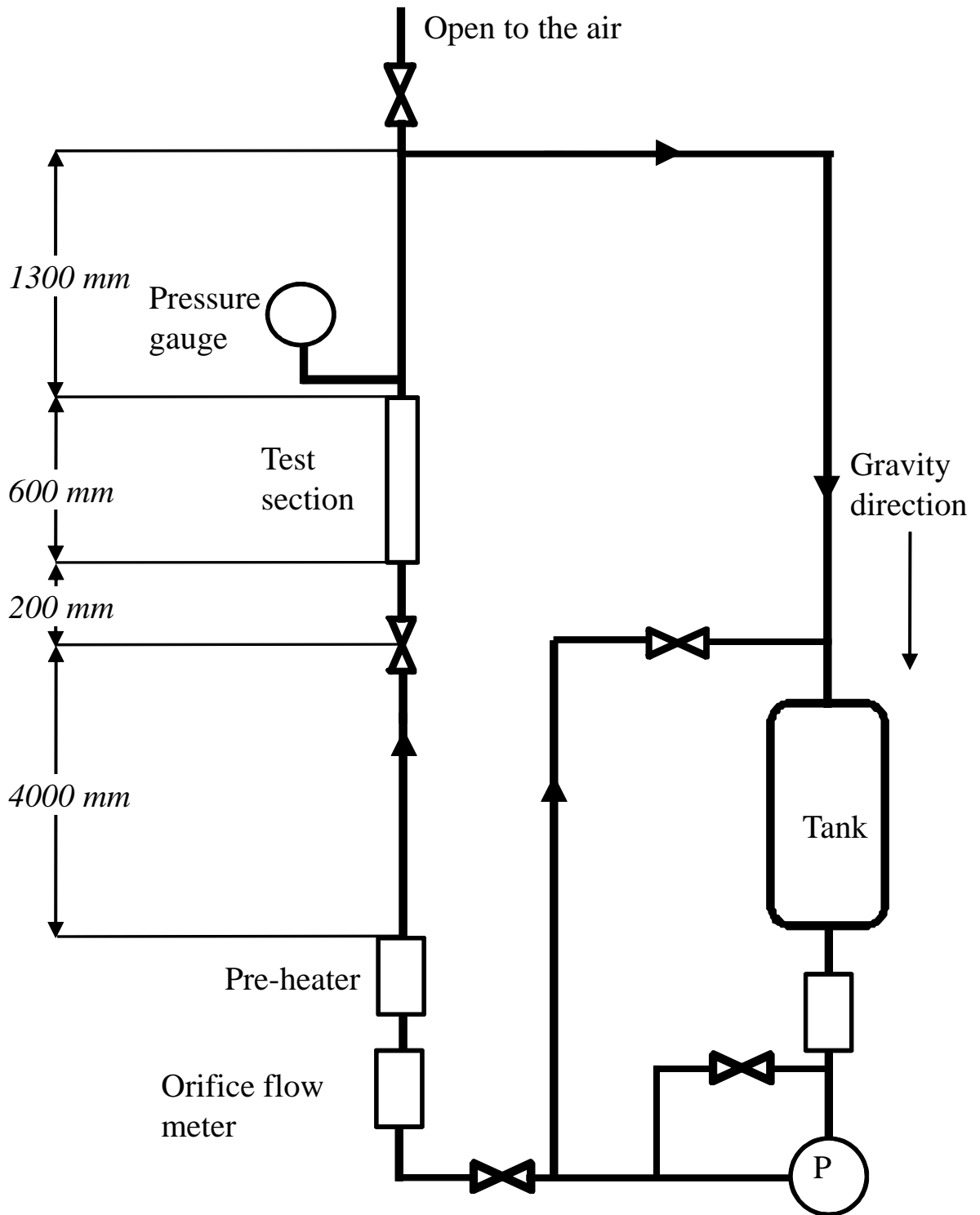


Fig.2.1 Schematic of the experimental apparatus



Fig.2.2 Experimental apparatus

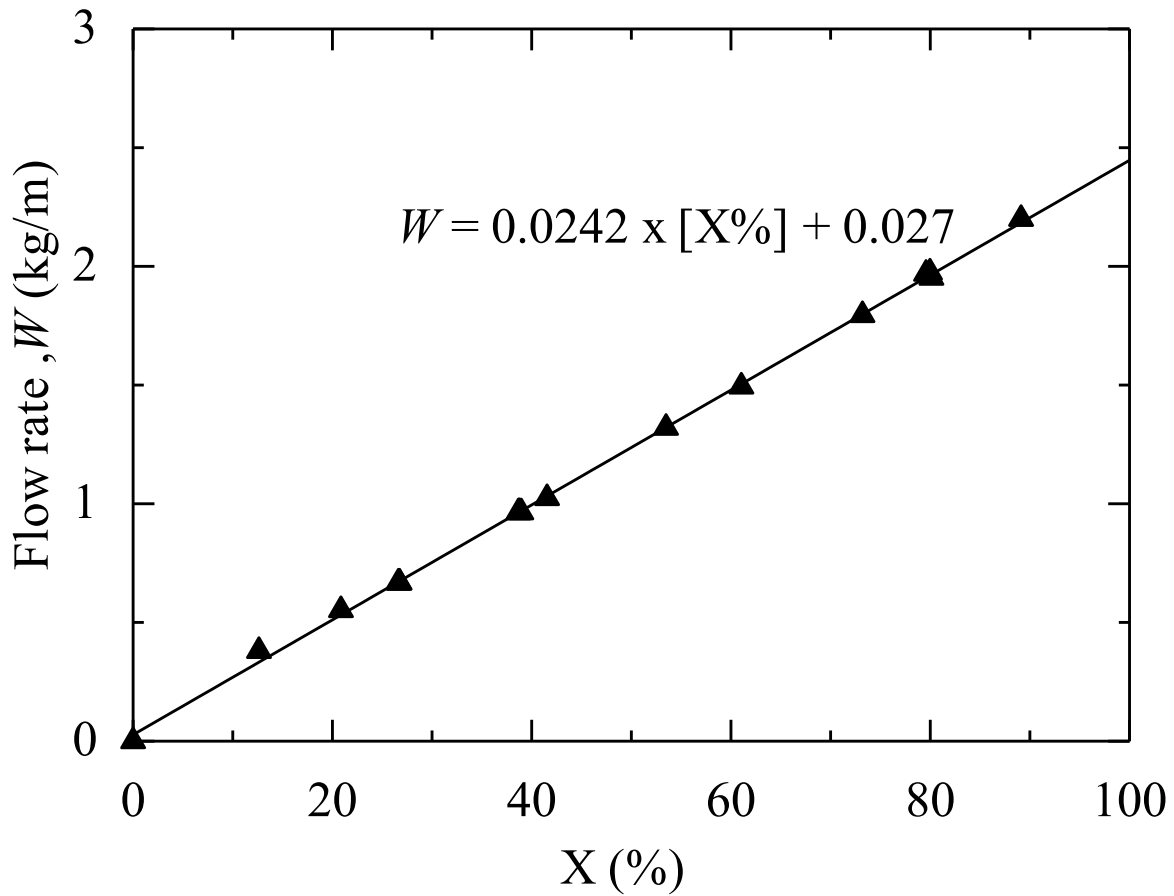


Fig.2.3. Calibration curve of the orifice

2.3. Single pin test Section

The single pin CHF test section is shown in Fig.2.4 with the oriented vertically. The cross section of the flow channel is shown in Fig.2.5. The test section were constructed from the heater pin, the upper and bottom copper electrodes, the glass tube, the thermocouples and the wire spacer in case of experiment for a heater pin with a wire spacer. In order to recognize the location of the reaching to the CHF,

the position indications were written on the outside surface of the glass tube. By using thermocouples, the length indications and the camera, the positions of burnout or the arrival to the CHF were recognized.

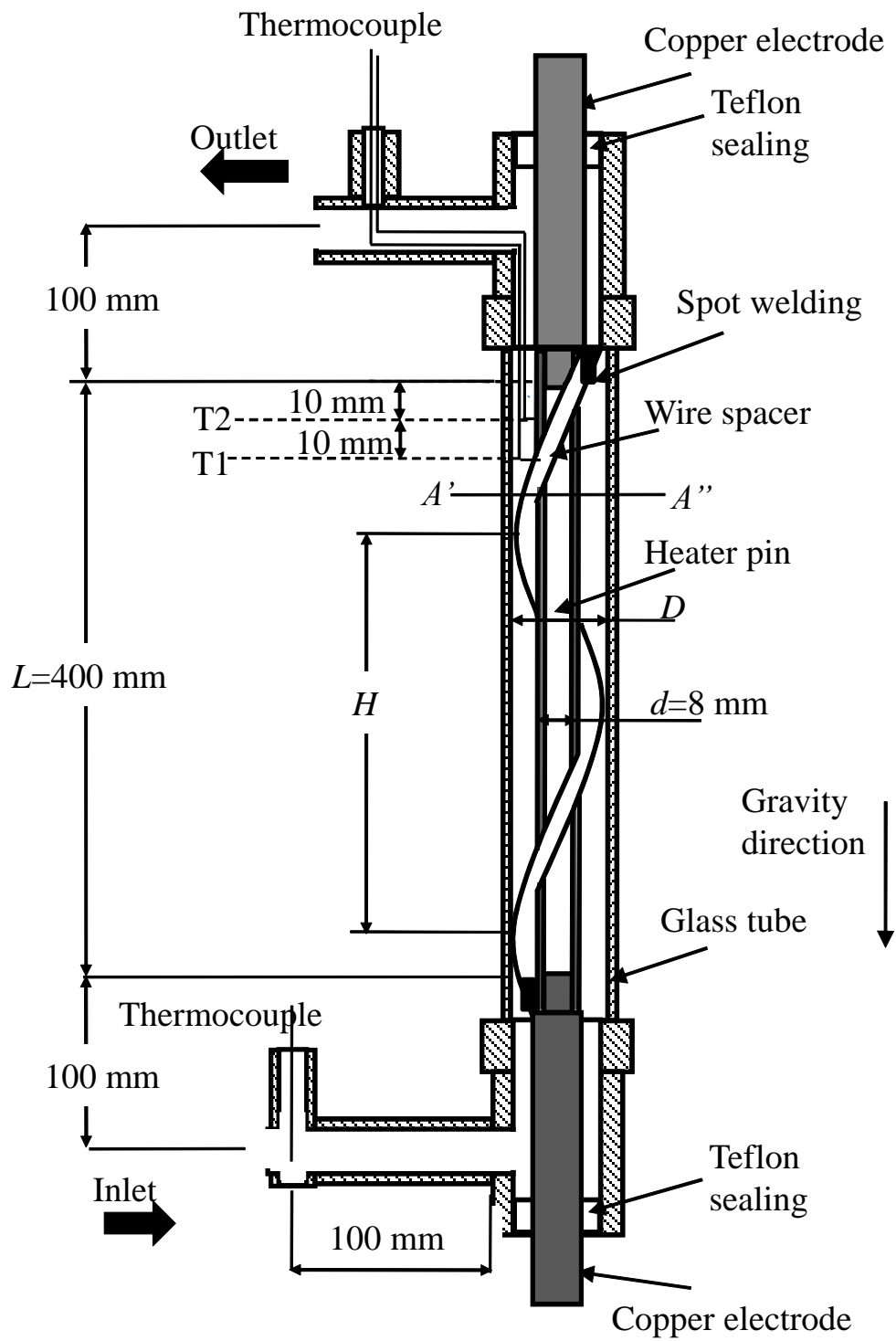


Fig. 2.4 Single pin test section.

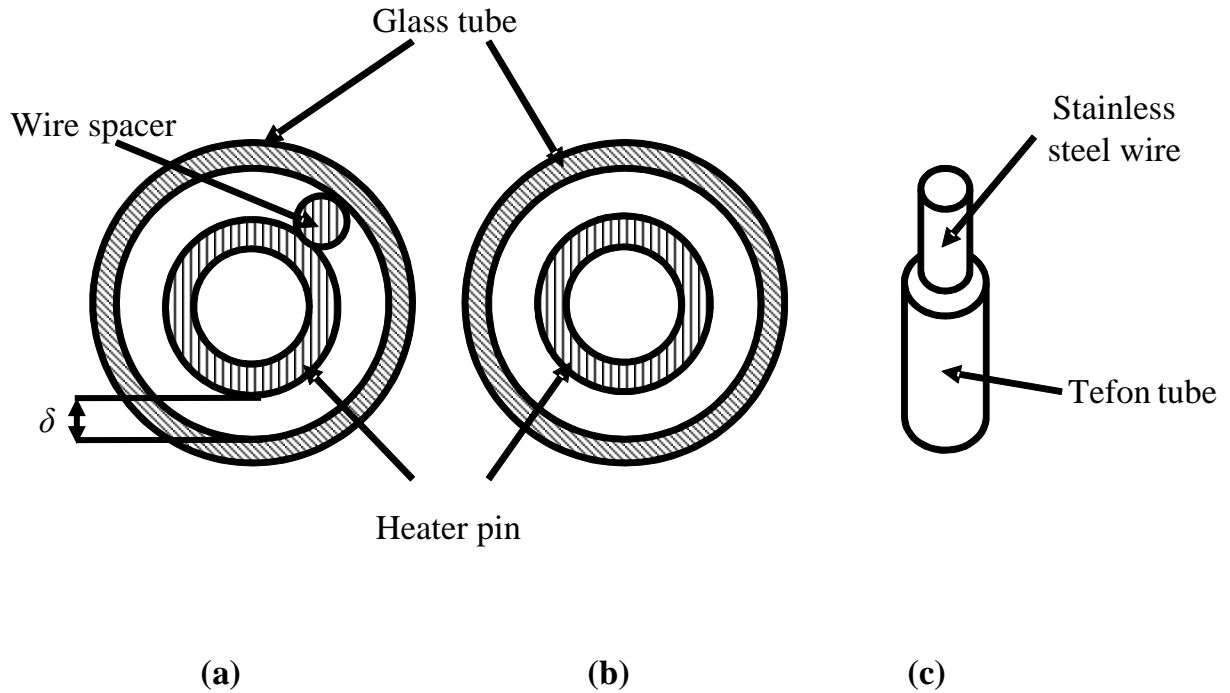


Fig. 2.5 Cross-section of the test section:

(a) heater pin with wire; (b) heater pin without wire; (c) wire structure

2.3.1. Heater pin

The simulated heater pin was made of a thin stainless steel tube with an outer diameter, d , of 8 mm, a length of 420 mm and a thickness of 0.25 mm. The electrodes were made by the copper and had a cylinder shape. The heater pin and the electrodes will be connected by silver soldering. At first, the copper electrodes were inserted into the inside of the stainless steel tube in the depth of 10 mm. The connected surface was covered by the flux to remove the oxygen layer on the

surface of the connected part which had an influence on the welding process. During the welding process, only the electrode part was heated to prevent the burn on stainless steel tube. Since the copper electrode was inserted into the inside of the heater pin in the depth of 10 mm, the heated length of the heater pin tube with a thin wall, L , was 400 mm. On the other hand, the length to diameter ratio, L/d , of around 50 was large enough to suppress the effect of heated length on CHF [10].

The copper electrodes were connected with the top and bottom part of the test section by the Swagelok filters. Before connecting the copper electrodes, the electrodes were covered by the Teflon tube for the purpose of electrically insulate. The Teflon ferrules were used in the connector part instead of stainless steel one to easy connect or remove.

The direct Joule-heating of the heater pin provided an uniform heat flux on the heater pin surface. The maximum power and current of the power in this experiment were 15 kW and 500 A, respectively.

2.3.2. Wire spacer

In the practical reactor, the metallic wire spacers are not covered by Teflon tube. Therefore, the heat can be conducted from cladding to the wire spacer. In the case of present study, the stainless steel wire was covered by Teflon tube so that there was no heat conduction from the heater pin to the wire spacer. In this

experiment, the heater pin was heat up by direct Joule-heating. Therefore, if there were no Teflon tube, the maximum heat could be generated from the wire without Teflon tube was nearly 4.9 kJ very 1 second with the wire diameter of 1.4 mm and voltage of 29.79 (V) at which the heat pin power was 19.6 kW. Thus, the heat generated from the wire spacer is nearly 25% of the total heat generated from the heater pin. Therefore, it is necessary to use the Teflon tube for electric insulation. Fig.2.5(c).

The Teflon tube working temperature is less than 200°C. Besides, the surface temperature of the heater pin during the experiment was around 110 °C. When the CHF occurs, the surface temperature was higher than 400°C so that the Teflon tube was damaged after the experiment. However, the purpose of this study is the onset of CHF phenomenon. Therefore, the burn of Teflon tube after the experiment did not have any matter to the experimental data.

In order to connect the wire spacer with the heater pin, the both end of wire spacer was fixed with the both end of the heater pin by using a thin stainless steel plate which has a thickness of 1 mm. The spot welding technique was used to embed the stainless steel plate on the surface of the heater pin. The axial coil pitch of the wire, H , is the axial distance over which the wire completely wraps around the heater pin as shown in Fig.2.4. The axial pitch of the wire spacer, H , was set with two different values 100 mm and 200 mm. For this two different values of the axial

pitch, the value of H/d less than 50 was the upper limit of the wire correlation for both CHF and pressure drop [10].

2.3.3. Glass flow channel

The glass tubes used as a flow channel were made by Pyrex glass and Crystal glass. The glass tube has a constant length of 500 mm. The thickness of the glass tube was change based on the experimental condition. Since the glass tube was use as a flow channel and also was used to connect the top and bottom part of the test section with each other, thus one of the most important points was to prevent the water leak from the experiment test section. Therefore, rubbers and stainless steel O-ring were used to prevent the water leak in the connection part.

Gap size, δ , is the distance from the outer surface of heater pin to the inner surface of the glass tube as shown in Fig.2.5(a). For the rod diameter of 8 mm, three different values of gap size were chosen: 1.1, 1.5 and 2.0 mm. By changing the wire diameter and glass inner diameter, the size of the gap values could be changed.

2.3.4. Thermocouples

To detect a sudden temperature rise on the heater pin surface at the CHF condition and quickly shutdown the heating power, type K thermocouple elements with diameter of 100 μm were used for the surface heater pin temperature measurement.

Fig.2.5 shows that, the ends of the thermocouple elements were spot-welded to the surface to be hot junction at positions of 20 mm and 10 mm upstream from the downstream end of the heated length, being marked as T1 and T2, respectively. The thermocouples were lead out from the test section through a small hole located at the outlet of the test section. The silicon glue was used to cover the around the hole to prevent the water leak. The effect of thermocouples on the CHF behavior can be neglected because its diameter is very small compared with the flow area.

Since the heater pin was the stainless steel tube with direct heating by the current, the three point junction technique [Fig.2.6] was used for compensation of voltage induced by the current between two points junctions, where C and A indicate the Chromel and Alumel thermocouple elements for Type K, respectively. The voltage induced by the current between C and A was eliminated by adjusting the resistance of the variable resistor under low power input condition where temperature did not increase appreciably.

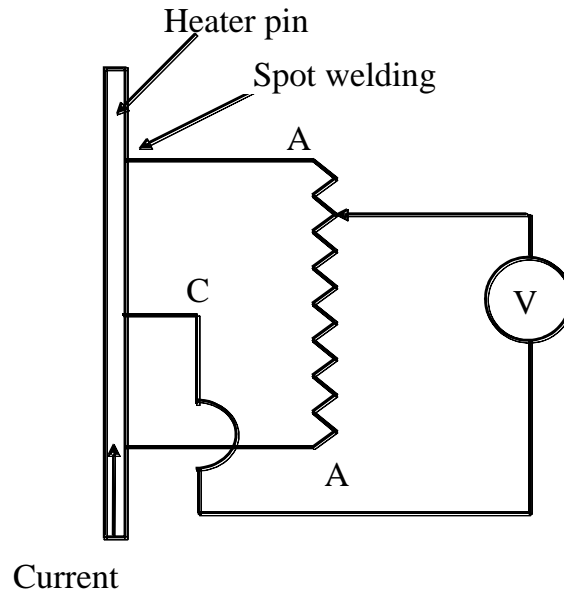


Fig.2.6. Three point junctions.

2.4. Three-pin bundle test section

The three-pin bundle test section is shown in Fig.2.7 and the cross section of the test section is shown in Fig.2.8. The test section were constructed from the heater pin, the upper and bottom copper electrodes, the top and bottom part, the glass triangular shape flow channel, the thermocouples and the wire spacer in case of experiment for a heater pin with a wire spacer. The schematic of top and bottom parts of the test section are shown in Fig.2.9.

The experiment can reach the maximum power of 12kW and current of 630 Ampere. Because of the high current, the electric cables are no longer in used due to the local heated by high current. Therefore, in the case of bundle experiment, the

copper plates which have the width of 60 mm and thickness of 5 mm are used instead of electric cables.

2.4.1 Bundle heater pin

Three-pin tight rod bundle was made by assembling three heater pins made of stainless steel tubes in the triangular arrangement. The heater pins were directly heated by Joule-heating and it had an uniform heat flux on the heater pin surface.

The heater pins were 4.57 mm in outer diameter and 400 mm in length. The pin pitch, p , was 5 mm and 5.4 mm, which corresponded to the pitch to diameter ratio, p/d , of 1.10 and 1.18, respectively.

Each heater pin was connected to the copper electrode at both ends by silver soldering. The copper electrodes are made by connecting three stick electrodes with the main electrode. The design of the stick electrodes and the main electrode are shown in Fig.2.10. Three stick electrodes were inserted from the bottom side of the main electrode into the inside of the main electrodes in the depth of 10 mm. By using the Tin handle soldering, the stick electrodes could be connected with the main electrodes.

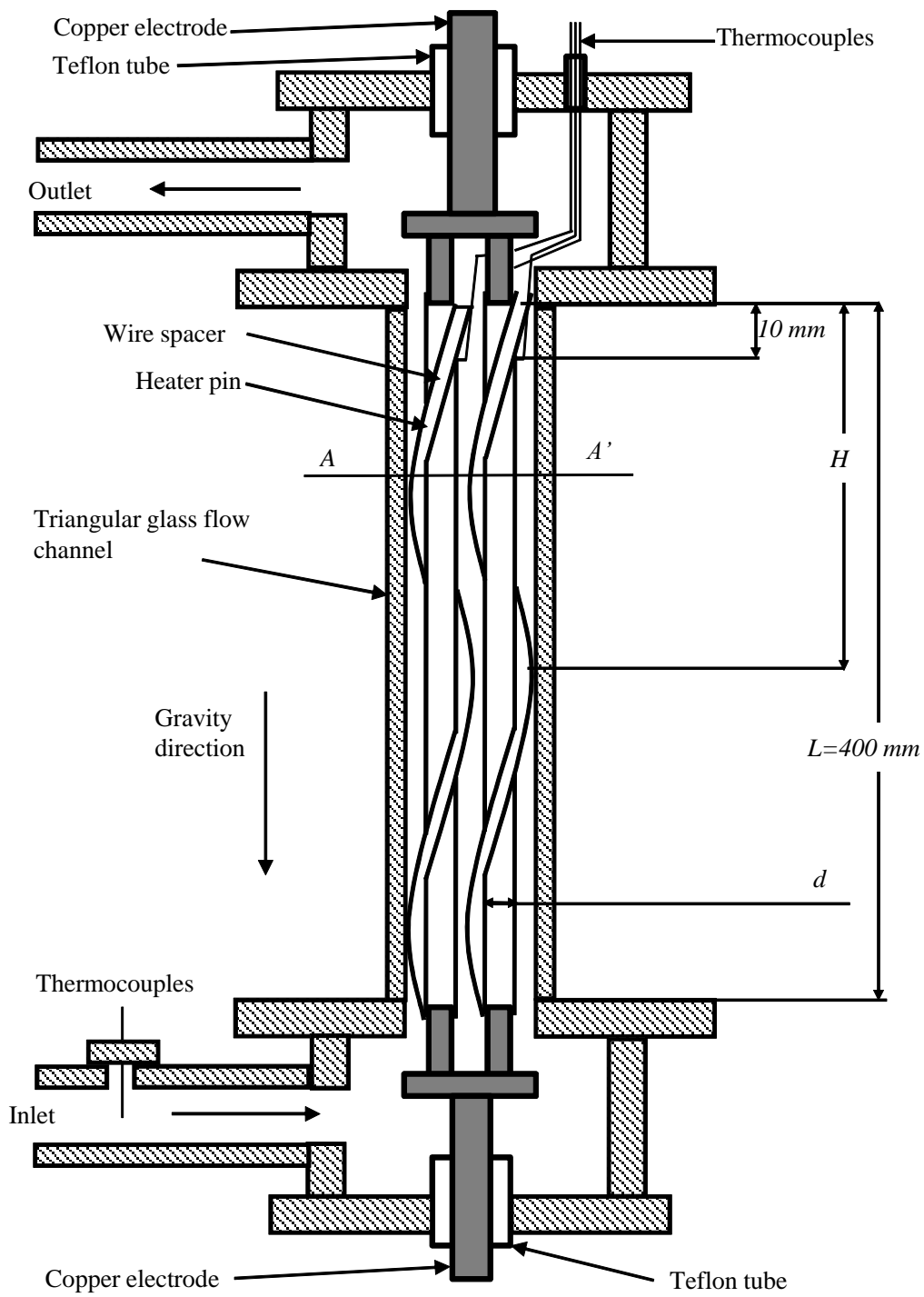


Fig.2.7 Three-pins bundle test section

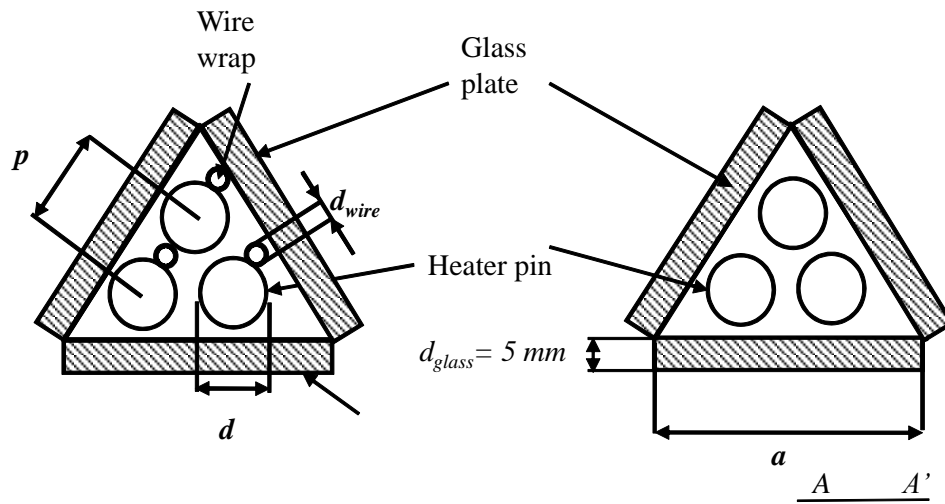


Fig.2.8 Cross section of flow channel

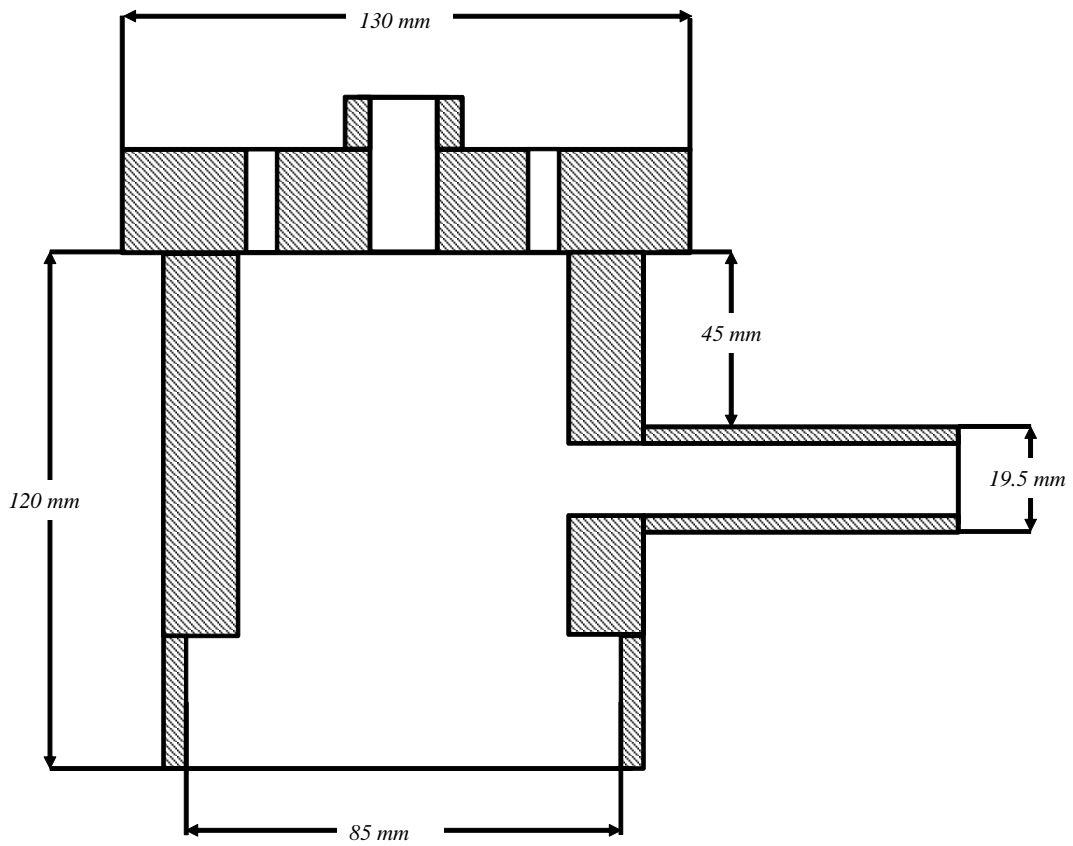


Fig.2.9 Schematic of the upper and lower part of the test section

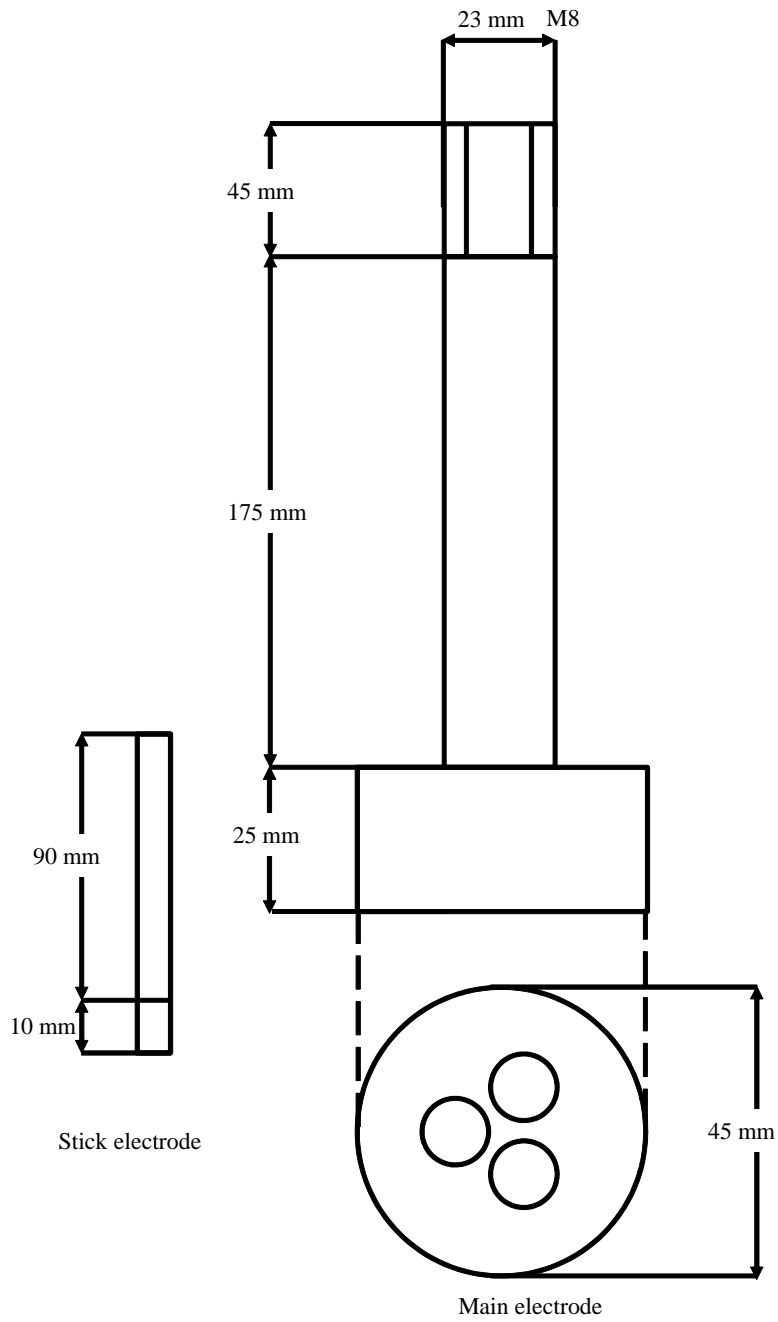


Fig.2.10 Copper electrode

2.4.2 Triangular glass flow channel

The flow channels were made from the glass plates, polycarbonate support plate, polycarbonate tube and the stainless steel tube. The schematic of the flow channel is shown in Fig.2.11.

The main flow channel had the triangular shape which was made from three Pyrex glass plate. The Pyrex glass plate has a length of 500 mm, the thickness of 5 mm and the width of 15 mm and 17 mm for the pitch to diameter of 1.10 and 1.18, respectively.

Three Pyrex glass plates were connected with each other along the edges by silicon glue. Before connecting with each other, the edge side of glass plate is filled with the special silicon glue which has a low viscosity [Fig.2.12]. The purpose of this step is to make a smooth surface on the edge side of glass plate to prevent the water leak from the side of flow channel. After connected with each other, the triangular flow channel is supported by connected with two polycarbonate plates at both ends. The polycarbonate plates are 65 mm in diameter and 5 mm in thickness [Fig.2.12]. After connected with the polycarbonate plates, the flow channel was inserted into the inside of the polycarbonate tube and sealed at the both end by silicon glue. To prevent the water leak from this part, the use of the silicon glue with the low viscosity was the best solution. The silicon glue was poured from the outside

through the windows which were cut on the surface of the polycarbonate tube. Another purpose of these windows was to prevent the damage from the expansion of the air storage between the flow channel and the outer polycarbonate tube.

The both end of the polycarbonate tube are connected with the stainless steel tube to be able to fit with the upper and bottom part of the test section. The details of flow channel parameters are shown in table 2.1.

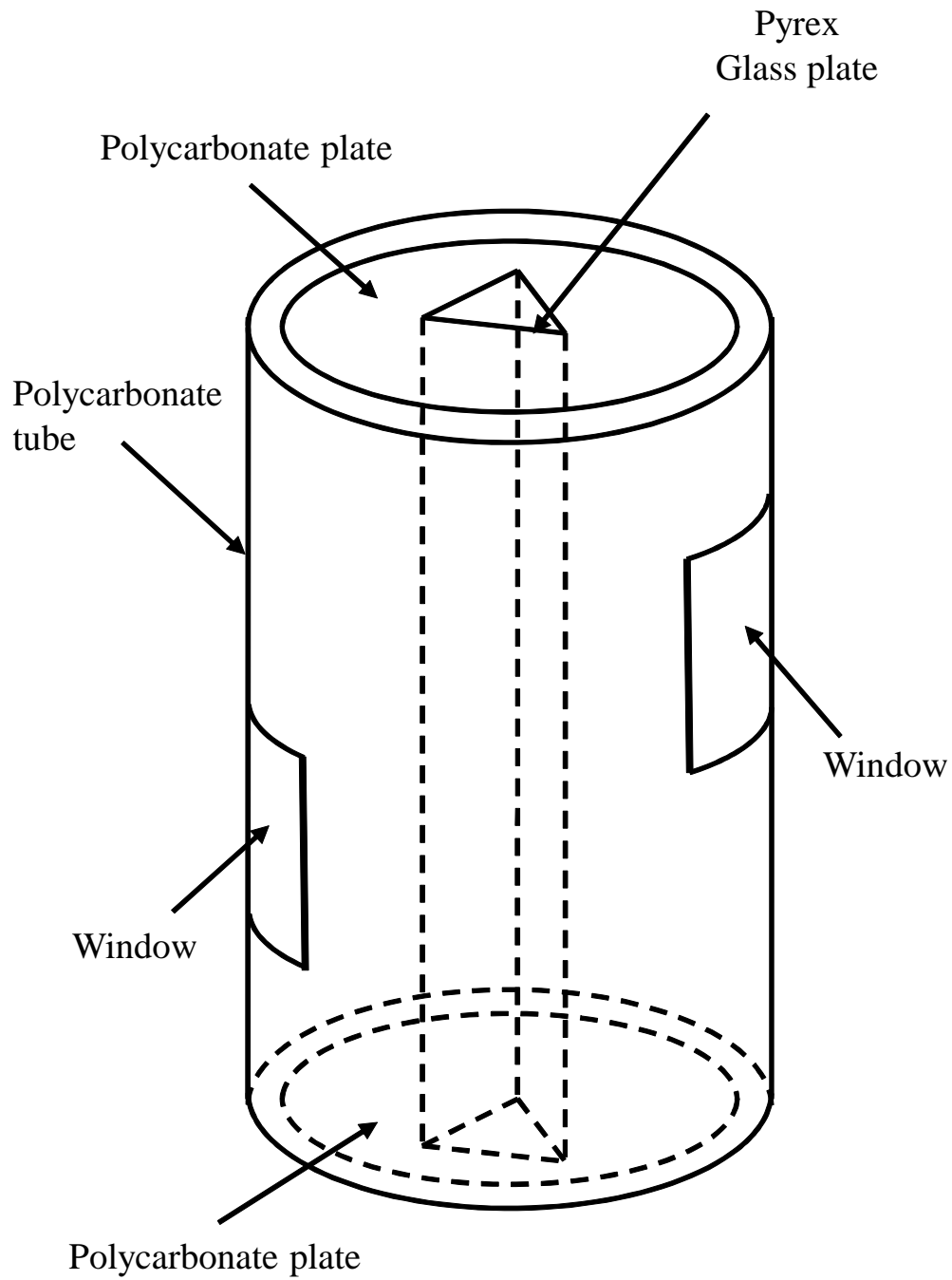


Fig.2.11 Structure of flow channel

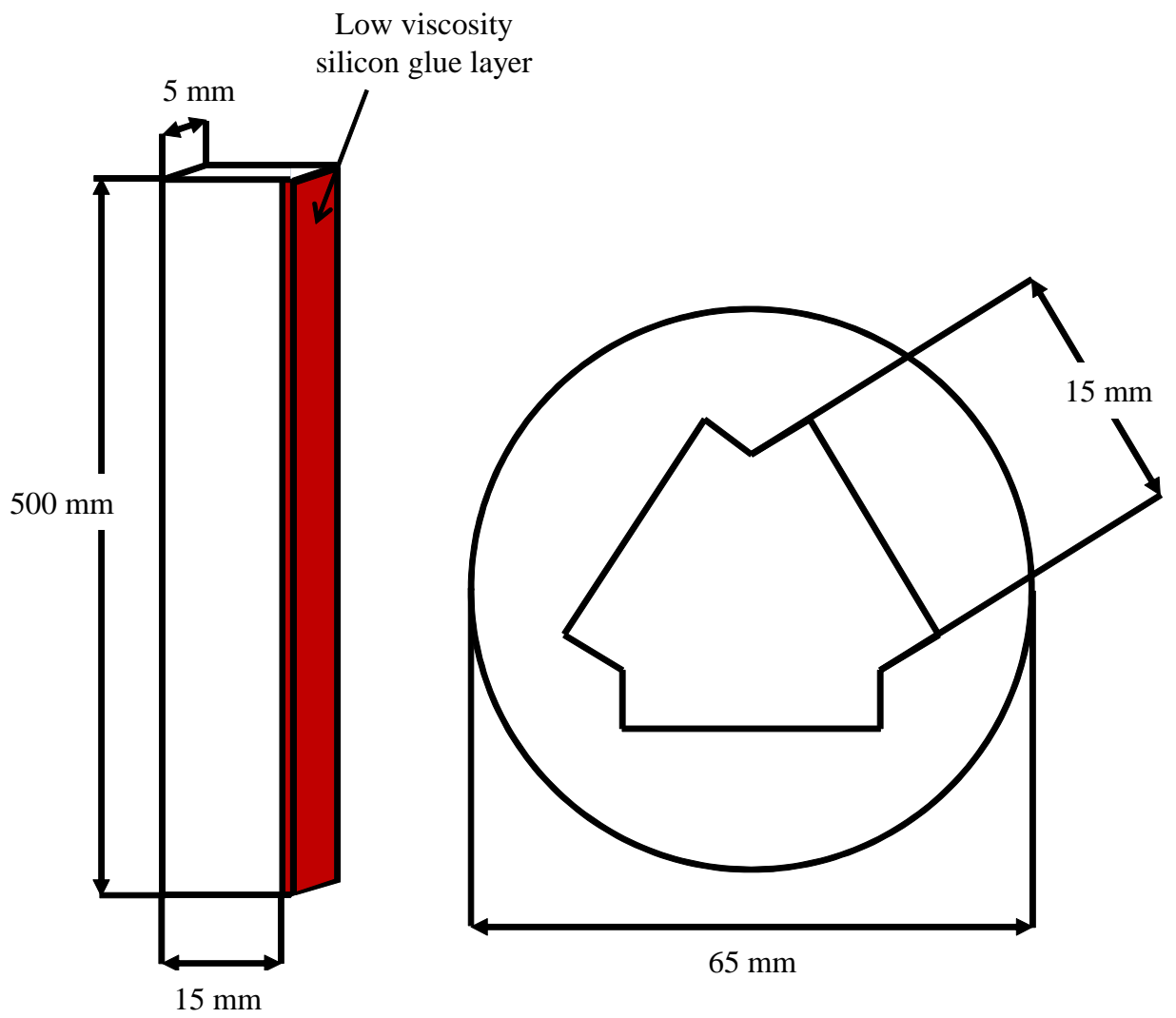


Fig.2.12 Cross section of the test section

Table 2.1 Flow channel geometric parameter

Crystal Glass tube	
Outer diameter	76 mm
Inner diameter	65 mm
Thickness	5 mm
Length	500 mm
Pyrex glass plate	
Width	variable
Thickness	5 mm
Length	500 mm
Polycarbonate plate	
Outer diameter	65 mm
Thickness	5 mm
Stainless steel tube	
Outer diameter	80 mm
Inner diameter	76 mm

2.4.3 Wire spacers

A wire spacer was wrapped around each of the heater pin with the axial winding pitch $H=200$ mm. The value of axial pitch of wire met the requirement of H/d less than 50 which was the upper limit of wire correlation for both CHF and pressure drop [10].

The wire spacer for $p/d = 1.18$ was a Teflon tube in outer diameter $d_w = 0.76$ mm in which a stainless steel wire was inserted, and that for $p/d = 1.10$ was a Holmal coated wire in outer diameter $d_w = 0.4$ mm. The reason for the use of Holmal coated wire is to satisfy the gap size of 0.5 mm in the case of p/d of 1.10. The wire spacer was electrically insulated from the heater pin by a Teflon tube or Holmal coating so that no heat was generated in the wire.

2.4.4 Thermocouples

Thermocouple elements were spot-welded on the surface of each heater pin. The surface temperature of the heater pin rapidly rose at the CHF condition. To determine the CHF, the temperature rise at the CHF condition was detected by thermocouples at the positions 20 mm upstream from the downstream end of heated length: T1, T2 and T3 [Fig.2.13].

Thin type K thermocouple elements with the diameter of $100 \mu\text{m}$ were used so that the thermocouples did not disturb the flow to change the CHF behavior.

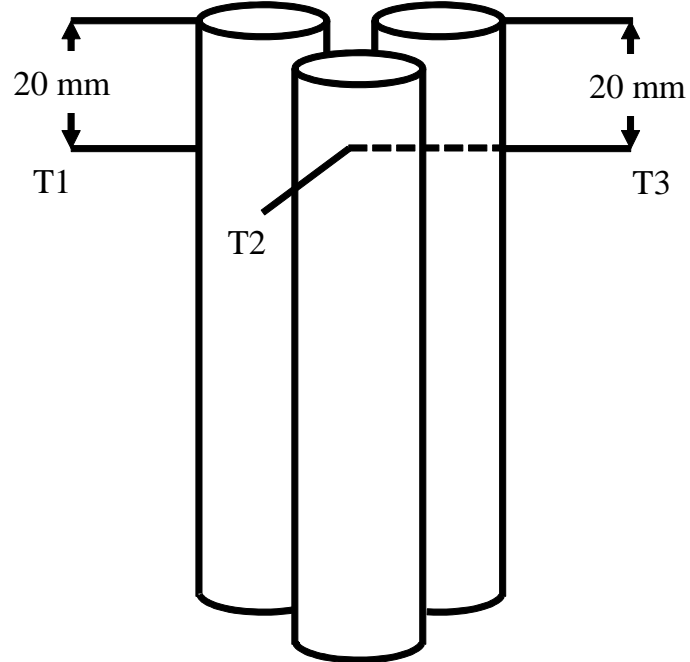


Fig.2.13 Thermocouple position

2.5. Experimental Procedure and Measurement Items

The water from the water tank was circulated in the loop by using the circulation pump. Water was heated up by the pre-heater before starting the experiment.

The water in the water circulation loop was degassed initially by boiling the water in the test section for a while until air dissolved in the water was removed sufficiently.

During the experiment, the water flow rate was kept constant. The flow resistance at the inlet valve of the test section was kept high enough to suppress the

instability of flow rate due to the instability of pressure drop of two-phase flow in the test section. When the water temperature was kept constant at the inlet of the test section reached the desired value by controlling the pre-heater, the electric power to the heater pin in the test section was increased gradually by remote controlling.

Surface temperature of the heat pin was measured and recorded by using the thermocouples with the sampling frequency of 100 Hz. The power of the heater pin was increased step by step until the surface temperature of the heater pin rapidly and suddenly increased because of reaching the CHF condition. Immediately after reaching the CHF condition, the power source was automatically shut down by the signal of sudden rise of surface temperature.

Fig.2.14 shows the behaviors of the measured surface and inlet temperatures in single pin test section, voltage and current during the operation. It can be seen that, the inlet temperature was kept constant. The surface temperatures T1 and T2 increased slightly due to the increase of the electric power to the heater pin, and then suddenly the surface temperatures of the heater pin T1 and T2 rapidly increased. It was judged that, at this time, the burn-out took place or the heat flux reached the CHF.

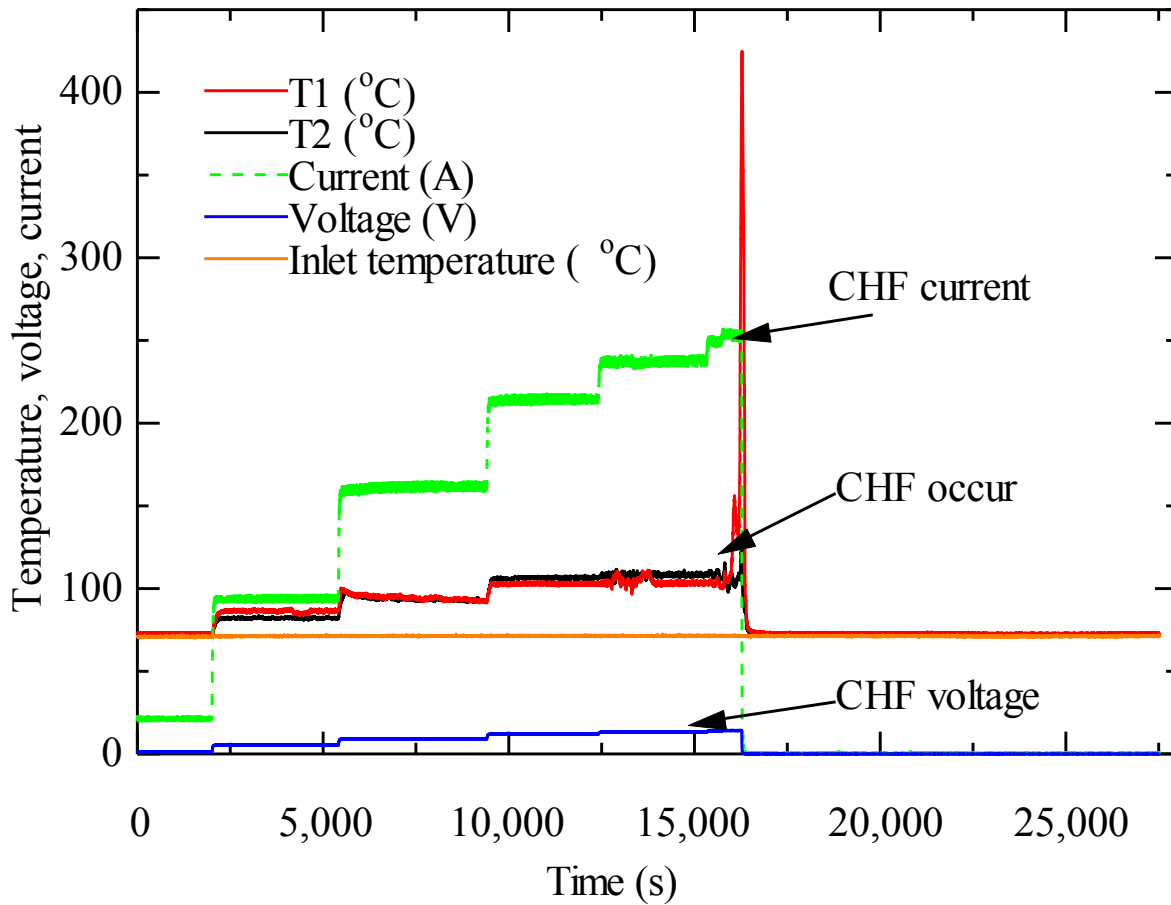


**Fig.2.14 Temperature behavior during the CHF experiment
in single pin test section.**

The electric power Q is calculated from measured voltage V and current I as

$$Q = VI \quad (2.1)$$

The CHF value is obtained by

$$q_{CHF} = \frac{Q_{CHF}}{S} \quad (2.2)$$

where Q_{CHF} is the electric power when CHF occurs, q_{CHF} is the critical heat flux (CHF) and S is the heated surface area of the heater pin. The local quality is defined as

$$x = \frac{h_z - h_f}{h_{fg}} \quad (2.3)$$

where h_f is the specific enthalpy of saturated liquid, h_{fg} is the latent heat of vaporization, and h_z is the local enthalpy that could be expressed by

$$h_z = h_{in} + \Delta h \quad (2.4)$$

where h_{in} is the inlet enthalpy, and Δh is the increase of enthalpy from the inlet of the test section to the measurement position of surface temperature on the heater pin with thermocouples. The inlet enthalpy and the increasing enthalpy are calculated as

$$h_{in} = h_f - (T_{sat} - T_{in})c_p \quad (2.5)$$

and

$$\Delta h = \frac{Q}{W} \quad (2.6)$$

where T_{sat} is the saturation temperature of liquid, T_{in} is the inlet temperature, c_p is

the specific heat capacity, and W is the water flow rate.

The experimental data of the CHF was obtained in the range of mass flux and inlet temperature. The measurements were made under the boiling two-phase flow condition. The measurement accuracy of the heat flux value was high enough since it was determined from measured voltage and current. In order to keep the uncertainty of the results small, only the experimental data obtained under the condition which met the following requirements were chosen:

- The flow rate was stable during the experiment;
- The inlet temperature fluctuated within 1 K.

2.6. Conclusion

The CHF experimental single pin and bundle pin test section are designed and setup successfully. The new techniques and design have been developed for the single pin and three-pin bundle CHF experiments:

1. Teflon tube and Teflon coated wire spacers.
2. Tight triangular arrangement of the heater pins.
3. Parametric changes of gap size, pitch to diameter ratio and axial pitch of wire spacer.
4. Three point junction method for detection of the surface temperature.

5. Thin thermocouple for detection of the rapid rise of surface temperature of the heat pins.
6. High current electrodes configuration for three-pin bundle.
7. Triangular flow channel with small cross section.

Chapter 3. Experimental study on CHF behavior in single pin with and without wire spacer

3.1. Introduction

Tight lattice with wire spacer can allow us to have a high conversion ratio event in LWRs, particularly BWRs. From the thermal-hydraulic point of view, it is necessary to consider about the coolability of tight lattice core due to its small flow area. On the other hand, CHF is the most important feature of coolability. The fundamental study on CHF in tight lattice core is needed to investigate the CHF behavior with the effects of mass flux, quality and geometric parameter on CHF. Therefore, the purpose of the CHF experiment in single pin test section with and without wire is as follow

- (1) To investigate the CHF behavior in tight lattice core with the effect of mass flux.
- (2) To clarify the effects of wire spacer on CHF behavior in tight lattice core.
- (3) To evaluate the effects of gap size on CHF in tight lattice channel: three difference values of gap size were chosen: 1.1, 1.5 and 2.0 mm
- (4) To investigate the effects of wire pitch on CHF: two difference values of wire pitch were taken into account: 100 and 200 mm.
- (5) To clarify the CHF mechanism in tight lattice core by measuring and analyze the axial position where CHF occurred.

(6) Comparison the experimental data with the CHF correlation

3.2 Experimental Conditions

The experimental parameters and conditions are given in table 3.1 Parameters in the experiment were the existence of the wire spacer, the gap size, δ and the axial coil pitch of the wire, H and the mass flux, G .

In order to investigate the effect of a wire spacer on CHF, two types of CHF experiments for both case of heater pin with and without a wire spacer were performed under the same mass flux condition.

To investigate the effect of gap size on CHF, there are three difference type of experiment with three difference values of gap size: 1.1, 1.5 and 2.0 mm were obtained at the same flow rate condition. From the nuclear reactor design point of view, the experiment with difference gap size value under the same mass flow rate condition is more important than the same mass flux condition. By changing the wire diameter and the inner diameter of the glass tube, the change of gap size values can be obtained.

The effect of wire pitch on CHF was considered with two experiments with two difference values of wire pitch: 100 and 200 mm under the same mass flux condition.

Table 3.1 Experimental condition

Parameter	Run No.1	Run No.2	Run No.3	Run No.4	Run No.5	Run No.6	Run No.7
	with wire	without wire	with wire				
Inner diameter of glass tube, D (mm)	12	12	11	12	11	10.2	11
Gap size, δ (mm)	2.0	2.0	1.5	2.0	1.5	1.1	1.5
Wire diameter, d_w (mm)	1.79	-	1.4	1.79	1.4	1.06	1.4
Wire axial pitch, H (mm)	200	-	200	200	200	200	100
Mass flux, G (kg/(m ² ·s))	400	400	658	-	-	-	-
Mass flow rate, W (kg/s)	-	-	-	0.018	0.018	0.018	0.018
Hydraulic diameter of flow channel, D_{hy} (m)	0.0035	0.004	0.0027	0.0035	0.0027	0.002	0.0027
Pressure, p (MPa)	0.1	0.1	0.1	0.1	0.1	0.1	0.1
Inlet temperature (K)	331-366	331-366	331-366	331-366	331-366	331-366	331-366

3.3. Results and Discussion

3.3.1. Effect of mass flux

The experiment in different mass flux value is needed for clearly understand the CHF behavior in tight lattice core. For that reason, the CHF experiments for heater pin with wire spacer were carried out under different mass flux condition.

Fig.3.1 and Fig.3.2 show the CHF values based on different mass flux. According to Fig.3.1, with the same gap size value of 1.5 mm, the CHF values were plotted as a function of exit vapor quality with three difference values of mass flux: 430, 550 and 658 kg/m²s. It can be seen that at the same exit quality condition, the CHF was enhanced with the increase of mass flux. The CHF values were increase up to 300 kW/m² with the rose of mass flux of 120 kg/m²s. Besides, with the gap size of 2.0 mm, the enhancement of CHF with the increase of mass flux also recorded [Fig.3.2]. Details, the CHF increase nearly two times higher when the mass flux increase from 330 kg/m²s to 400 kg/m²s at the similar exit vapor quality. Therefore, it is clearly seen that the CHF values increased with the increase of the mass flux. With the increase of the mass flux, the bubble detachment from the heated surface was enhanced. On the other hand, the increase of mass flux leads to the rise of flow velocity that was related with higher heat transfer coefficient. Therefore, the CHF values increased with the mass flux.

Fig.3.1 and 3.2 also shows that the difference in CHF values between two dissimilar of mass flux were clearer in smaller values of mass flux and also in larger flow area.

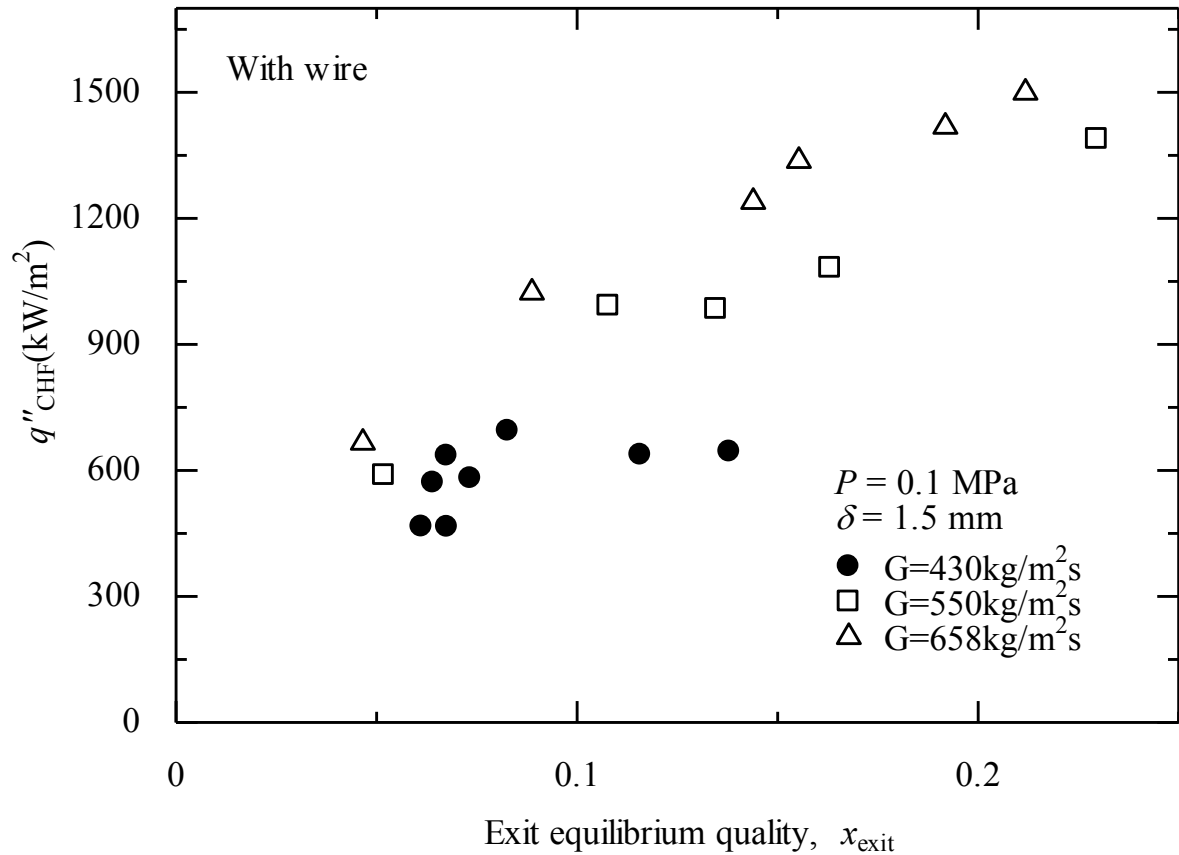


Fig.3.1 Effect of mass flux on CHF (gap size, $\delta = 1.5 \text{ mm}$)

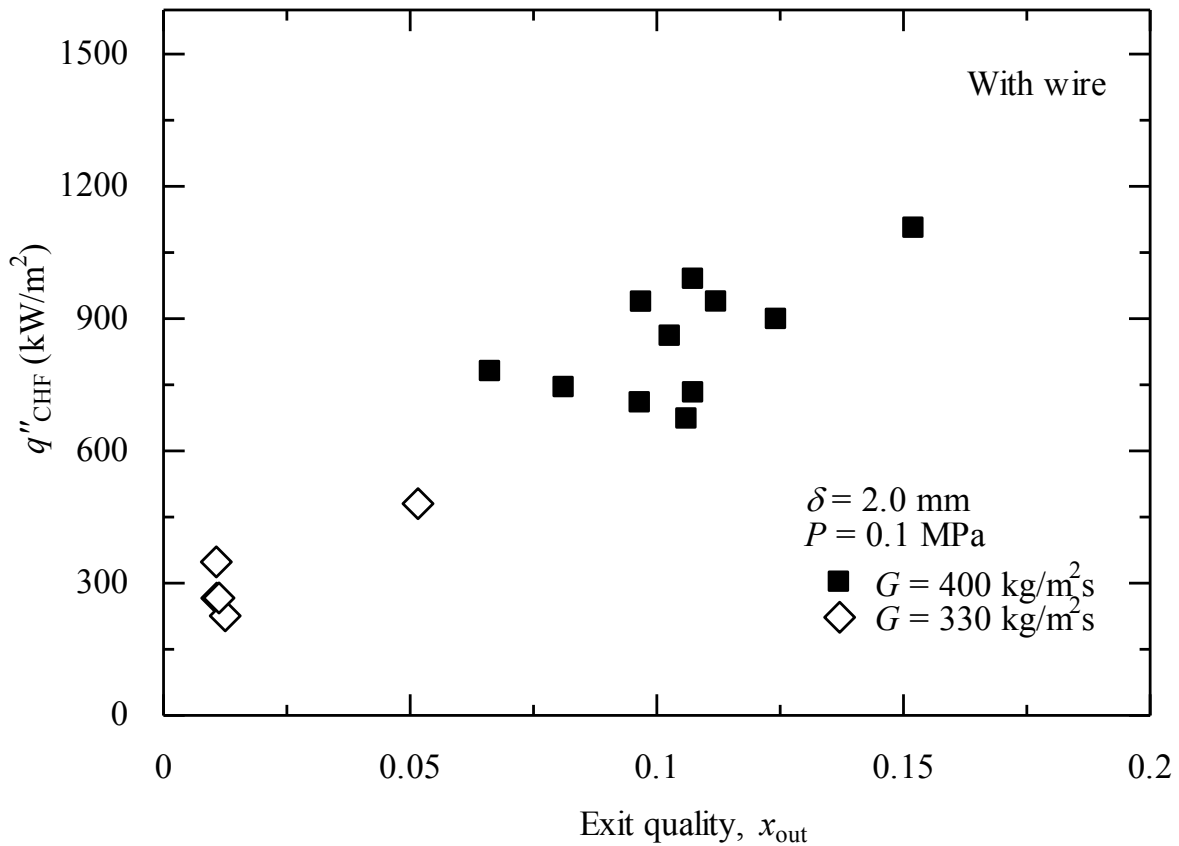


Fig.3.2 Effect of mass flux on CHF (gap size, $\delta = 2.0$ mm)

3.3.2 Effect of Wire Spacer

Fig. 3.2 shows the comparison of the CHF values of single pin channels between with the wire spacer and without the wire spacer. The experimental data were obtained at the same mass flux condition of 400 kg/m²s and pressure of 0.1 MPa. It was found that, the CHF values in both types of heater pin decreased with the decrease of the inlet equilibrium steam quality, x_{in} .

Besides, at the similar inlet quality values, the CHF values were higher in case of heater pin with the wire spacer than that in case of heater pin without the wire spacer. In more details, the CHF improved up to 25% in the case of heater pin with wire spacer compared with that without wire spacer. On the other hand, the difference in the CHF values between heater pin with and without wire spacer was larger in qualities ranged from -0.08 to -0.04 compared with the difference of CHF values in qualities region higher than -0.04.

The promotion of CHF in the case of heater pin with wire spacer can be explained by the enhancement of bubble removal from the heated surface due to the effect of wire and spiral flow. Moreover, the single pin experiments were obtained in the annulus channel, thus there were two parallel liquid films which flow along the heated surface and the inner surface of the flow channel. By using the wire spacer, there is an effect of the water film along the inner surface of the channel (glass tube) on CHF values. In detail, the vapor velocity became higher under the effect of wire spacer and spiral flow. Therefore, it may disturb the water film which flow along the inner surface of the channel and bring the droplets to the heated surface, which cause of increasing of droplet deposition rate then lead to the improvement of CHF [Fig.3.3].

Compared with the work of Cheng and Müller [7] [Fig.3.4], it clearly seen that the CHF values of wire type were still higher than those without wire type even

if the inlet equilibrium steam quality was close to zero. Details, the experimental data of Cheng and Muller were obtained at the range of inlet quality from -1.2 to -0.3. It also showed the improvement of CHF by wire spacer at the inlet quality region from -1.2 to -0.9. However, with the inlet quality ranged from -0.9 to -0.3 the CHF in the case of wire spacer were similar to that in the case of without wire spacer. Nevertheless, by analyzing the experimental data in present study, it was found that the CHF in the case of heater pin with wire spacer still higher than that without wire spacer even at the inlet vapor quality close to zero.

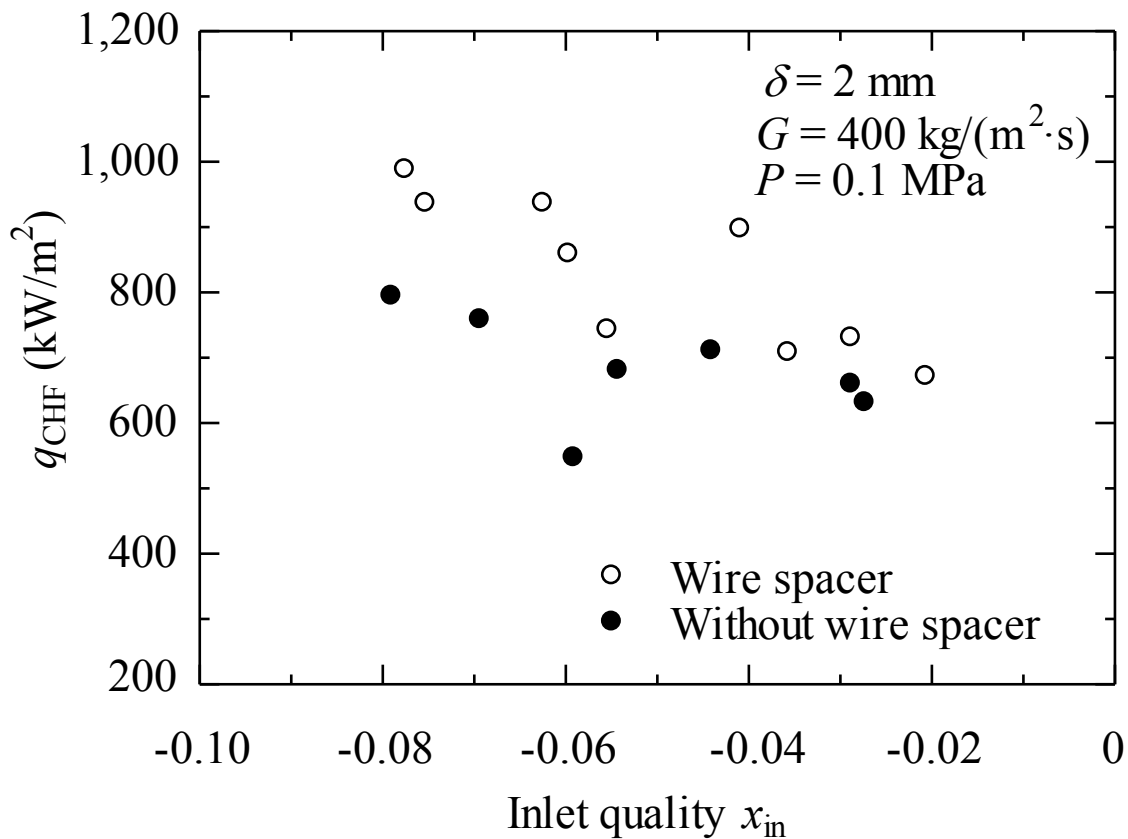


Fig. 3.2 Critical heat flux base on inlet condition.

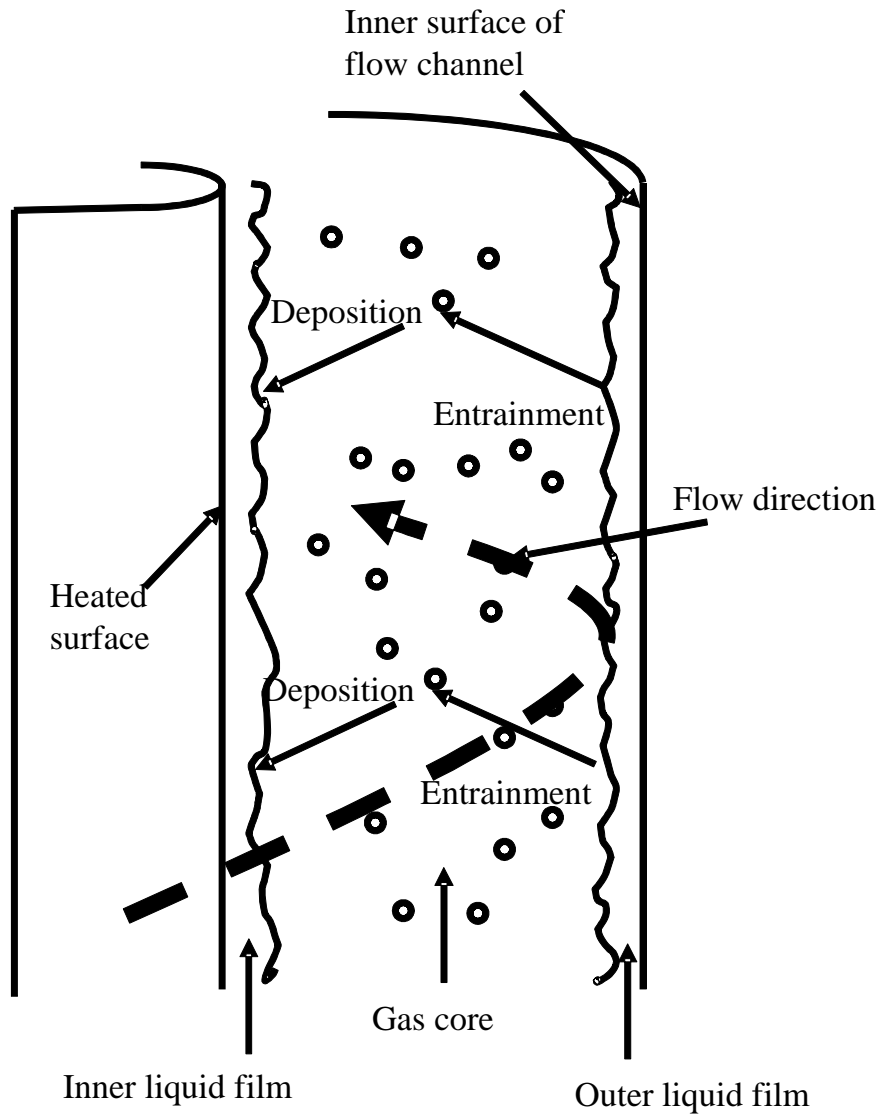


Fig.3.3 Effect of wire on the entrainment and deposition rate

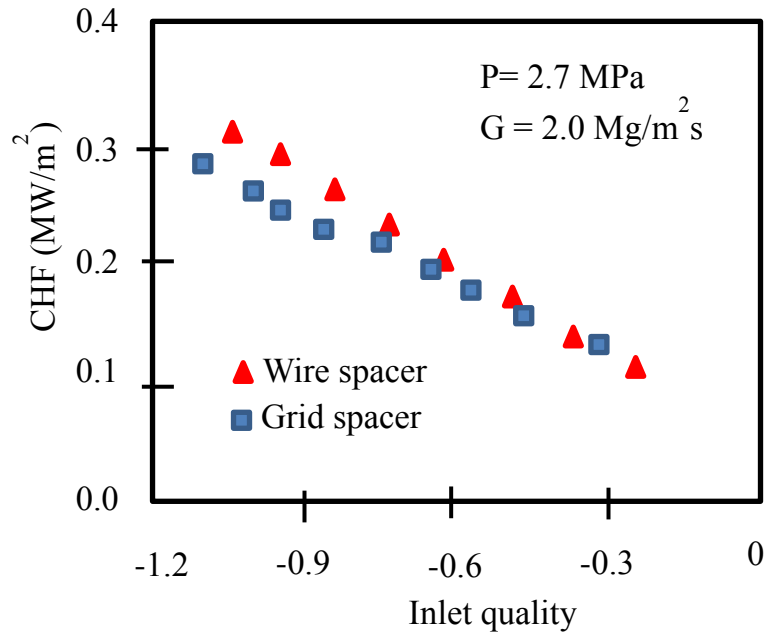


Fig. 3.4 Critical heat flux base on inlet condition[7] .

3.3.3 Effect of gap size and wire pitch

In furtherance of the investigation of CHF behavior under the effect of the wire spacer, the change in wire spacer size is needed. Therefore, the CHF experiment with different value of δ and H was performed to deal with such kind of study. From reactor design point of view, the consideration of the same water flow rate rather than the same mass flux is needed to be able to keep the best coolability for difference core design. Thus, these experiments were performed under the same flow rate condition of 0.018 kg/s and also at the constant pressure condition of 0.1 MPa.

Fig.3.5 shows the comparison of the CHF values between three different values of gap size: 1.1, 1.5 and 2.0 mm at the same flow rate. It can be seen that, at the same local quality, x_z , the CHF values were enhanced with the decrease of gap size under the same flow rate condition. In more detail, the CHF values were higher in case of smaller gap size and it was the highest in case of the smallest gap size. The channel with the gap size of 1.1 mm could reach the CHF values nearly 900 kW/m². That is because the channel which has the smallest flow area has the highest mass flux at the same water mass flow rate which leads to the enhancement of CHF values. On the other hand, as mentioned above, the disturbance of wire spacer also has a larger effect of the outer liquid film in the case of flow channel with smaller gap size, compared with that in bigger gap size values. Besides, with the smaller gap size, the droplet concentration in the vapor phase also higher compared with it in case of bigger gap size. This is another reason which contributed for the increase of CHF values.

According to Fig.3.5, also based on the disturbance of wire spacer the experiment with smaller gap size could reach higher CHF values and also could go to the higher local quality, x_z . In the case of bigger gap size ($\delta = 2.0$ mm), the CHF value tended to decrease with the increase of quality. However, in case of flow channel with small gap size, the CHF values were nearly constant value or slightly increase with the increasing of quality.

Moreover, the CHF were sharply increased up to 100 % by reducing the gap size values from 2.0 mm to 1.1 mm. Therefore, it is evident that the effect of wire spacer on CHF was stronger in the case of small gap size. Besides, the cool wall effect was also higher in the case of small gap size.

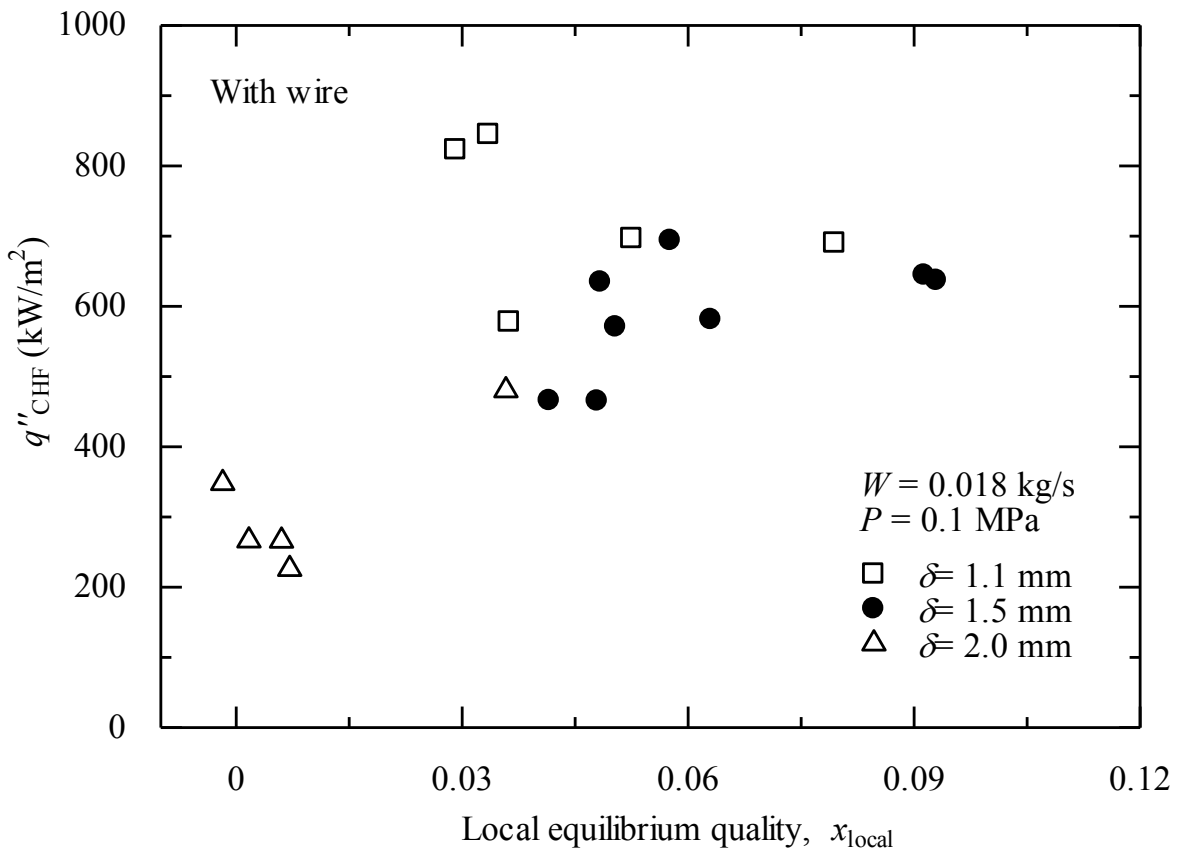


Fig. 3.5 Critical heat flux of three different values of gap size.

Fig.3.6 illustrates the CHF results in two different values of wire pitch, H of 100 and 200 mm. The experiments were obtained at the constant flow rate of 0.018 kg/s and pressure of 0.1 MPa. It can be seen that, the CHF values were nearly the

same between two different values of wire pitch. It can be explained that there were two flow channels with two different values of wire pitch, velocity was the same. Since the velocity was the same, the mass flux was the same. Therefore, it is clear that, the axial pitch did not have a large influence on the CHF.

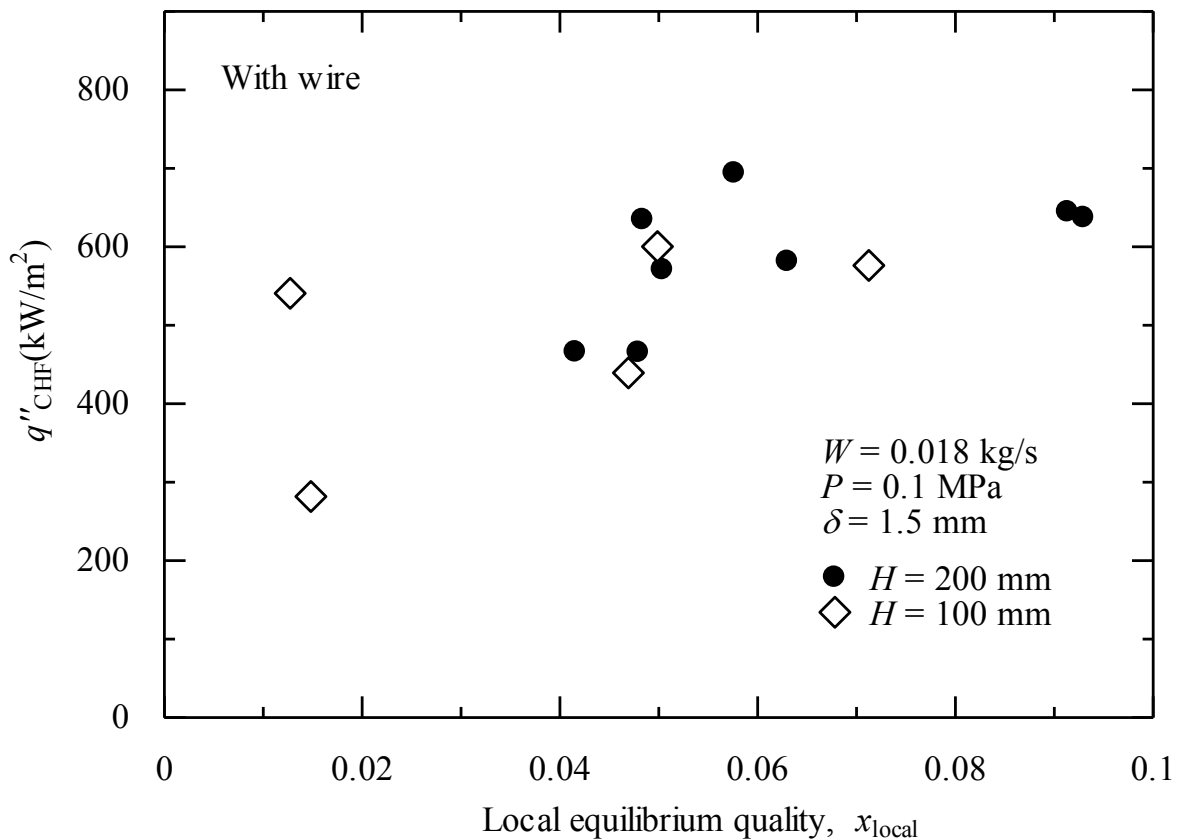


Fig. 3.6 Critical heat flux of two different values of wire pitch, H .

3.3.4 Axial Position of CHF

The relation between the CHF values and the heated length to the position of arriving at CHF is shown in Fig.3.7. At the same mass flow rate of 0.018 kg/s, the

CHF occurred mostly in the downstream of the flow channel which related to the dryout phenomenon.

Fig.3.7 also shows the comparison of CHF position among three different values of gap size. In case of gap size of 1.5 mm and 2.0 mm, the CHF positions were located at the position from 0.3 to 0.4 m downstream from the upstream of the heater pin, which were mainly at the downstream of flow channel. As mention in chapter 1, the CHF which occurs at the downstream of the flow channel is based on the dryout phenomenon. Therefore, the CHF values which were obtained with a gap size of 1.5 and 2.0 mm were principally caused by liquid film dry-out.

On the other hand, with the smallest flow area which had the gap size of 1.1 mm, with the increase of heat flux values, the CHF positions were shifted from the downstream to the upstream of the flow channel. In details, with the CHF values of nearly equal 700 kW/m^2 the CHF was occurred at the position from 0.3 to 0.4 m downstream from the upstream of the flow channel. Nevertheless, when the CHF values increase to nearly equal 900 kW/m^2 , the CHF positions were shifted to the middle and also very upstream of flow channel, which related to the DNB phenomenon. In the channel with the gap size of 1.1 mm, due to the very small flow area, at the high heat flux values the bubbles were easy formed with each other to become the larger bubbles then covered the heated surface which related with the DNB mechanism. Therefore, under the high heat flux and mass flux condition in the

small gap size value, there were the possibility of CHF occurring based on the DNB mechanism. In summary, the CHF positions changed slightly with different values of the gap size. The CHF positions tended to move from downstream to the upstream of the flow channel due to the decrease of gap size. In other words, the CHF mechanism may change from dryout phenomenon to DNB phenomenon by reducing the gap size values under the same flow rate condition.

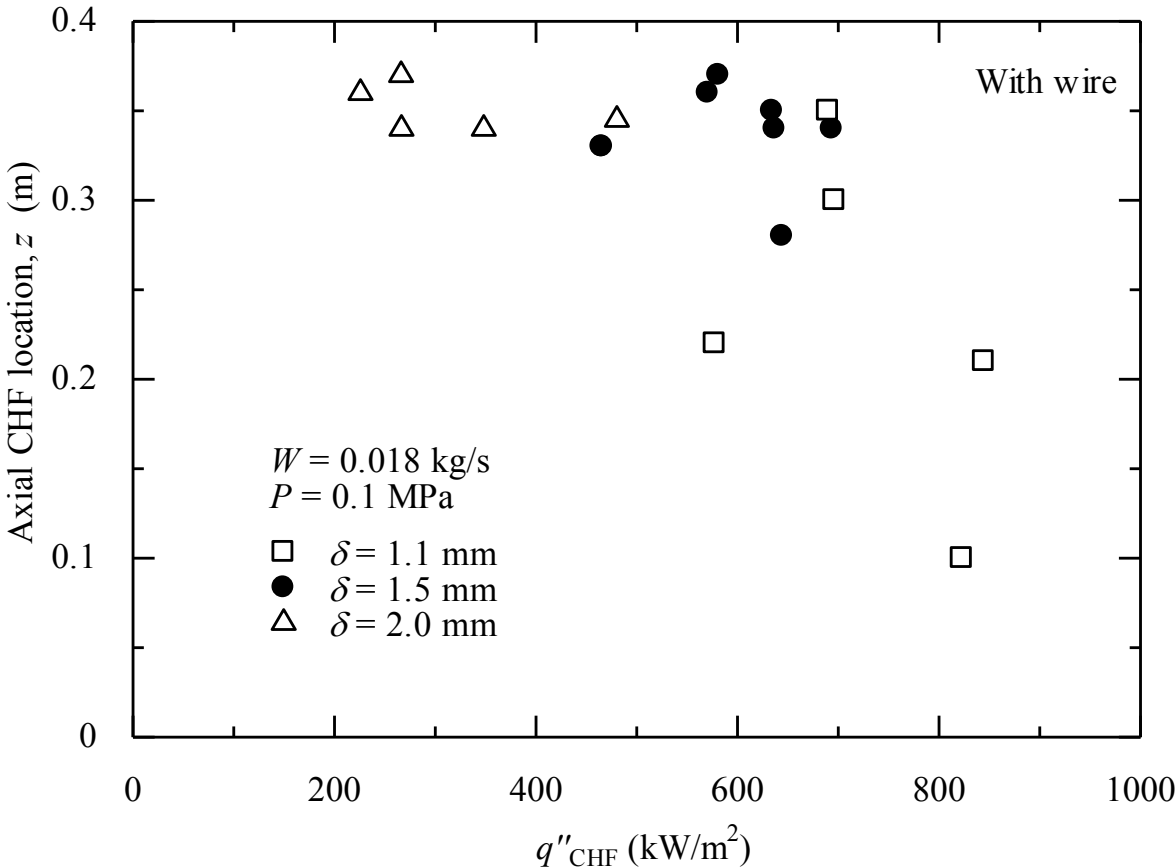


Fig. 3.7 Critical heat flux base on the heated length.

Fig.3.8 show the position where CHF occurred in both cases of heater pin with and without wire spacer under the same mass flux of $650 \text{ kg/m}^2\text{s}$ and gap size of 1.5 mm . It is clear that at the same position, the CHF in the case of heater pin with wire spacer were higher than that without wire spacer. On the other hand, with the CHF nearly equal 1000 kW/m^2 , the CHF position in the case of heater pin without wire spacer was 0.1 m downstream from the upstream of the flow channel which related with the DNB mechanism. Nevertheless, also with the CHF value of 1000 kW/m^2 , the CHF position in the case of heater pin with wire spacer was located 0.37 m downstream from the upstream of the heated length, which was occurred based on the liquid film dryout mechanism. Therefore, it can be seen that with the same heat flux values, the CHF positions were shifted to the downstream of the flow channel under the effect of wire spacer. That was also the reason why the CHF in the case of heater pin without wire spacer were mostly obtained at the middle or near the upstream of the flow channel under the high mass flux condition while the CHF in the case of heater pin with wire spacer were mostly recorded at the downstream of the flow channel.

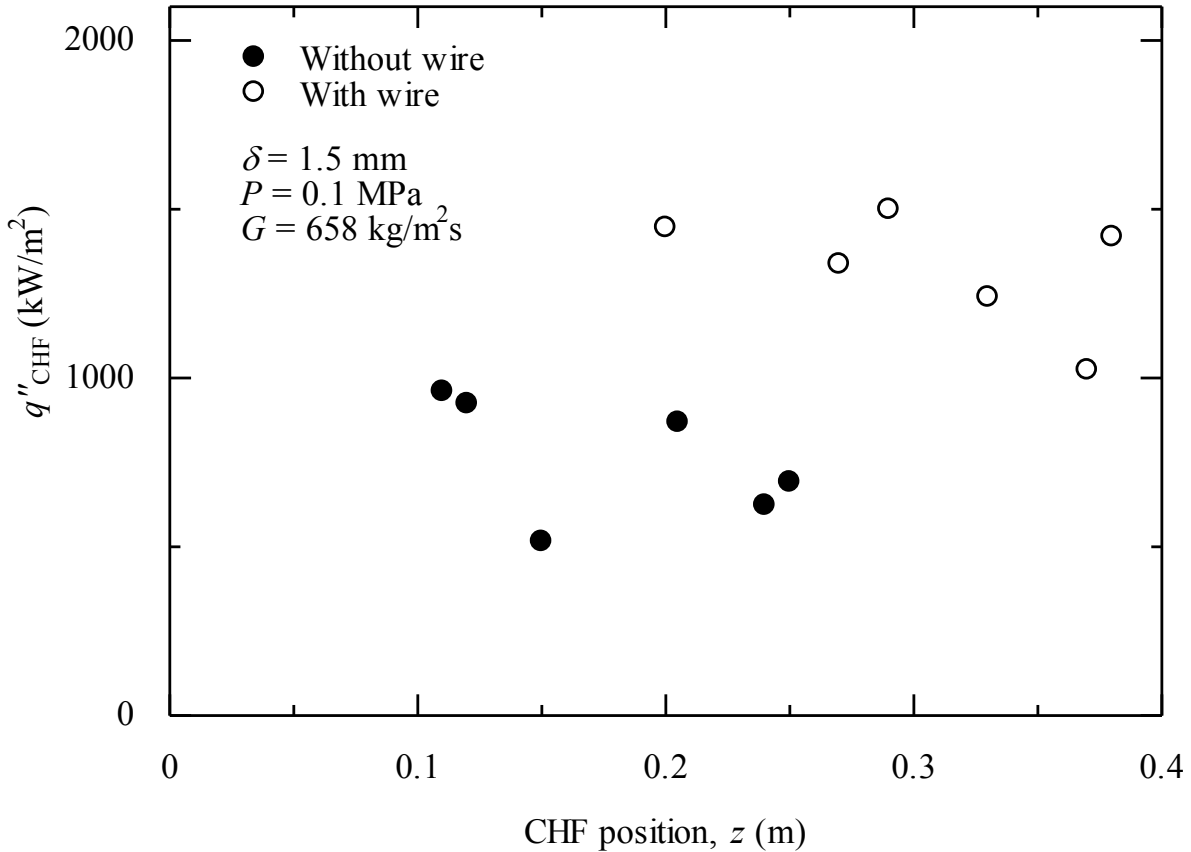


Fig.3.8. CHF position for heater pin with and without wire spacer

3.4. Comparison with previous study and prediction methods

Various CHF experiments were obtained in previous study. However, the single pin experiment with the special experimental condition at mass flux of $400 \text{ kg/m}^2\text{s}$ and pressure of 0.1 MPa and with a narrow gap width, only the study of Haas [18] can be used as a comparison.

Fig.3.9 shows the comparison between the CHF experimental data of single pin test section without wire spacer of present study with Haas [18] results. It can be

seen that at the same condition mass flux of $400 \text{ kg/m}^2\text{s}$ and pressure of 0.1 MPa , the CHF data for heater pin without wire spacer in present study had the same tendency in comparison with that in previous study. Details, the CHF values were increase with the increase of exit quality in the channel with narrow gap width and at the high quality condition. The CHF data for heater pin without wire spacer in present study close with that in previous study of Haas[18].

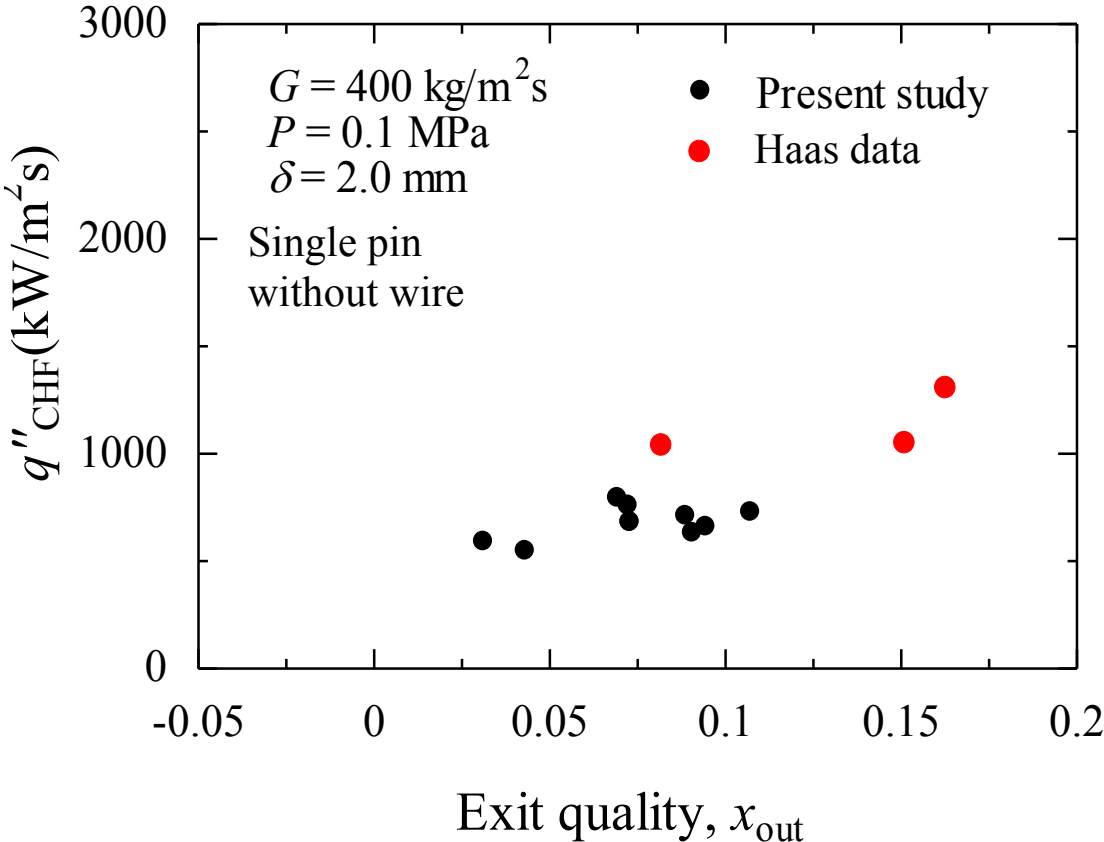


Fig.3.9 Comparison between CHF experimental data without wire spacer with Haas's results[18]

Beside, in the case of prediction method, Doerffer et al. proposed the CHF prediction methods for annuli with inside heating [11]. The prediction methods were based on the 1986 CHF look-up table [15]. Base on their explanation, the critical quality, gap size and pressure are three main factors that have the strongest influence on the CHF ratio between annuli channel and round tube channel. Thus, the authors developed a correlation based on three main factors as mentioned above. In this correlation, the CHF values in the 1986 look-up table of Grovneveld et al.(1986) were multiplied with three correlation factors representing for critical quality, gap size and pressure. The CHF correlation for the annuli channel is

$$q_{CHFAn,conc} = q_{CHFd=8} k_x k_\delta k_p \quad (3.1)$$

where $q_{CHFd=8}$ is the CHF values for a tube with the diameter of 8 mm from the 1986 CHF look-up table. However, in this study, we used the Doerffer et al.(1994) correlation [Eq.3.1] with the CHF values derived from the 2006 look-up table [14] for higher accuracy. k_x , k_δ , k_p are three factors representing the effect of quality, gap size and pressure, respectively. The three factors are calculated by

$$k_x = 0.859 - 16.179x^{1.5} + 15.6x^2 - 7.195x^2 \ln x \quad (3.2)$$

$$k_\delta = 0.2872 + 1.209\delta^2 - 1.156\delta^{2.5} + 0.2873\delta^3 \quad (3.3)$$

$$k_p = 0.9 \quad (3.4)$$

where x is the quality ($x > 0.025$), δ is the gap size ($\delta < 4.26$ mm), p is the pressure ($p < 3.30$ MPa).

Fig.3.10 shows the comparison between CHF results for heater pin with the wire spacer and the calculated values of Eq.3.1 using the 2006 look-up table [14]. It can be seen that the experimental values of CHF for heater pin with wire spacer were higher than the calculated values of CHF for heater pin without wire. Therefore, it is evident that the CHF values were enhanced by the effect of the wire spacer.

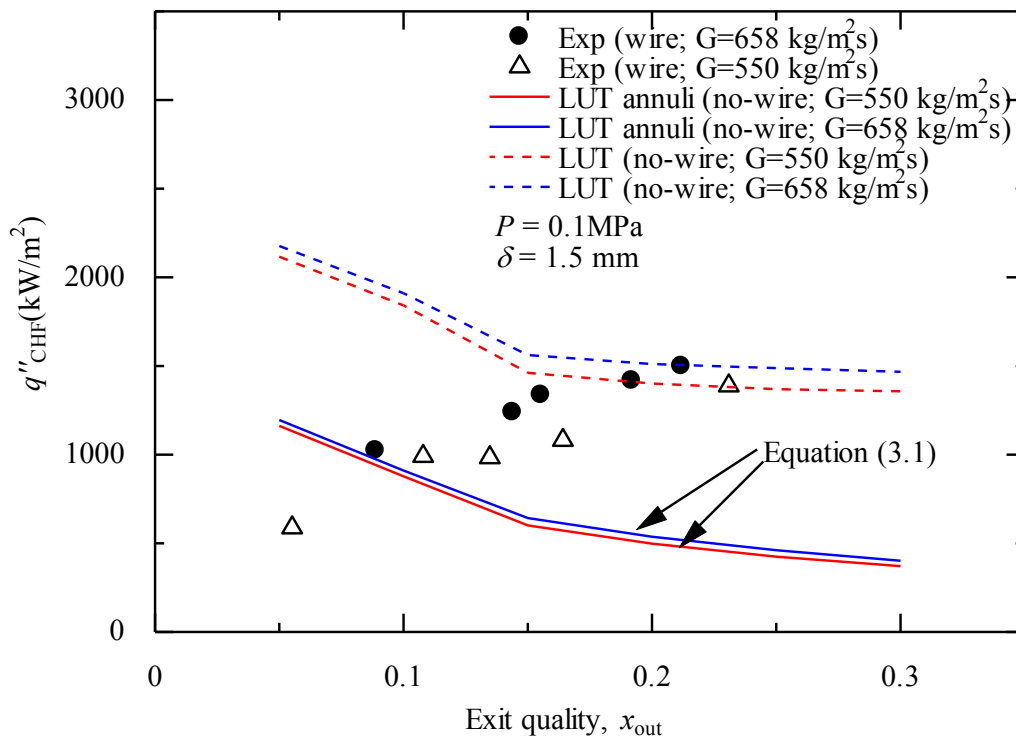


Fig.3.10 Comparison of experimental results of wire type with the calculated results of non-wire type using concentric annuli correlation of Doerffer et al.(1994) for the 2006 CHF look-up table of Groeneveld et al.(2007)

Fig.3.11 compares the experimental results obtained in the flow channel with a wire spacer and without a wire spacer with the 2006 CHF look-up table [14] which is calculated Eq.3.1 for annuli channel. The ratio of the measured CHF to the calculated CHF is obtained at the same pressure, mass flux and exit vapor quality. As shown in Fig.3.11, the CHF values in case of heater pin without wire spacer become closer to the calculated values in high quality region. On the other hand, the different values between CHF values of heater pin with a wire spacer and the calculated CHF values without a wire spacer have an upward trend with the increase of the exit vapor quality.

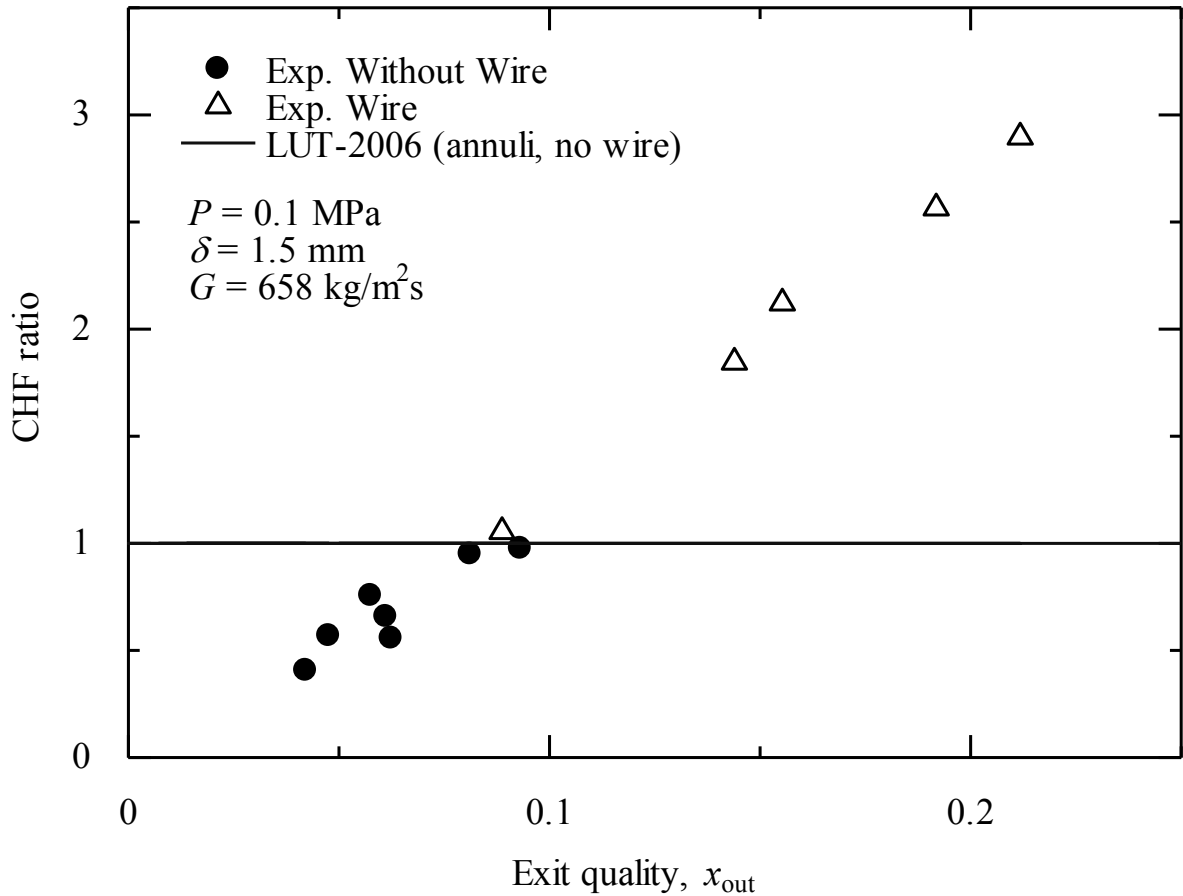


Fig.3.11 CHF ratio of experimental results to calculated results obtained from Eq.3.1

The correlation shown in Eq.3.1 is the annuli correlation. However, there are two type of annuli channel which are concentric annuli and eccentric annuli [Fig.3.12].

In this study, the heater pin was located at the center of the flow channel which was a concentric annuli channel, so that the comparison between experimental data and the calculated values for the rod-centered case is needed. In

the study of Doerffer et al.(1994), the authors also proposed the CHF correlation for the rod-centered approach (concentric annuli).

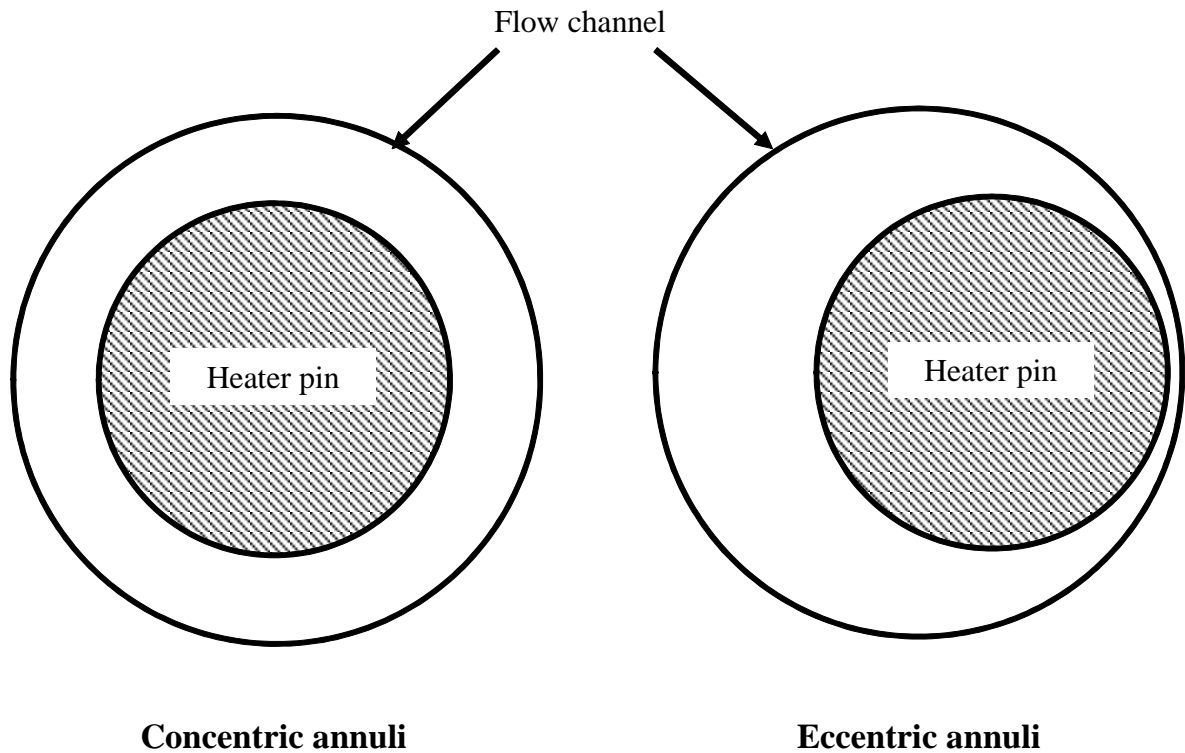


Fig.3.12 Concentric and eccentric annuli

According to this correlation, the vapor quality in annular channel is calculated by

$$x' = x + \Delta x \quad (3.5)$$

where x is the quality that given from Eq.2.3. The calculation for Δx is given by

$$\Delta x = 0.658 - 0.33 p^{0.428} G^{0.108} \delta^{-0.453} D_{he}^{0.37} \quad (3.6)$$

where D_{he} is the heated equivalent diameter in centimeters, and G is the mass flux in $\text{Mg/m}^2\text{s}$. Finally, the CHF in an annular channel is obtained by

$$q_{CHFAn}(P, G, x) = q_{CHFd=8}(P, G, x') \quad (3.7)$$

Following Fig.3.13, the calculated values were obtained by CHF correlation for the rod-centered approach (Doerffer et al.,1994) were closer to the experimental results, compared with the concentric annuli correlation (Doerffer et al.,1994).

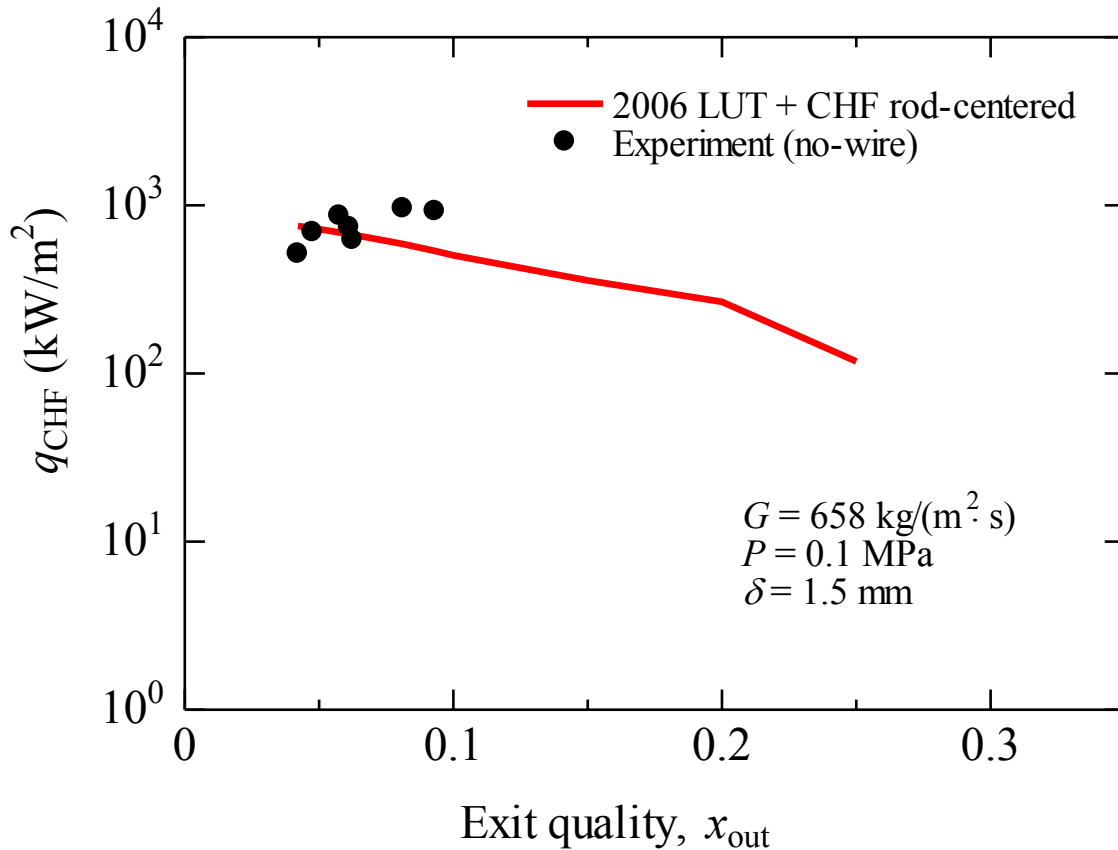


Fig.3.13. Comparison of experimental results with the calculated results using CHF correlation for the rod-centered approach of Doerffer et al.(1994) for the 2006 CHF look-up table of Groeneveld et al.(2007)

3.5. Conclusion

The CHF phenomena for the tight lattice fuel arrangement with the effect of wire spacer were investigated by mean of the experiment for single fuel pin with and without wire spacer and three difference values of gap size of 1.1, 1.5, 2.0 mm.

Besides, the effect of wire pitch was made clear by the experiment with two dissimilar wire pitch value of 100 mm and 200 mm. The conclusions are as follows:

- (1) The CHF values increased with the rise of mass flux under the same geometric and quality condition because of the increasing of mass flux lead to the change in heat transfer coefficient of the heater pin.
- (2) The CHF in case of heater pin with circular shape wire was enhanced up to 25% compared with it in case of without wire space under the same flow condition. Therefore, the coolability or heat removability was enhanced by the existence of the wire spacer and spiral flow.
- (3) With the same flow rate condition, the CHF values can be increased up to 100% with the decrease of gap size. Therefore, the flow channel with smaller gap size a higher coolability compared with the flow channel with larger gap size.
- (4) The change in a pitch of wire, H , with two difference values of 100 mm and 200 mm did not have a large influence on the CHF if the mass flux was kept constant. The experiment data was nearly the same value even with two different cases of wire pitch.
- (5) The CHF in boiling two-phase flow was mostly caused by liquid film dry-out. Nevertheless, the CHF positions changed slightly with different values of the gap size. The CHF positions tended to move from downstream to the upstream of the flow channel due to the decrease of gap size. In other words, the CHF

mechanism may change from dryout phenomenon to DNB phenomenon by reducing the gap size values under the same flow rate condition.

- (6) Directly comparison with the CHF look-up tables of Groeneveld et al. (2007) had a big different with the test results because of the different in geometric condition. In case of the CHF look-up tables Groeneveld et al. (2007) the CHF was performed in a round tube which was different with the CHF in annuli flow as shown in our experiment. The experimental values of single pin without wire spacer agreed well with the predicted method by using the rod-centered approach method of Doerffer et al.(1994). It also shown the predicted values of CHF in case of channel without wire spacer were lower than the experimental data of channel with wire spacer. That agreed with the experimental results.

Chapter 4. Experimental study on CHF behavior in bundle pin with and without wire spacer

4.1. Introduction

To design the new type of high conversion boiling water reactor, the study on CHF in tight lattice core is needed. The single pin experiment was created as a first step to evaluate the CHF behavior in tight lattice channel under the effect of single wire spacer. In the practical reactor core, there are many heater pin and wire spacer, the flow behavior is much difference from the flow behavior in single pin and wire channel. Therefore, to evaluate the coolability of the tight lattice core with wire spacer, it is necessary to investigate the effect of wire spacer on CHF in tight rod bundle by means of CHF experiment in three-pin bundle test section with wire spacer. The purpose of the CHF experiment in three-pin bundle test section with and without wire is as follow

- (1) To investigate the effect of mass flux on CHF in tight rod bundle with wire spacer.
- (2) To evaluate the effect of wire spacer on CHF in tight rod bundle with wire spacer.
- (3) To investigate the effect of pitch to diameter ratio on CHF at the constant mass flow rate, two difference values of pitch to diameter ratio were chosen: 1.10 and 1.18.
- (4) To investigate the effect of pitch to diameter ratio on CHF at the constant mass flux value.

- (5) To clarify the effect of wire pitch on CHF behavior in tight rod bundle with two difference values of wire pitch: 100 mm and 200 mm.
- (6) To evaluate the CHF mechanism in tight lattice rod bundle by measuring the CHF position.
- (7) Comparison the experimental data with the prediction correlation.

4.2 Experimental Conditions

The experimental parameters and conditions are given in Table 4.1.

From the thermal-hydraulic point of view, the effect of a wire spacer on CHF in tight rod bundle at constant mass flux is interesting. Thus, the CHF experiments for both case of heater pin with and without a wire spacer were conducted under the same mass flux condition.

On the other hand, from the viewpoint of the design of the practical reactor, it is important to know how the coolability changes with the change of core tightness under constant mass flow rate. Thus, the experiments were conducted for two different values of p/d at the same flow rate condition.

Also, the experiments for different values of wire pitch were performed to investigate the effect of wire pitch on CHF.

Table 4.1 Experimental condition.

Parameter	Run No.1	Run No.2	Run No.3	Run No.4	Run No.4
	Without Wire	Wire	Wire	Wire	Wire
Heater pin diameter, d (mm)	4.57				
pitch, p (mm)	5.4				5.0
Pitch to diameter ratio, p/d	1.18				1.1
Wire diameter, d_w (mm)	-	0.76			0.4
Wire axial pitch, H (mm)	-	200	100	200	
Mass flux, G (kg/(m ² ·s))	435		-	435	-
Mass flow rate, W (kg/s)	-		0.0208	-	0.0208
Hydraulic diameter of flow channel, D_{hy} (m)	0.0032	0.0029			0.0021
Pressure, p (MPa)	0.1				
Inlet temperature (K)	343-365				

4.3. Results and discussion

4.3.1. Effect of mass flux

The effect of mass flux on CHF in tight lattice core was made clear by performing two experiments for the constant values of pitch to diameter ratio of 1.18 at mass flux of 280 kg/m²s and 435 kg/m²s.

Fig.4.1 shows the comparison between CHF values for dissimilar mass flux values. It can be seen that the CHF tendency was the same even with the change of mass flux from 280 kg/m²s to 435 kg/m²s. Nevertheless, at the same local quality condition the CHF values were promoted up to 200% by increasing the mass flux values from 280 kg/m²s to 435 kg/m²s.

The same results were also plotted as a function of inlet enthalpy as shown in Fig.4.2. It can be seen that at the same inlet enthalpy and pitch to diameter condition, the CHF values in three-pin bundle with wire spacer with the mass flux of 435 kg/m²s were higher than that with the mass flux of 280 kg/m²s.

Therefore, it is evident that the mass flux has a large influence on the enhancement of CHF. By increasing the mass flux, the turbulent rate is increased, thus it also improved the bubbles transport from the heated surface and lead to the increase of CHF values.

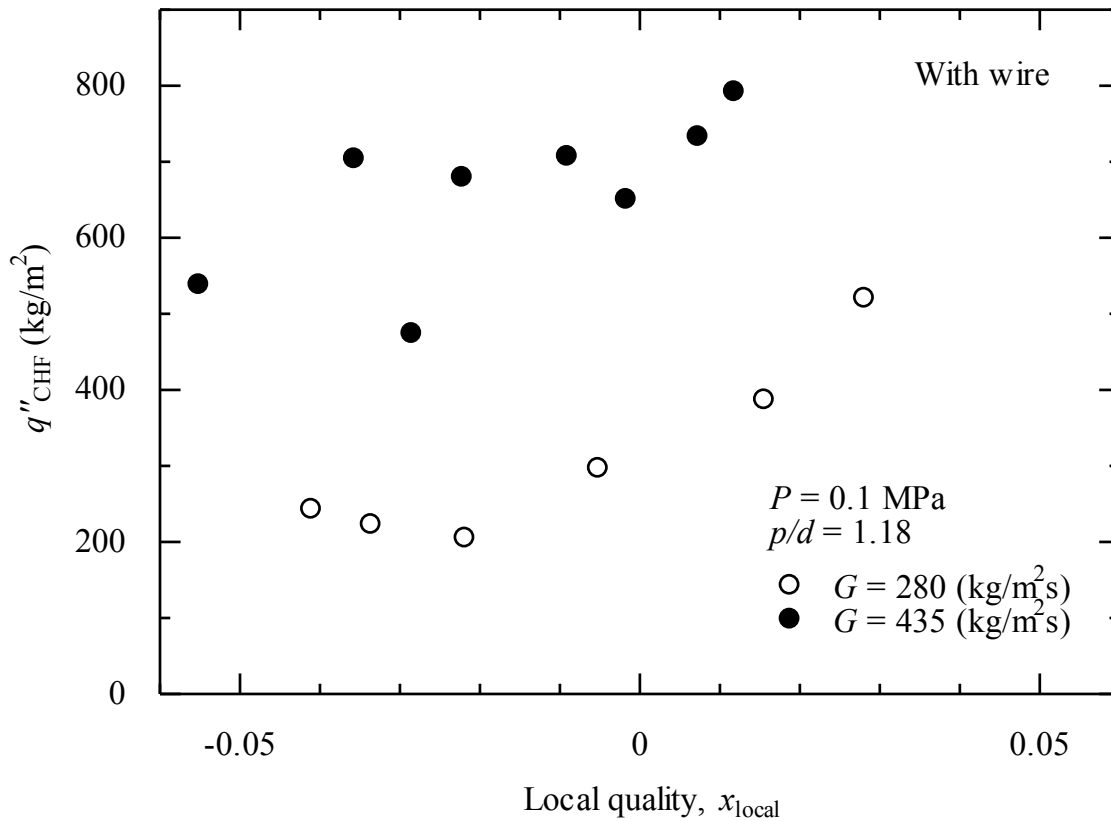


Fig.4.1 Effect of mass flux on CHF in tight lattice bundle

In comparison with the effect of mass flux on CHF for single pin with wire spacer, the effect of mass flux on the promotion of CHF in bundle pin experiment was based on the same mechanism with that in single pin experiment. Moreover, the effect of mass flux on CHF in three-pin bundle was stronger than that in single pin channel. As discussed above, the enhancement of CHF with the increase of mass flux was based on the turbulent. On the other hand, in three-pin bundle flow channel, due to the effect of three wire spacers, the turbulent mixing was much higher than that in single pin channel which was affected by only single wire spacer. Thus, in

the bundle pin channel, the effect of mass flux on CHF was clearer in comparison with that in single pin channel.

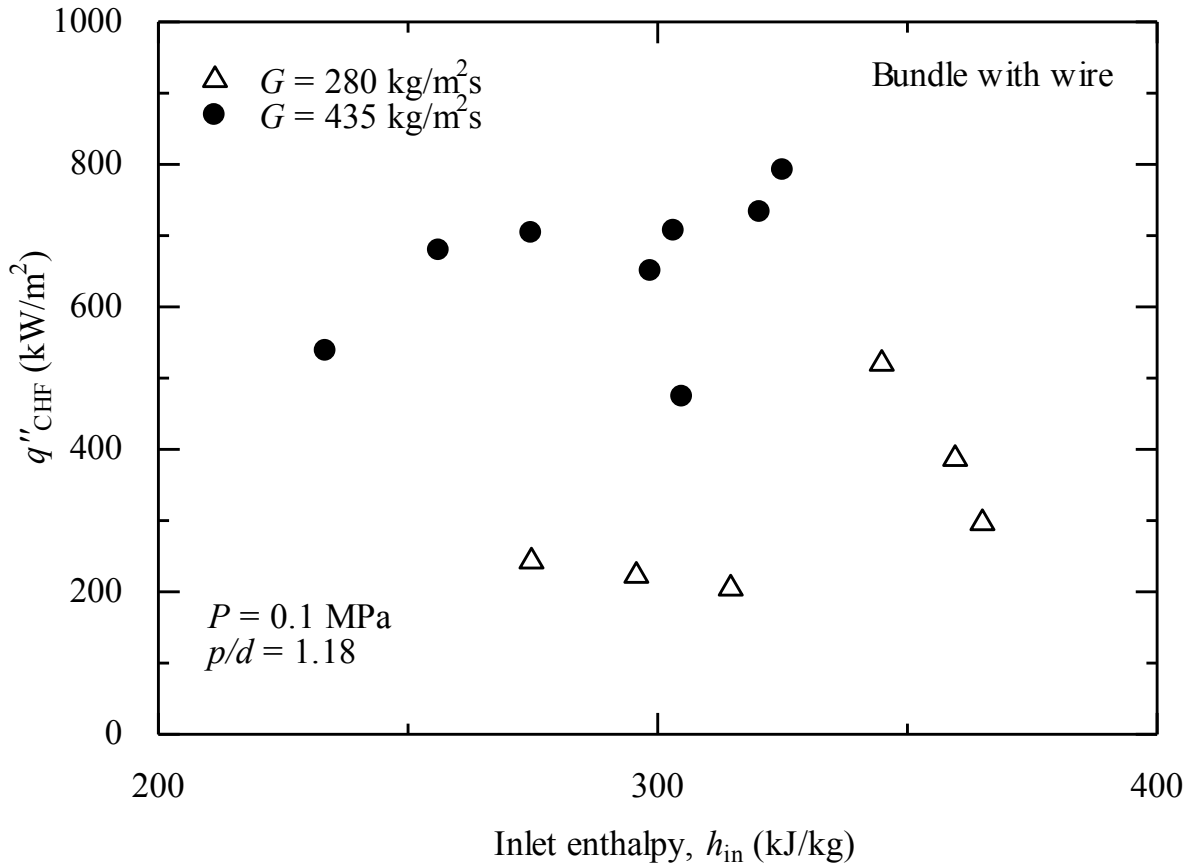


Fig.4.2 CHF in three-pin bundle with two difference mass flux values as a function of inlet enthalpy

4.3.2 Effect of wire spacer

The effect of wire spacer on the enhancement of CHF was made clear through Fig.4.3. The experiments were performed with the three-pin bundle which

had a pitch to diameter ratio of 1.18 at the constant pressure of 0.1 MPa and mass flux of 435 kg/m²s.

The CHF values in a three-pins bundle with wire spacer were higher compared with it in the case of bundle without wire spacer. The difference in CHF value was larger at the quality region from $x_{\text{local}} = -0.06$ to 0 than at the quality region from $x_{\text{local}} = 0$ to 0.02. The CHF was enhanced by up to 50% with wire spacer compared with it without wire spacer under the constant mass flux condition of 435 kg/m²s. The enhancement was more significant at the low quality region. Therefore, the coolability in tight lattice core could be optimized by using wire spacer. The reason for the enhancement can be explained by divide into two part base on the local vapor quality region.

In the range of the quality from -0.06 to 0, the enhancement of CHF was very clear, which was possibly caused by the increase of disturbance by wire spacer. In the low quality region, the turbulent mixing caused by the disturbance became higher, which enhanced the bubble removal from the heated surfaces. As a result, CHF increased. The existence of the wire spacer induced a spiral flow, which increased coolant velocity. Therefore, the CHF increased in comparison with the case of straight flow.

Under the effect of wire spacer, the coolant flow along the heated rod with the swirling motion. In more details, the wire spacer was wrapped from the bottom to the top of the heater pin with the clockwise direction. Along each heater pin, under the effect of wire spacer, the swirling flow motion would flow with the clockwise direction. Therefore, from the bottom view, inside the subchannel of three-pin bundle, the coolant would flow with the counter clockwise direction. Thus, the centrifugal force may occur at the interior subchannel. The centrifugal as a result of swirling flow also have an effect on the promotion of CHF values. Details the centrifugal force which is appeared in the gas core due to the effect of wire spacer and swirling flow has an effect on the liquid droplets in the gas core. Under the effect of centrifugal force, the radial velocity of the droplets in the gas code are enhanced, thus the droplets tend to wet again the heated surface, in other word the deposition rate is enhanced [Fig.4.4] . The result is the improvement of CHF values.

Besides, in the range of positive local vapor quality, the CHF was nearly the same in the cases of bundle pins with wire and without wire spacer. It has been known that the liquid film flow becomes thinner compared with it in the low quality region in the high quality region. In the condition of the thin liquid film flow, the wire spacer may break the liquid film flow, and consequently the dry-out more easily occur. Since the boiling heat transfer rate become higher in the high quality

region than in low quality region, the disturbances of the bubbles become higher and tend to break the liquid film, which leads to the decrease of CHF values.

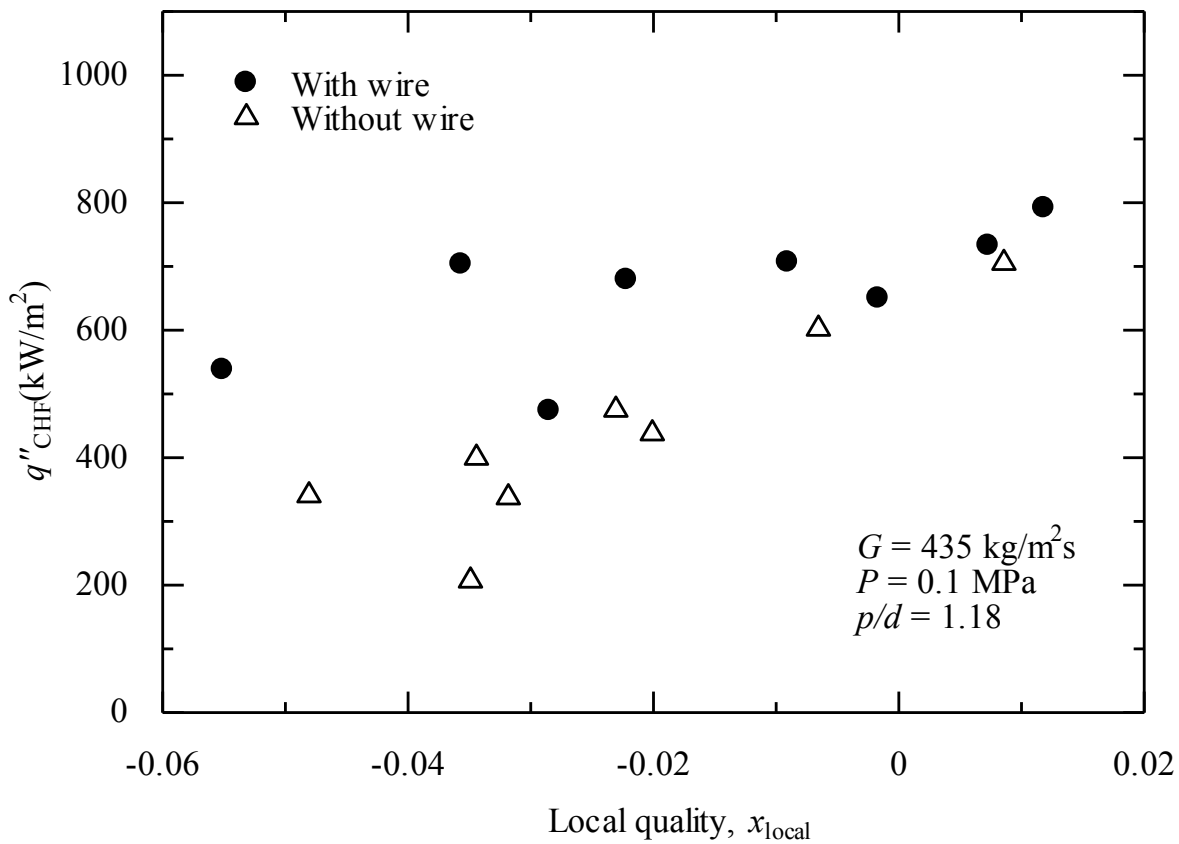


Fig. 4.3 Critical heat flux in bundle with and without wire spacer.

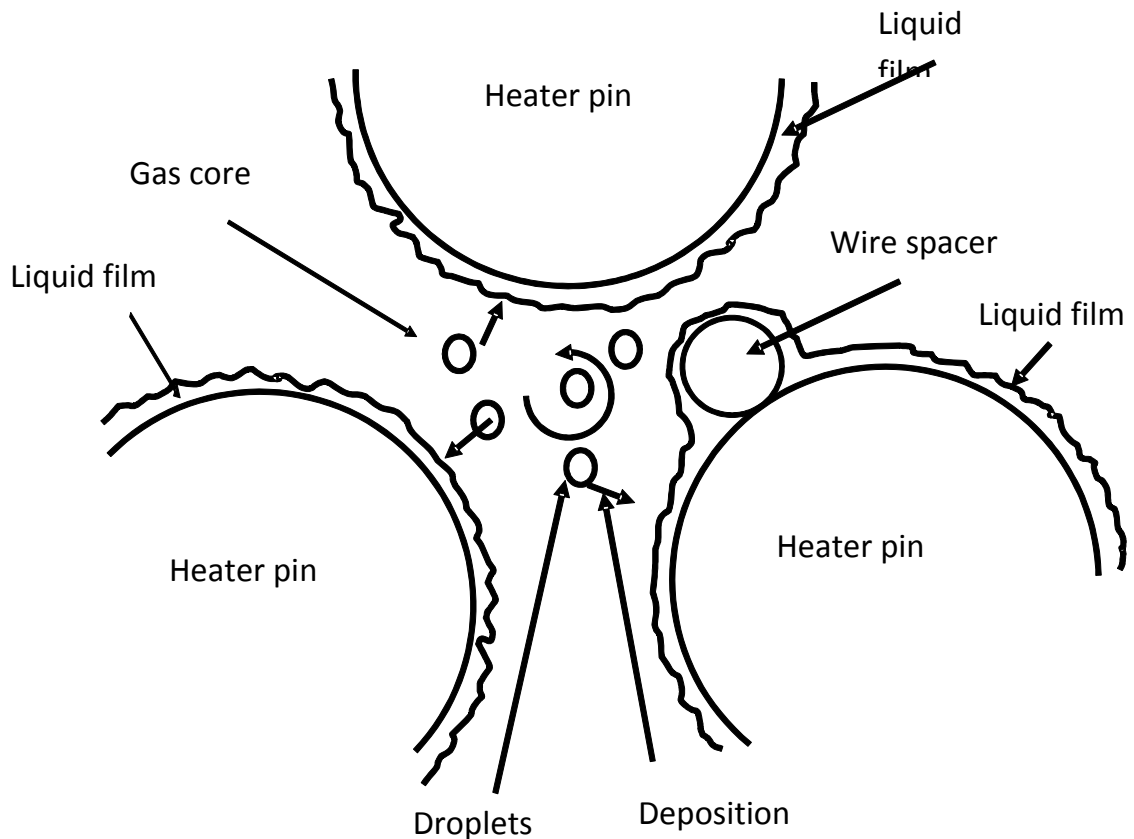


Fig.4.4 Enhancement of deposition rate by centrifugal force

Assume that an operational quality of the BWR is around 0.2 and then the degree of subcooling is around 10°C to 15°C , the CHF in case of bundle pin with wire still higher than that at subcooling temperature of 15°C according to the plot of the experimental data as a function of subcooling [Fig4.5]. Therefore, it can be concluded that the wire spacer still can enhance the CHF when the experiment data are extracted to local quality of 0.2 which is nearly the same condition with the practical case.

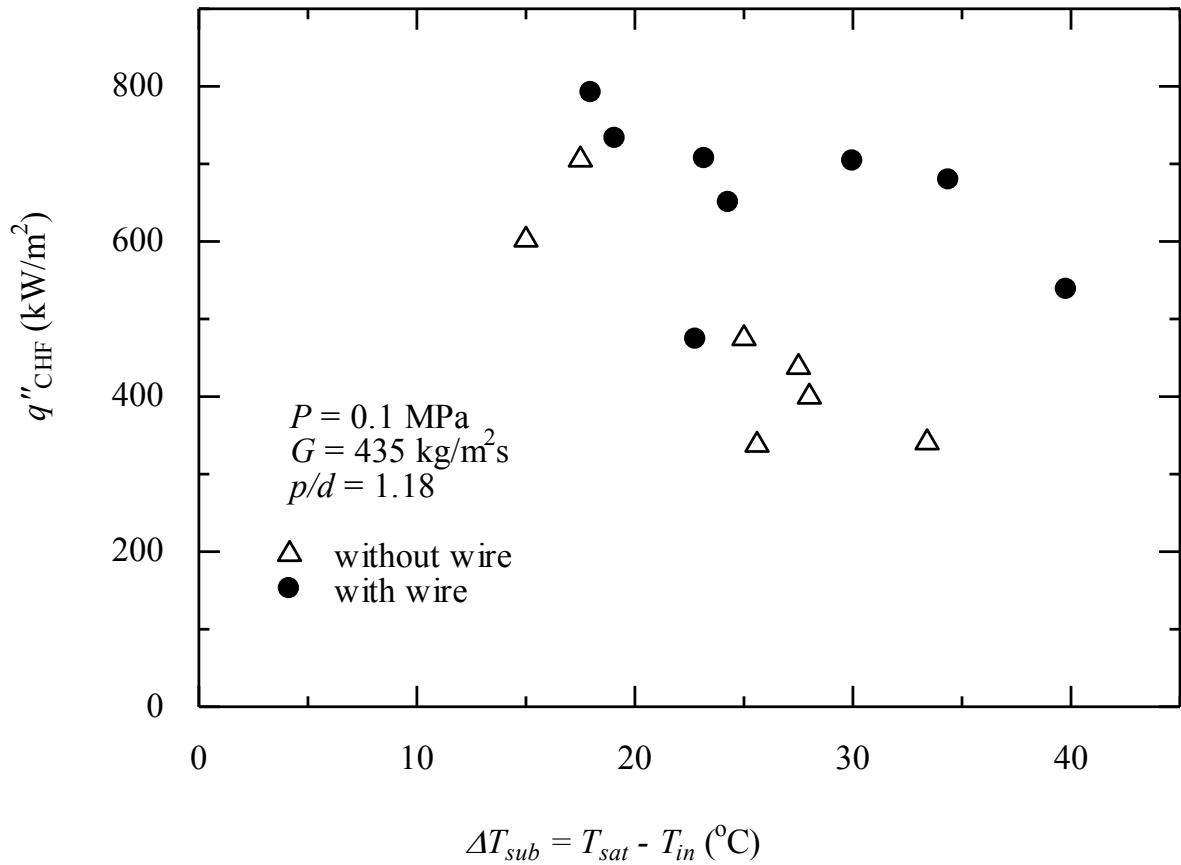


Fig. 4.5 Critical heat flux in bundle with and without wire spacer as a function of inlet subcooling temperature

Summary, at the same local steam quality, the CHF was enhanced by up to 50% with wire spacer compared with it without wire spacer under constant mass flux condition, which was based on the enhancement of turbulent mixing and droplet deposition rate. The enhancement was more significant at the low quality region. Thus, the coolability in tight lattice core could be optimized by using wire spacer.

4.3.3 Effect of pitch to diameter ratio

Fig.4.6 shows the collation in CHF values for three-pin bundle experiment with two difference pitch to diameter equal to 1.10 and 1.18 under the same mass flux condition. It is found that the CHF values have a similar tendency even with the difference value of pitch to diameter ratio. Thus, the characteristics of CHF were not change even with the difference mass flux condition, in other word there are no significant differences of CHF were carried out for pitch to diameter of 1.10 and 1.18.

Additionally, the CHF data with the pitch to diameter ratio of 1.10 was slightly lower than that in the case of pitch to diameter ratio equal to 1.18 under the same mass flux condition because of lower coolant velocity. Details in the quality region from -0.04 to 0.01, the difference in CHF values were nearly 100 kW/m^2 .

However, in the region of higher quality $x > 0.01$, the difference in CHF values were nearly 200 kW/m^2 which nearly two time larger than that in the quality region from -0.04 to 0.01. Thus, it can be seen that the difference became larger in the region of higher quality $x > 0.01$, that is, the CHF values for pitch to diameter ratio of 1.18 were higher those for pitch to diameter ratio equal to 1.10.

The same CHF results were plotted as a function of inlet enthalpy [Fig.4.7]. It can be seen that at the same inlet enthalpy and mass flux, the CHF values in three-

pin bundle with wire spacer with $p/d = 1.10$ were also lower than that with $p/d = 1.18$.

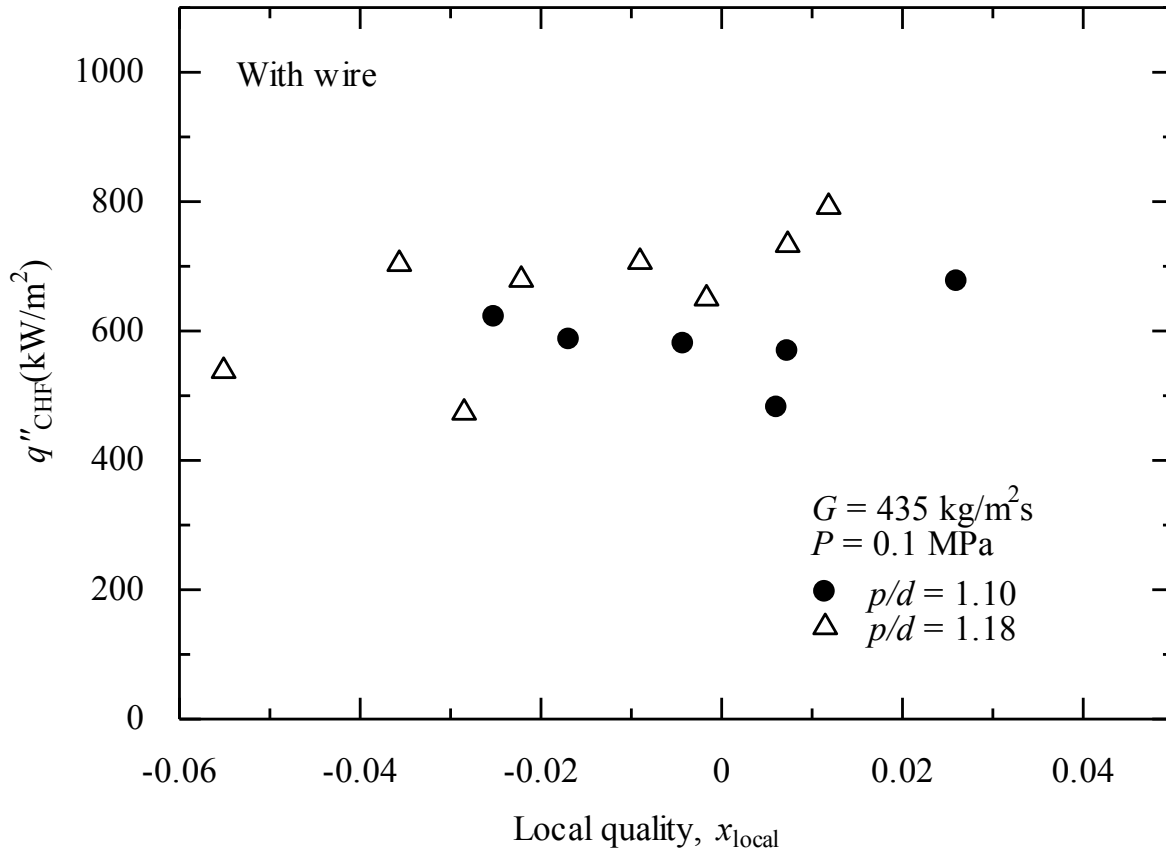


Fig. 4.6 CHF of difference values of p/d under the same mass flux condition.

The reason for this result is related to the geometric factorial. For the pitch to diameter ratio equal to 1.10, the flow area is smaller than that for pitch to diameter ratio equal to 1.18. Hence, in the flow channel with the pitch to diameter ratio of 1.10, the bubbles coalesce with each other into larger bubbles more easily, and cover the heated surface, and as a result hinder the cooling of heater pin by the liquid film,

which lead to lower CHF values in the case of pitch to diameter ratio equal to 1.10 compared with those for pitch to diameter ratio of 1.18. In summary, at the constant mass flux conditions, the tendency of CHF values did not change even with different values of pitch to diameter ratio. The CHF decrease around 5% when changing the pitch to diameter ratio from 1.18 to 1.10. The difference in CHF values tend to become larger at the quality region higher than 0.1.

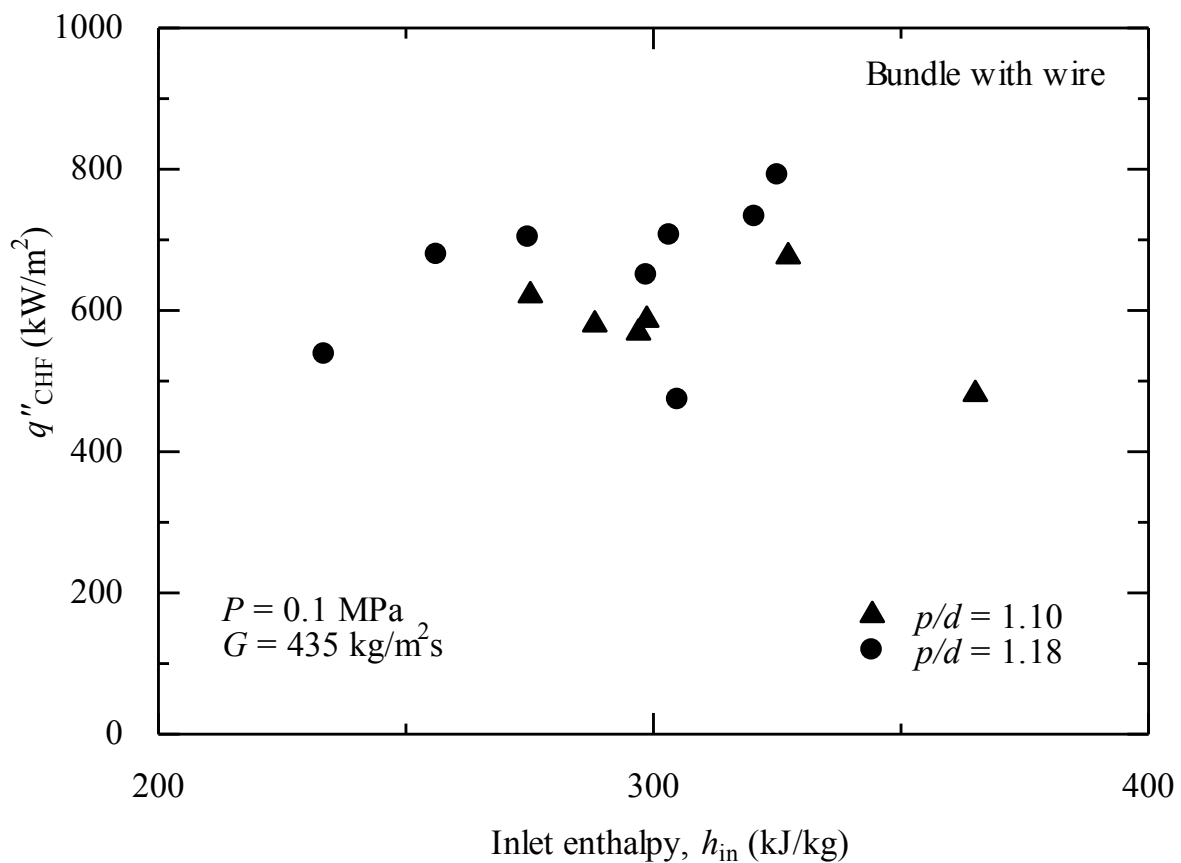


Fig. 4.7 CHF of difference values of p/d under the same mass flux and inlet enthalpy condition.

As mentioned above, from the nuclear reactor design point of view, to evaluate the coolability performance, the experiment for difference value of pitch to diameter ratio at the same mass flow rate condition is necessary. The experiments were obtained with two difference channel which had the pitch to diameter ratio of 1.10 and 1.18, respectively. The experiments were performed at the constant mass flow rate of 0.0208 kg/s and the pressure of 0.1 MPa.

The comparison of CHF between two difference values of the pitch to diameter ratio is showed in Fig.4.8. It can be seen that the CHF values for pitch to diameter equal to 1.10 were much higher than that for the pitch to diameter of 1.18 under the same mass flow rate condition particularly in lower range of x_{local} .

It can be explained by the enhancement of mass flux. With the same flow rate condition, the flow channel which has a smaller value of pitch to diameter ratio would have a smaller flow area which leads to a higher mass flux. Therefore, the coolant velocity in case of pitch to diameter equal to 1.10 was higher than that in the case of pitch to diameter equal to 1.18 at the same flow rate condition. Therefore, the coolability was enhanced by tighter core lattice under the constant mass flow rate condition, which turned to a higher CHF values. Additionally, the difference in CHF values between two difference values of pitch to diameter ratio of 1.10 and 1.18 values became smaller with the increasing quality. In detail, at the quality nearly equal -0.03, the CHF in the case of pitch to diameter ratio of 1.10 (600

kW/m^2) was nearly three time higher than that in the case of pitch to diameter ratio of 1.18 (200kW/m^2). Nevertheless, when the quality increase to nearly equal to 0.03, the difference in CHF values between two dissimilar pitch to diameter ratio value was nearly equal to 200 kW/m^2 , which was equal to 50% in enhancement. Besides, Fig.4.9 shows CHF of difference values of p/d with the same flow rate and inlet enthalpy condition. It also can be seen that the CHF values in three-pin bundle with wire spacer with $p/d = 1.10$ were higher than that with $p/d = 1.18$ at the constant mass flow rate and inlet enthalpy condition.

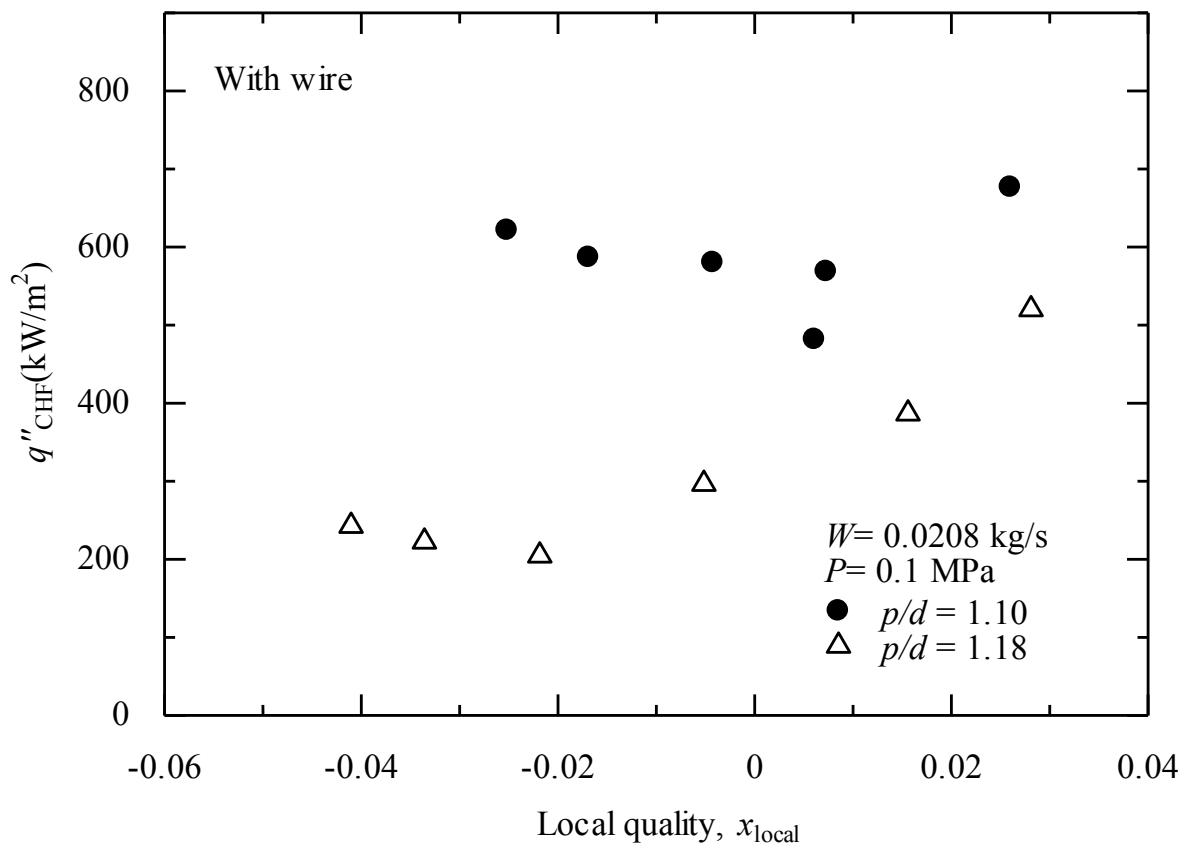


Fig. 4.8 CHF of difference values of p/d with the same flow rate condition.

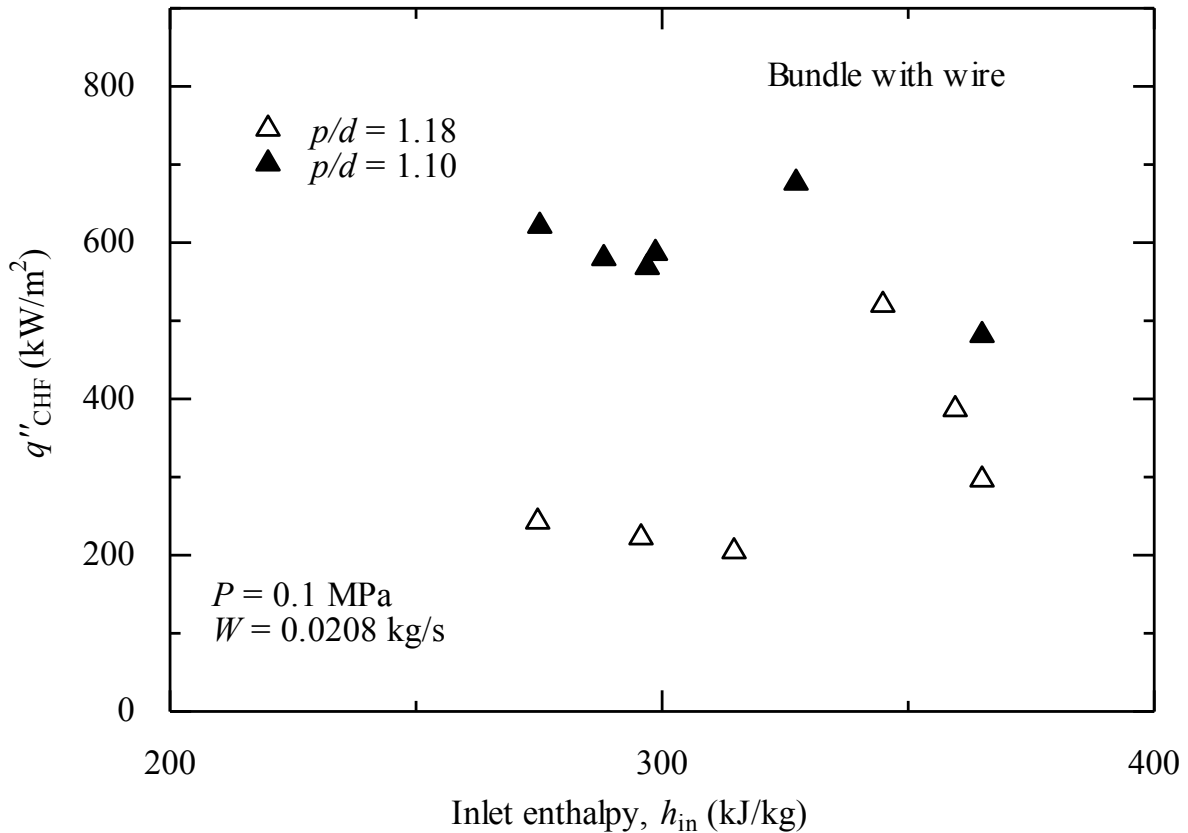


Fig. 4.9 CHF of difference values of p/d with the same flow rate and inlet enthalpy condition.

The reason for such kind of these results can be explained as follow: as mentioned above, under the same mass flow rate condition, the mass flux in the case of pitch to diameter ratio equal to 1.10 was higher than that in the case of pitch to diameter ratio of 1.18. On the other hand, as mentioned in subsection 4.3.1, at the low quality region, with the higher mass flux values the turbulent mixing become higher, thus the CHF in the flow channel with the pitch to diameter of 1.10 were much higher than that with the pitch to diameter ratio of 1.18. On the other hand, at

the high quality region, the bubbles were easily to form with each other and covered the heated surface, which turned to the decrease of CHF in the case of pitch to diameter ratio equal to 1.10.

Summary, the CHF values increased by up to 150% when decrease the pitch to diameter ration from 1.18 to 1.10 under the constant flow rate condition. The enhancement was larger in the low quality region compared with that in high quality region.

4.3.4 Effect of wire pitch

The experiments were performed with the three-pin bundle test section which had a pitch to diameter ratio of 1.18 at the constant mass flux values of $435 \text{ kg/m}^2\text{s}$ and pressure of 0.1 MPa. Fig.4.10 shows the CHF data with two difference values of wire pitch: 100 and 200 mm under the same flow rate condition.

It can be seen that, the CHF experimental data of two difference values of wire pitch were close with each other. Since the flow area was the same even with difference values of wire pitch, thus the coolant velocity is also the same. Therefore, the CHF values did not have a large difference even with difference values of wire pitch. It can be concluded the effect of wire pitch on CHF in bundle pin was similar with that in single pin experiment, hence the wire pitch did not has a large influence on CHF.

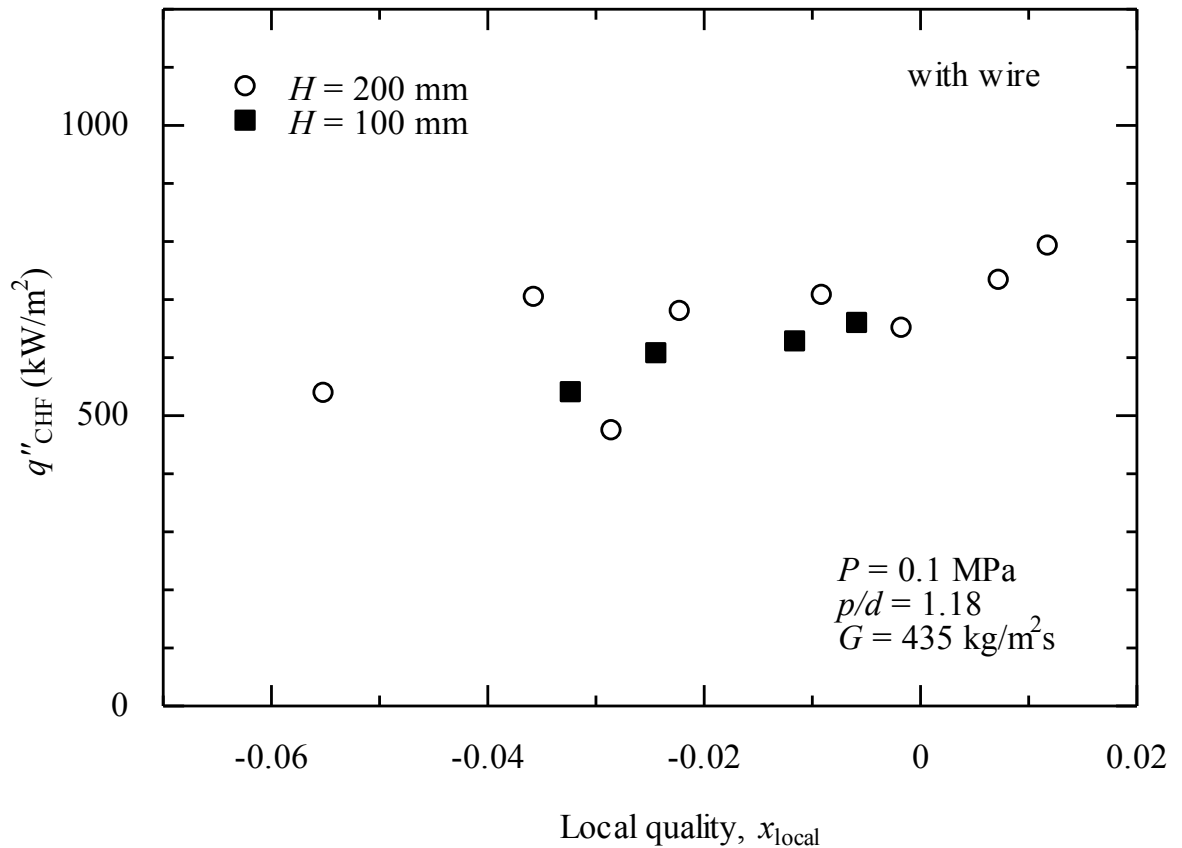


Fig.4.10 Effect of wire pitch on CHF in tight rod bundle

4.3.5 Axial CHF position

The result of the measured position at which CHF occurred along the heated length suggests that CHF mechanism changed with changing the value of pitch to diameter ratio and mass flux. Fig.4.11 and Fig.4.12 show the position where CHF occurred in all the experiment. According to Fig.4.11, the positions of most of CHF at the pitch to diameter values equal to 1.18 and mass flux of 280 kg/m²s were located in the downstream region of the flow channel. However, when the mass flux

was increased from 280 to 435 kg/m²s, the CHF occurred in the middle of the heater pin. In the case of the lowest mass flux of 280 kg/m²s in the flow channel with the pitch to diameter equal to 1.18, the CHF positions were mostly in the downstream region of the flow channel, which suggested the occurrence of liquid film dryout along the heater pin. On the other hand, at higher mass flux, 435 kg/m²s, CHF positions were shifted to the middle of the flow channel, which suggested the departure from nucleate boiling (DNB) phenomenon. In short words, the CHF mechanism changed from the liquid film dryout phenomenon to DNB phenomenon with an increase of mass flux.

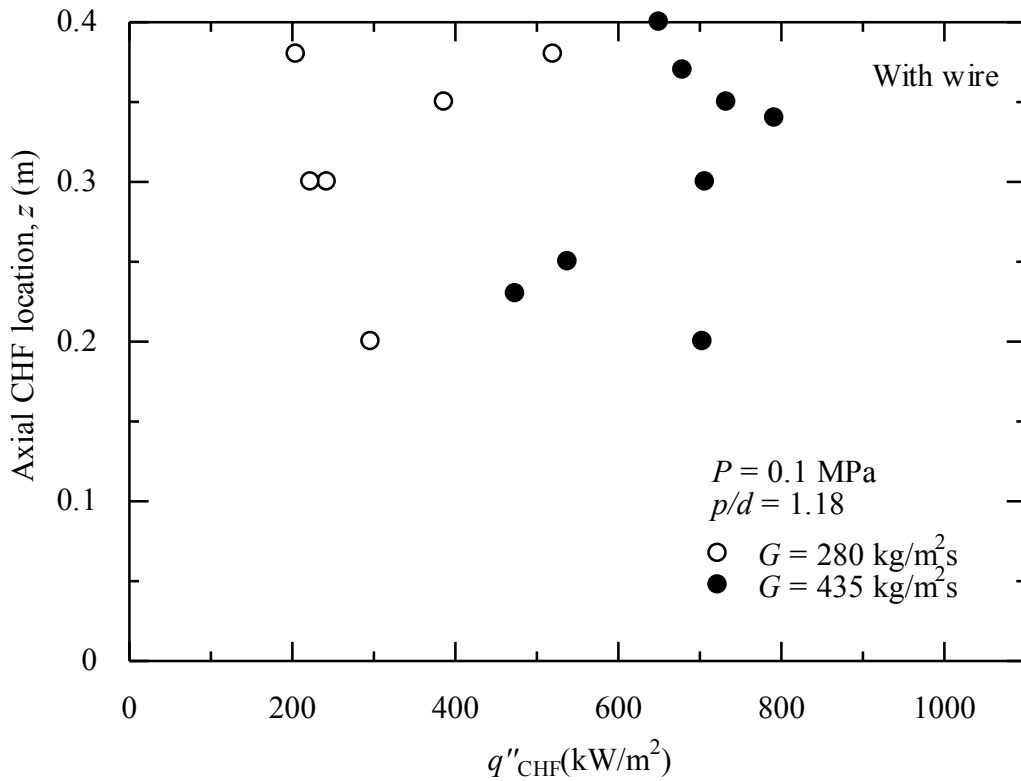


Fig.4.11 CHF position along the heated length with the effect of mass flux.

On the other hand, the CHF positions for difference values of p/d are shown in Fig.4.12. At the same mass flux condition, the CHF positions were nearly the same even with two difference values of pitch to diameter ratio. It can be concluded that the CHF position or the mechanism of CHF values are mostly depend on the mass flux values.

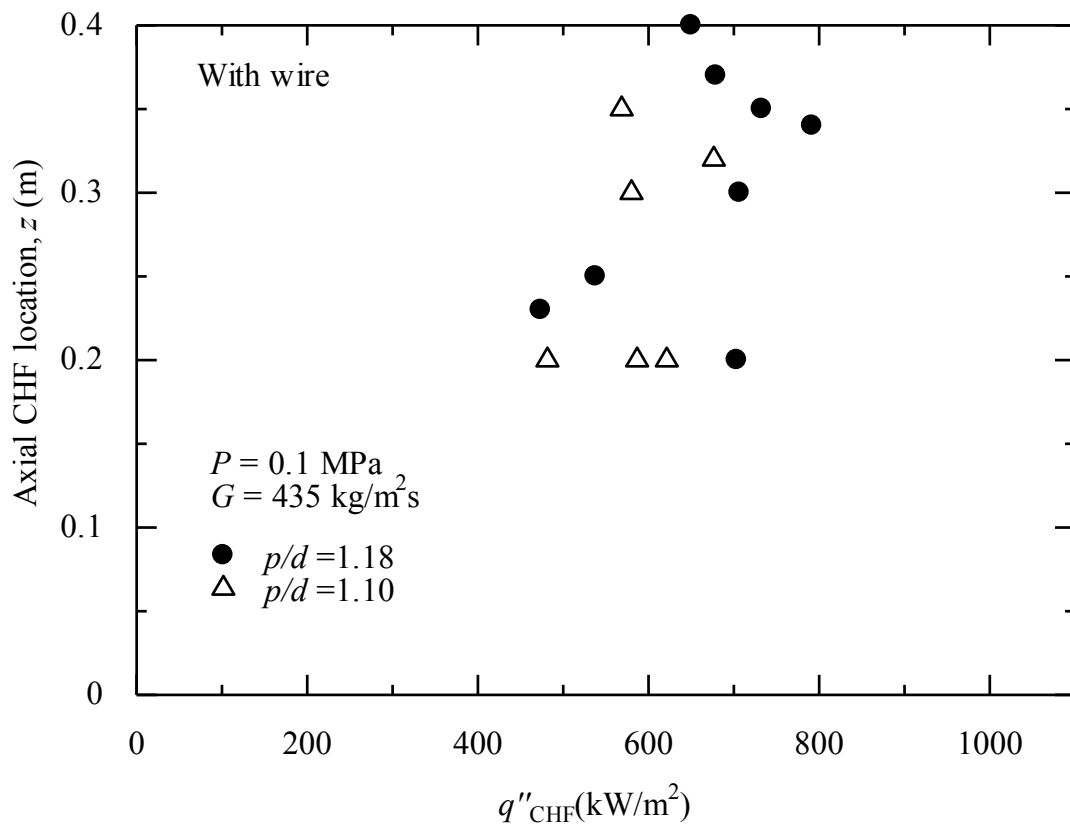


Fig.4.12 CHF position along the heated length with the effect of p/d .

4.4. Comparison with previous study and prediction methods

Many CHF studies were obtained but the studies on CHF in tight lattice core were limited. On the other hand, at the special condition with pressure of 0.1 MPa, mass flux of $435 \text{ kg/m}^2\text{s}$ and the $p/d = 1.18.$, there are no experimental data was obtained in previous studies. Nevertheless, the experiment data in present study can be compared with the experiment data of JAEA [28] which has the closest condition with present study.

The experimental data of RMWR (JAEA) is critical power and in present study it is critical heat flux data. Thus, it is difficult to plot all the data of RMWR in the same figure with present study results. However, it can be compare with present study by picking up the data at similar condition and estimate the CHF value.

At the subcooling temperature of 25°C and mass flux of $400 \text{ kg/m}^2\text{s}$, the critical power is nearly 700 kW. This experimental data was obtained by the 37-rods bundle with the rod diameter of 13.0 mm and the heated length of each rod is 1.26 m. On the other hand, the CHF can be obtained by using equation 2.2. The results are showed in Fig 4.13. It can be seen that at the subcooling temperature of 25°C and mass flux of $400 \text{ kg/m}^2\text{s}$, the CHF data in JAEA study is nearly 370 kW/m^2 . Thus, the present study result was close to JAEA result at the same mas flux and inlet subcooling temperature condition.

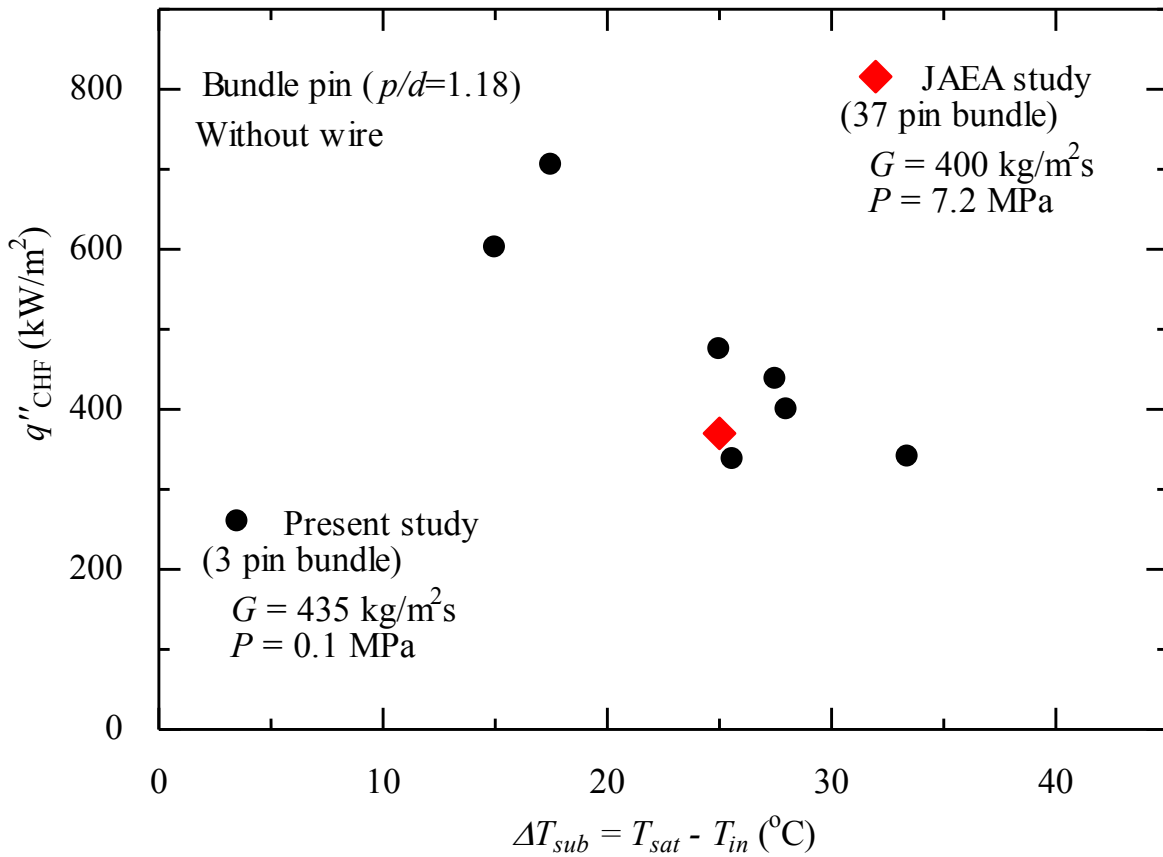


Fig. 4.13 Comparison of CHF experimental data in three-pin bundle without wire spacer with JAEA data in 37-pin bundle [28]

Besides, the experimental data of present study also compared with the prediction method. CHF look up table [16] is well known as one of the best correlation for CHF prediction. However, the look up table [16] was obtained for the tube channel which has the coolant flow internally and the heater part is surrounding the coolant part. Therefore, to be able to compare the look up table data with the three-pin bundle experiment data, it is necessary to use the additional correlation to

convert the look up table data. Min Lee [30] proposed the CHF prediction method for bundle pin channel base on the 1995 CHF look up table [16]. The prediction method includes various correction factors such as hydraulic diameter factor, heated length factor, bundle factor, cold wall effect factor, spacer factor, radial power distribution factor, non-uniform heat flux distribution factor. The CHF correlation for bundle pin is shown as follow

$$q''_{CHF} = q''_{CHF-Table}(P, G, x_{out})K_{Correction-factors} \quad (4.1)$$

As mentioned above, there were many correction factors but in present study only the correction factor of hydraulic diameter factor, K_{hy} , heated length factor, K_{hl} , bundle factor, K_{bf} , cold wall effect factor, K_{cw} were taken into account because the experiments were obtained with the uniform heat flux. The Eq.4.1 can be rewrite as follow

$$q''_{CHF} = q''_{CHF-Table}(P, G, x_{out})K_{hy}K_{hl}K_{bf}K_{cw} \quad (4.2)$$

The correction factors are shown as follow

Hydraulic diameter factor

$$K_{hy} = \left(\frac{D_{hy}}{0.008} \right)^{-\frac{1}{2}} \quad (4.3)$$

where D_{hy} is the hydraulic diameter.

Heated length factor

$$K_{hl} = \exp\left(\frac{D_{hy}}{L} e^{2\alpha}\right) \quad (4.4)$$

where

$$\alpha = \frac{x}{x + \frac{\rho_G}{\rho_F}(1-x)} \quad (4.5)$$

where L is the heated length, x is the quality, ρ_G is the vapor density, ρ_L is the liquid density.

Bundle factor

$$K_{bf} = A \times B \quad (4.6)$$

$$A = \min[c_1, c_1 \exp(-1.12x)] \quad (4.7)$$

$$B = \exp\left[-0.073 + 0.035\left(\frac{G}{1000}\right)\right] \quad (4.8)$$

where c_1 is set equal to 0.419 for triangular pin array, G is the mass flux.

Cold wall effect factor

$$K_{cw} = 1.03\left(\frac{D_{hy}}{D_{he}}\right)^{0.115} \quad (4.9)$$

where D_{he} is the heated equivalent heat diameter.

Fig.4.14 shows the comparison between the calculation data of Eq.4.2 based on the CHF look up table data [14] and the CHF experimental data in the case of three-pin bundle without wire spacer. It can be seen that, the experimental data agrees with the calculation results within $\pm 50\%$. The experimental data close to the calculation results of the quality from -0.02 to 0.01. At the quality lower than -0.02 and higher than 0.01, the agreement becomes lower.

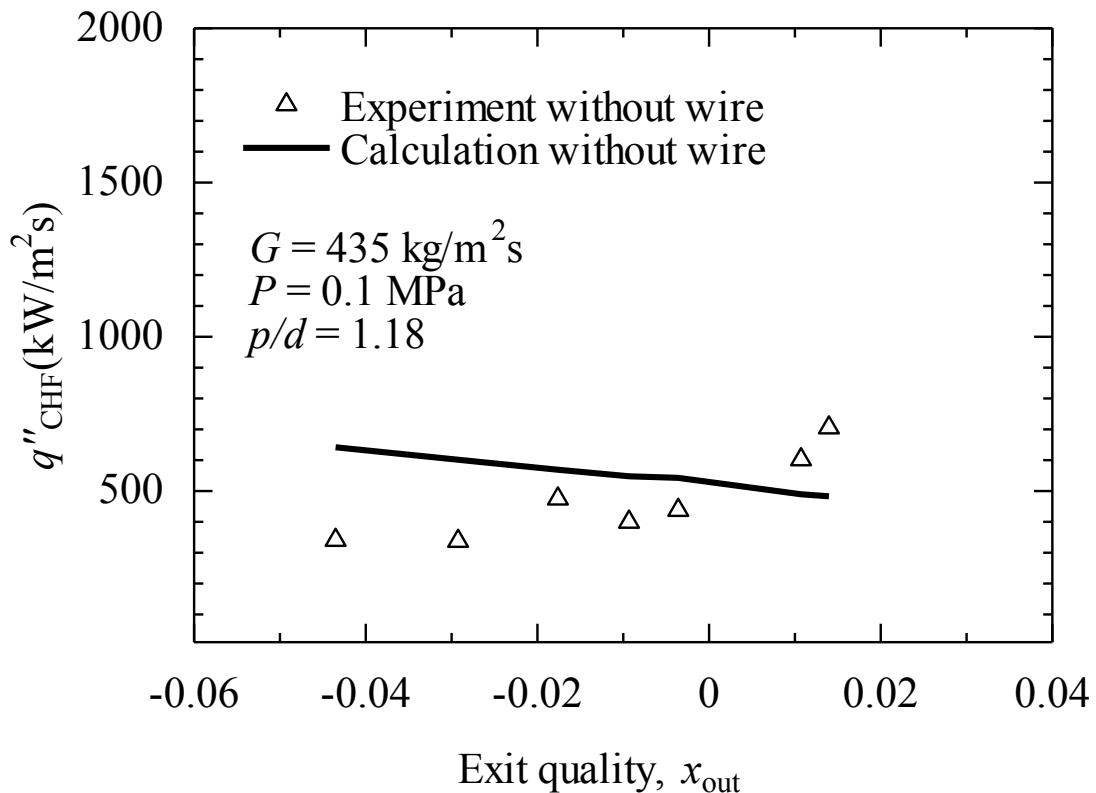


Fig.4.14 Comparison between CHF experimental data in three-pin bundle without wire spacer and the calculation results [Eq.4.2]

In previous study of Haas [Fig.4.15], the CHF in the channel with a bigger gap size decrease with the increase of quality but in the channel with a smaller gap size, the CHF tend to increase with the increase of the quality. In present study, with a narrow flow channel, the CHF experimental data enhanced with the increase of quality due to the increase of the flow disturbance at the high quality region. Therefore, the experimental data look like increase with quality while the calculation results seem like decrease.

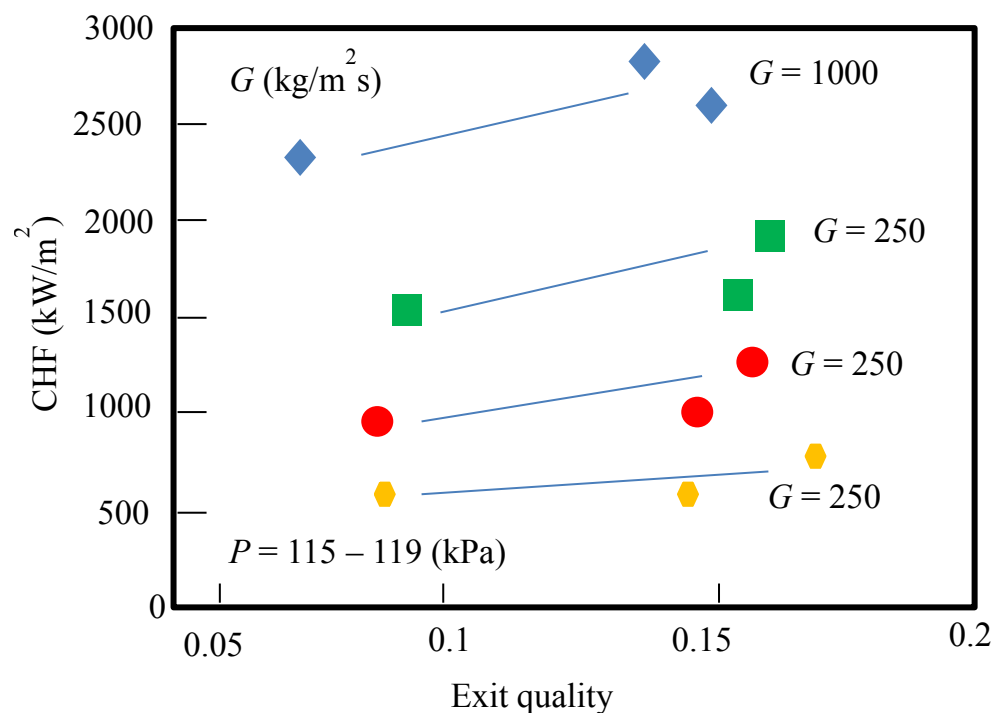


Fig.4.15 Critical heat flux in heated annuli [18]

Fig.4.16 shows the CHF ratio between CHF experimental data in three-pin bundle with wire spacer and the calculated CHF values which were obtained from

by Eq.4.2 for the case of without wire spacer. It can be seen that the CHF in the case of three-pin bundle with wire spacer were higher than that without wire spacer under the same mass flux, pressure and exit quality condition.

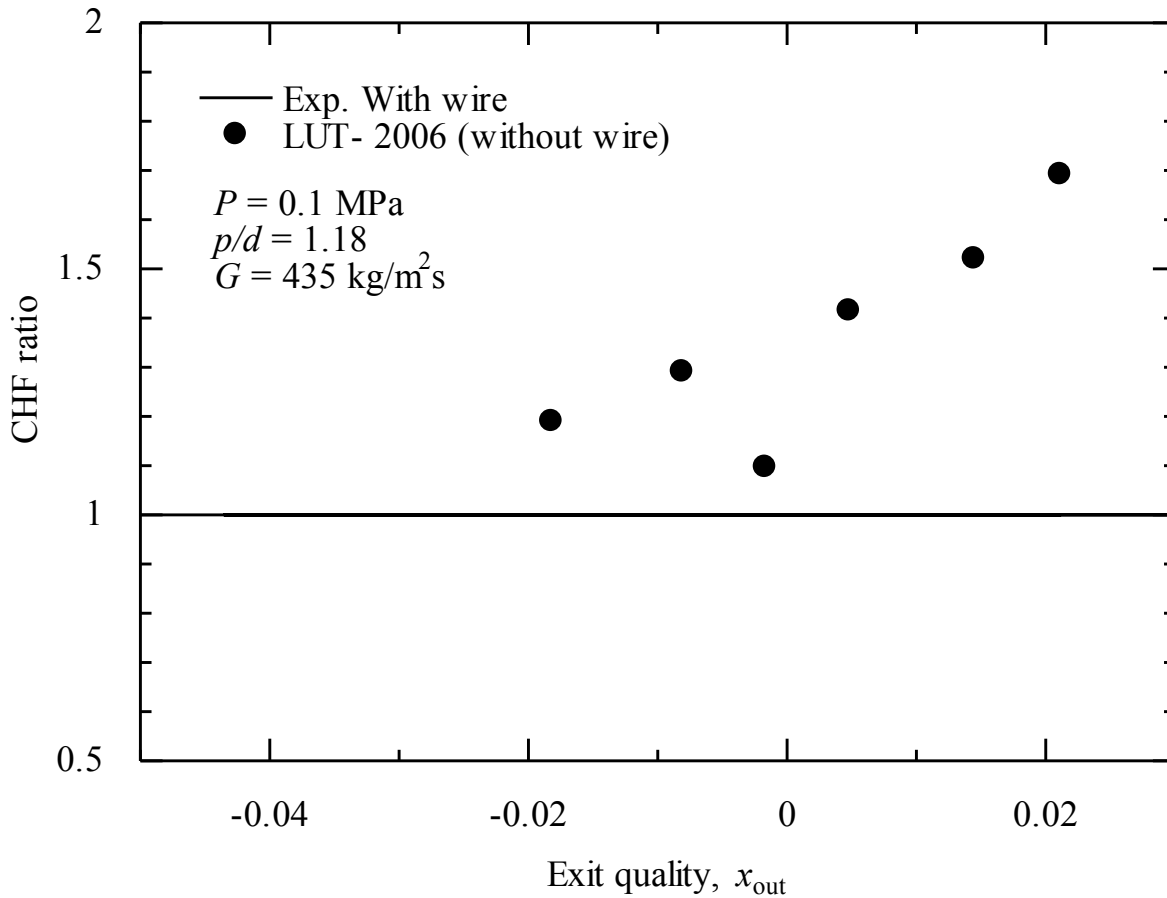


Fig.4.16 CHF ratio of experimental data to calculated results

4.5. New CHF empirical correlation

There are three type CHF correlations which are fitting correlation, dimensional analysis correlation and physical model correlation. Fitting correlation

is the correlation which is the composition of all related factors. In order to obtain such kind of correlation, the experimental data are plotted as a function of related factors and the related factors are obtained by fitting all the values. Dimensional analysis correlation is the composition of dimensionless factors. The dimensionless factors in the correlation are showed as exponential function. To obtain the exponent of the dimensionless factors, the experimental data are plotted as a function of dimensionless factors in the logarithmic scale. Physical model correlation is obtained by considering the mechanism of phenomena. In this study, the fitting CHF correlation for bundle pin with wire spacer was created base on the CHF experimental data in three-pin bundle with wire spacer.

According to the experimental results, the CHF can be written as a function of quality, mass flux and gap size as follow

$$q_{CHF}'' = f(x, G, \delta) \quad (4.10)$$

or

$$q_{CHF}'' = K_x K_G K_\delta \quad (4.11)$$

where K_x is the quality factor, K_G is the mass flux factor and K_δ is the gap size factor.

In order to obtain the quality factor, K_x , the experimental data of three-pin bundle with wire spacer was plotted as a function of local quality, x_{local} . The quality factor, K_x , can be obtained by fitting all the values of the experimental data [Fig.4.17]. Then the CHF to quality factor ratio plotted as a function of mass flux values at the same quality condition [Fig.4.18]. The mass flux factor, K_G , can be obtained by fitting the experimental data. Finally, at the same quality and mass flux condition, the CHF to quality and mass flux factor ratio plotted as a function of gap size [Fig.4.19]. The gap size factor, K_δ , can also be obtained by fitting the experimental data. By fitting the experimental data, the new CHF empirical correlation can be obtained as follow

$$q_{CHF}'' = K_x K_G K_\delta \quad (4.12)$$

where

$$K_x = 264777 \times x^2 + 4233.4 \times x + 710.45 \quad (4.13)$$

$$K_G = G \times 0.0035 - 0.536 \quad (4.14)$$

$$K_\delta = \delta \times 0.5608 + 0.5348 \quad (4.15)$$

This correlation was created base on CHF experimental data for three-pin bundle with wire spacer at which the rod diameter of 4.57 mm and length of 400

mm. Besides, this correlation was obtained with the local quality ranged from -0.06 to 0.02 ($-0.06 \leq x \leq 0.02$), the mass flux ranged from 280 to 435 kg/m²s ($280 \leq G \leq 435$ kg/m²s) and the gap size range from 0.43 to 0.83 mm ($0.43 \leq \delta \leq 0.83$) which had a pitch to diameter ranged from 1.10 to 1.18 respectively.

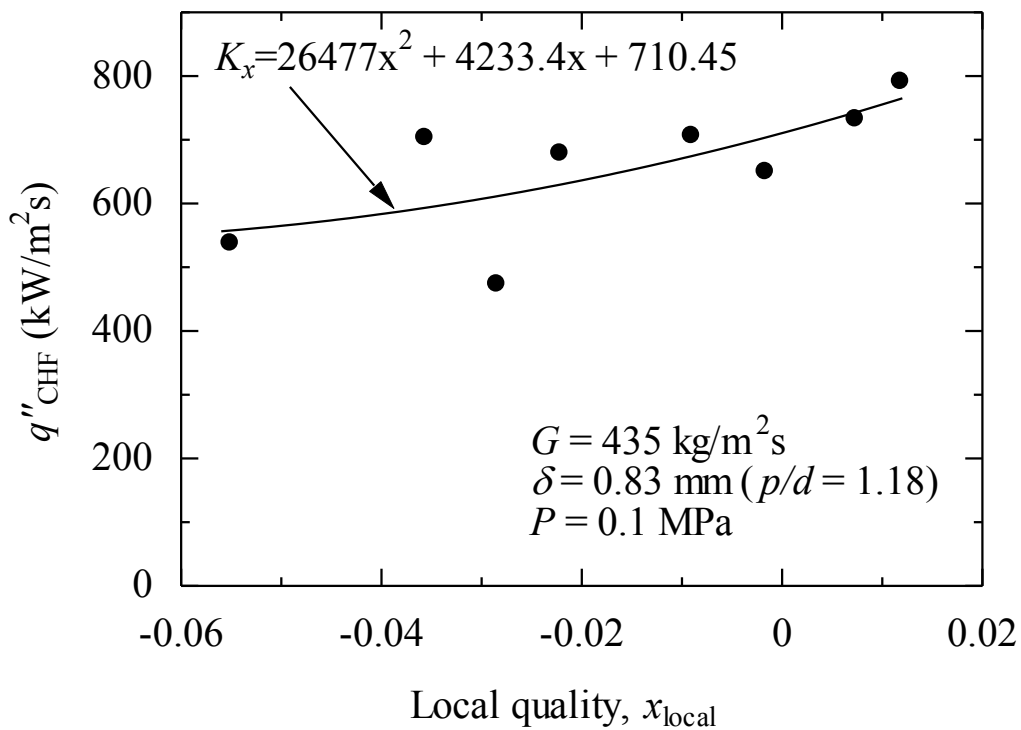


Fig.4.17. CHF in three-pin bundle with wire spacer as a function of local quality

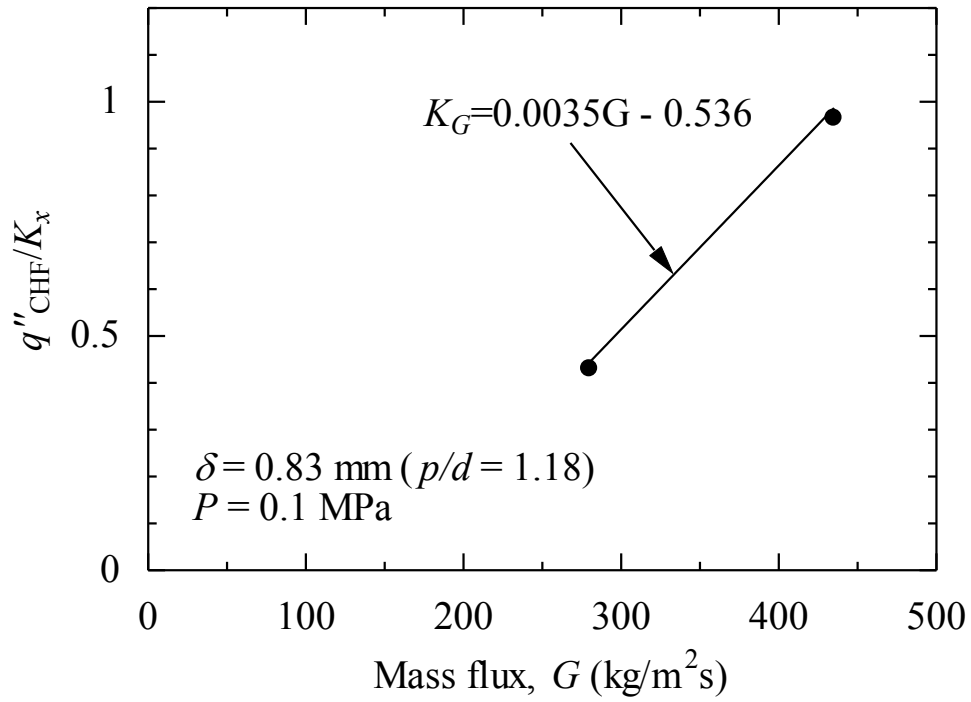


Fig.4.18 CHF to quality factor ratio as a function of mass flux

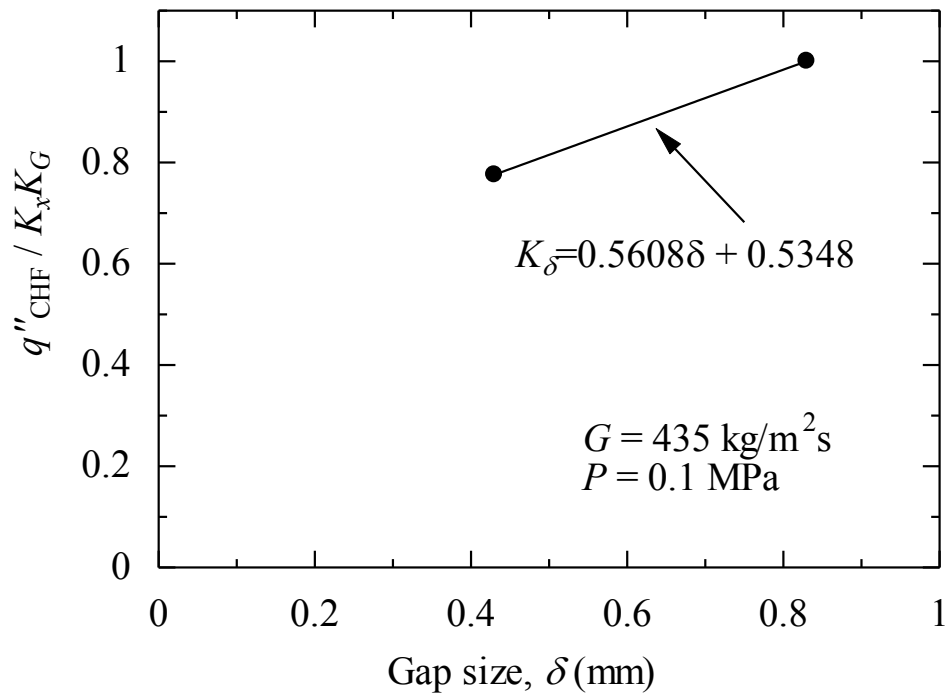


Fig.4.19 CHF to quality and mass flux factor ratio as a function of gap size.

Figure 4.20, 4.21 and 4.22 show the comparison between the calculation results obtained with the experimental data at different mass flux and gap size condition. It can be seen that the prediction values were agreed with the experimental data within the range of $\pm 25\%$.

Moreover, in order to determining the thermal limits of the BWRs, the critical power ratio (CPR) is used. The CPR is that power in the assembly that is calculated by application of the correlation to cause some point in the assembly to experience boiling transition (CHF), divided by the actual assembly operating power. In the practical reactor, the minimum CPR (MCPR) is around 1.3 which means the minimum critical power is about 30% higher than the operating power. Therefore, the correlation with the deviation of lower than 30% is the good correlation. On the other hand, two phase flow is the complicated phenomena with the low repeatability in experimental data. Thus, the CHF correlation with the deviation of $\pm 25\%$ is good enough.

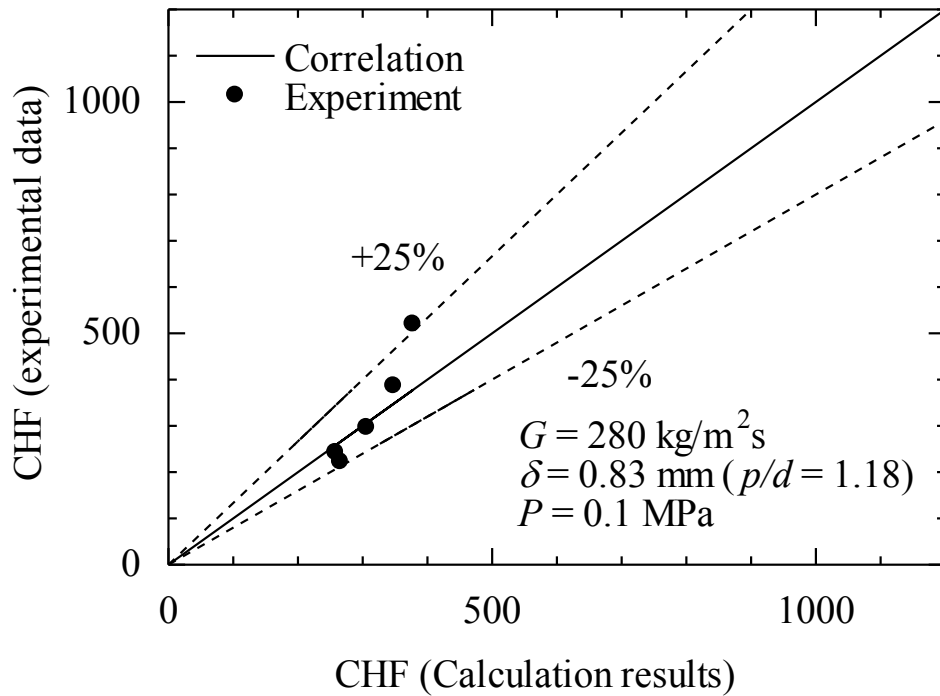


Fig.4.20 Experimental data and calculation results at $G=280 \text{ kg/m}^2\text{s}$

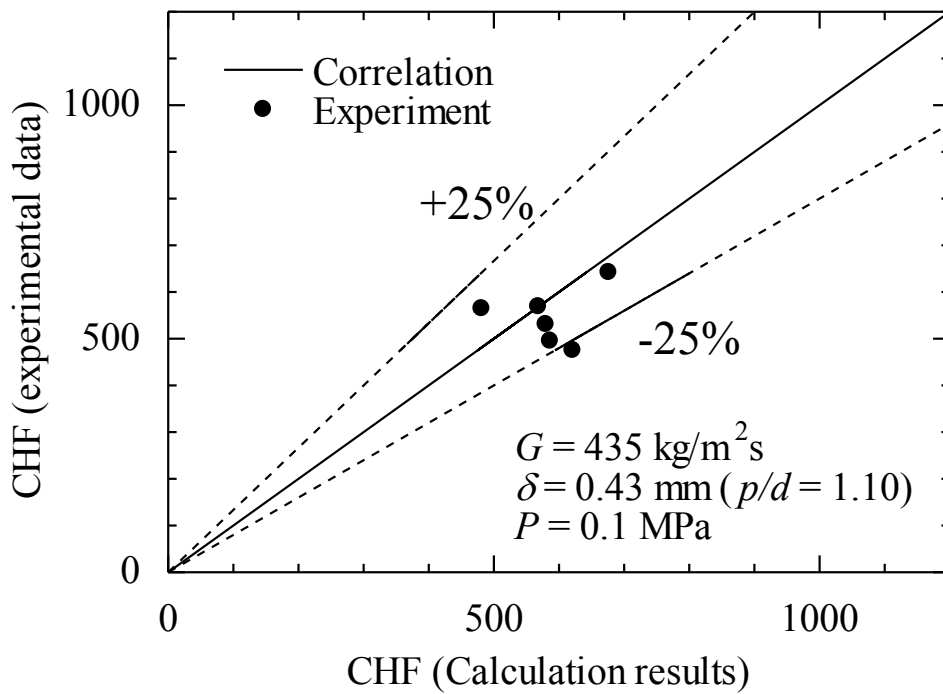


Fig.4.21 Experimental data and calculation results at $\delta=0.43 \text{ mm}$

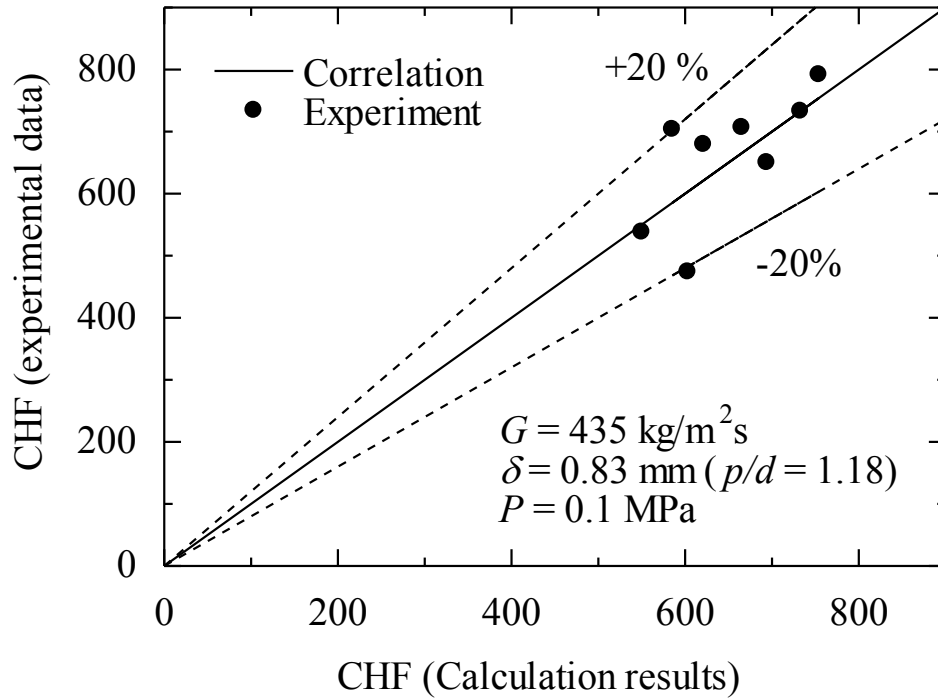


Fig.4.22 Experimental data and calculation results at $G=435 \text{ kg/m}^2\text{s}$

4.5. Conclusions

Critical heat flux in boiling water flow in a tight rod bundle was investigated experimentally for a three-pin bundle with and without wire spacers. Two different values of pitch to diameter ratio were chosen: 1.10 and 1.18. The conclusions are as follows:

- (1) The CHF values increased with the increase of the mass flux values under the same quality condition. The effect of mass flux on CHF in tight rod bundle with wire spacer was the same with that in single pin channel.

- (2) The CHF was enhanced by up to 50% with wire spacer compared with it without wire spacer under constant mass flux condition. The enhancement was more significant at the low quality region. Thus, the coolability in tight lattice core could be optimized by using wire spacer.
- (3) Under constant flow rate conditions, the CHF values increased by up to 150% when decrease the pitch to diameter ration from 1.18 to 1.10.
- (4) Under constant mass flux conditions, the tendency of CHF values did not change even with different values of p/d . the CHF decrease around 5% when changing the p/d from 1.18 to 1.10.
- (5) Under the same mass flux condition, the CHF is nearly the same even with difference values of wire pitch.
- (6) The positions of CHF at $p/d = 1.18$ and low mass flux were located in the downstream region of the flow channel. However, when the mass flux was increased, the CHF occurred in the middle of the heater pin. Under constant mass flux condition, CHF occurred at nearly the same position for both of $p/d = 1.10$ and 1.8.
- (7) The CHF experimental data in the case of three-pin bundle without wire spacer were agreed with the prediction method given by Min Lee within $\pm 50\%$ of deviation. On the other hand, the CHF experimental data with wire

spacer were higher than the calculated results for bundle without wire spacer at the same quality condition.

- (8) The new correlation of CHF in bundle pin with wire spacer was created by the fitting method. The correlation was shown as a function of mass flux, quality and gap size value. The new correlation can predict the CHF data with the deviation of $\pm 25\%$ which is good enough in the case of boiling two-phase flow phenomena.

**Chapter 5. Analytical study on CHF behavior in
tight rod bundle using CHF simulation method**

5.1. Introduction

The experimental study on CHF behavior in tight lattice core with wire spacer was presented in the previous chapter. The enhancement of CHF with the wire spacer is also discussed in detail. However, for the better understanding of such kind of phenomenon, the analytical study on CHF behavior in tight lattice core is necessary. On the other hand, the CHF in high conversion BWR is occurred mostly depend on the liquid film dryout mechanism which base on the deposition and entrainment rate of droplets. Therefore, the three-fluid model (liquid phase, gas phase, droplet phase) is the best approach method to simulate for such kind of phenomenon.

Therefore, the purpose of the study which is presented in this chapter is to clarify the CHF behavior in tight lattice channel with and without wire spacer base on the three-fluid model method.

Besides, in order to clarify the mechanism of the enhancement of CHF in tight lattice core with wire spacer, the parametric studies were also obtained.

5.2. Dryout simulation method and boundary condition

As mentioned in chapter 1, the CHF can be occurred base on two mechanisms: dryout mechanism and DNB mechanism. However, the main purpose of this study is to investigate the CHF behavior in boiling two phase flow for the

high conversion boiling water reactor. Therefore, this study is focus on the dryout mechanism which is occurred base on the droplet deposition rate and entrainment rate. Hence, in order to analyze the CHF behavior in tight lattice core, the dryout simulation is required.

Therefore, dryout simulation method which can simulate the dryout phenomena base on the deposition and entrainment rate of droplets should be taken into account. To simplify the calculation, the simulation method was based on the one dimensional calculation method. In order to simulate the dryout phenomenon, the three-fluid model is considered with the liquid phase, gas phase and droplets phase. In order to simulate the CHF phenomenon, the conservation and constitutive equations were taken into account. The conservation equations are created to simulate two separated liquid film in the case of single pin channel and also to simulate the single liquid film in the case of bundle test. The constitutive equations were Sugawara [44-46] equations which can be simulated the CHF phenomena base on the dryout mechanism at which the droplet deposition and entrainment rate was taken into account.

The calculation is assumed start to calculate from the entrance with the single phase water flow, then the flow regime evolution is simulated along the vertical axial of the flow channel. The bubbly and slug flow can be defined by the vapor quality. The annular flow can be defined from the initial transition vapor quality.

Finally, the liquid film dryout is defined as the breakdown or disappearance of the liquid film flow along the head surface. The boundary conditions are the inlet mass flux, inlet enthalpy, outlet pressure and the heat flux of the wall. The boundary conditions for single pin channel and three-pin bundle are given in table 5.1 and 5.2.

Table.5.1. Single pin experiment calculation

Outlet pressure P [MPa]	Inlet mass flux G [kg/m ² s]	Subcooling enthalpy, Δh_{sub} [kJ/kg]	
		Without wire	Wire
0.1	658.0	73.08	51.66
		81.09	68.04
		107.10	77.70
		130.20	112.98
		146.58	121.80
		168.42	161.00

Table.5.2 Three-pin experiment calculation

Outlet pressure P [MPa]	Inlet mass flux G [kg/m ² s]	Subcooling enthalpy, Δh_{sub} [kJ/kg]	
		Without wire	Wire
0.1	658.0	73.08	92.4
		81.09	97.02
		107.10	114.24
		130.20	118.86
		146.58	142.8
		168.42	161.28

5.3. Dryout simulation for annulus channel

5.3.1. Three fluid model in annulus channel

The single pin test section is an annulus channel which has two separate liquid films flow along the heated surface and the flow channel [Fig.5.1]. Therefore, in order to analyze the dryout phenomenon in annulus channel, it is necessary to simulate the two separate liquid film flow.

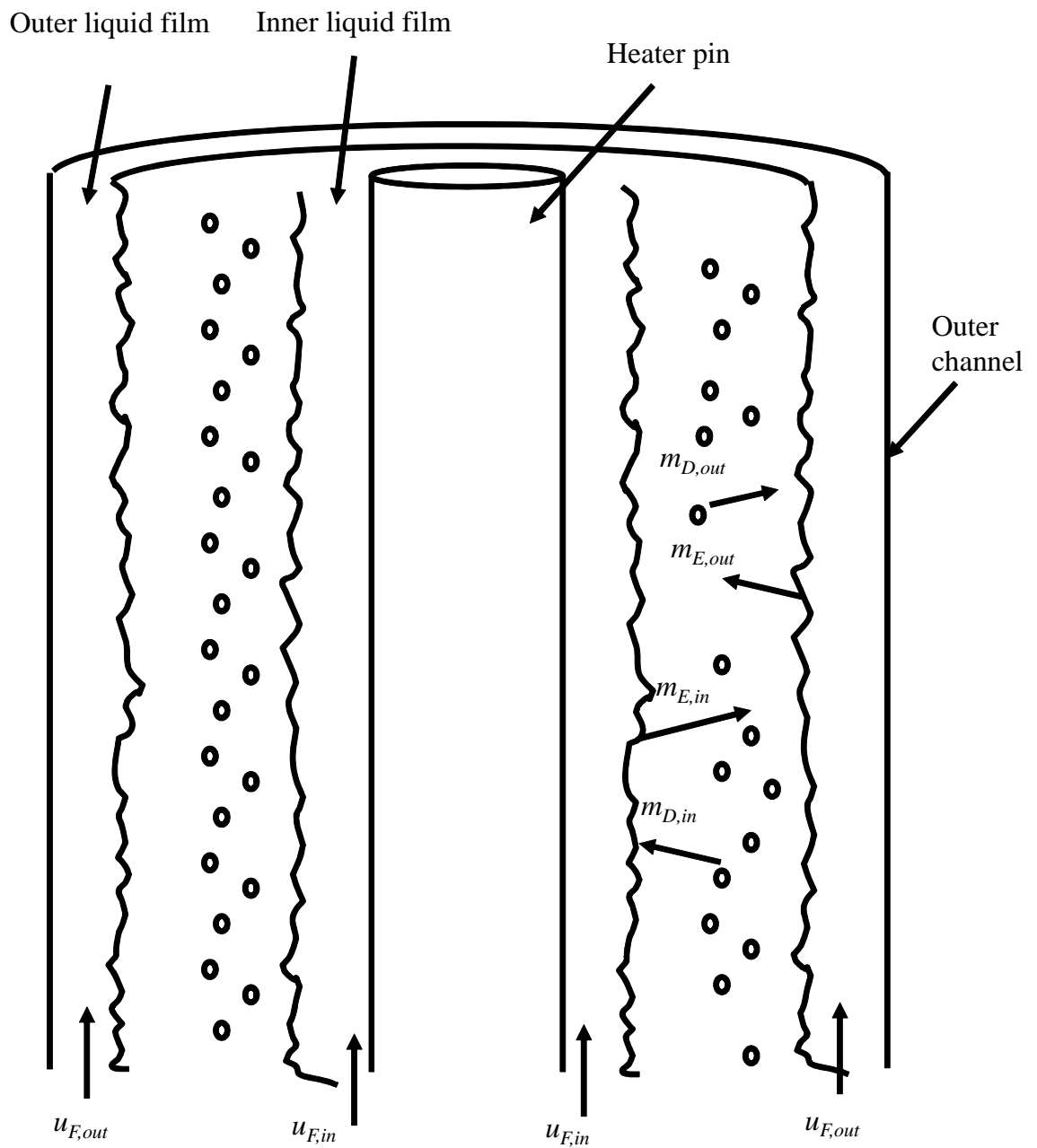


Fig.5.1 Flow behavior in annulus channel

As mentioned above, to simulate the dryout the three-fluid model is considered with the liquid phase, gas phase and droplets phase. The field equations are given as follow

Continuity equation

Gas phase

$$\frac{\partial}{\partial z} (\alpha_G \rho_G u_G A) = P_{heat} \frac{q_w}{h_{fg}} \quad (5.1)$$

Liquid phase

- Inner liquid film

$$\frac{\partial}{\partial z} (\alpha_{F,in} \rho_F u_{F,in} A) = P_{wet,in} (m_{D,in} - m_{E,in}) - P_{heat} \frac{q_w}{h_{fg}} \quad (5.2)$$

- Outer liquid film

$$\frac{\partial}{\partial z} (\alpha_{F,out} \rho_F u_{F,out} A) = P_{wet,out} (m_{D,out} - m_{E,out}) \quad (5.3)$$

Droplets phase

$$\frac{\partial}{\partial z} (\alpha_E \rho_E u_E A) = P_{wet} (m_E - m_D) \quad (5.4)$$

where

$$\alpha_{F,in} + \alpha_{F,out} + \alpha_G + \alpha_E = 1 \quad (5.5)$$

Momentum equation

Gas phase

$$\begin{aligned} \frac{\partial}{\partial z} (\alpha_G \rho_G u_G^2) + \alpha_G \frac{\partial P}{\partial z} = & -A_{FG,in} \tau_{FG,in} - A_{FG,out} \tau_{FG,out} \\ & -A_{EG} \tau_{EG} + \frac{P_{heat}}{A} \frac{q_w}{h_{fg}} u_{F,in} - \alpha_G \rho_G g \cos \theta \end{aligned} \quad (5.6)$$

Liquid phase

- Inner liquid film

$$\begin{aligned} \frac{\partial}{\partial z} (\alpha_{F,in} \rho_F u_{F,in}^2) + \alpha_{F,in} \frac{\partial P}{\partial z} = & A_{FG,in} \tau_{FG,in} - A_{WF,in} \tau_{WF,in} \\ & + \frac{P_{wet,in}}{A} (m_{D,in} u_E - m_E u_{F,in}) \\ & - \frac{P_{heat}}{A} \frac{q_w}{h_{fg}} u_{F,in} - \alpha_{F,in} \rho_F g \cos \theta \end{aligned} \quad (5.7)$$

- Outer liquid film

$$\begin{aligned} \frac{\partial}{\partial z} (\alpha_{F,out} \rho_F u_{F,out}^2) + \alpha_{F,out} \frac{\partial P}{\partial z} = & A_{FG,out} \tau_{FG,out} - A_{WF,out} \tau_{WF,out} \\ & + \frac{P_{wet,out}}{A} (m_{D,out} u_E - m_E u_{F,out}) - \alpha_{F,out} \rho_F g \cos \theta \end{aligned} \quad (5.8)$$

Droplets phase

$$\begin{aligned}
\frac{\partial}{\partial z}(\alpha_E \rho_E u_E^2) + \alpha_E \frac{\partial P}{\partial z} &= A_{EG} \tau_{EG} + A_{EF} \tau_{EF} \\
&+ \frac{P_{wet,in}}{A} (m_E u_{F,in} - m_{D,in} u_E) \\
&+ \frac{P_{wet,out}}{A} (m_E u_{F,out} - m_{D,out} u_E) - \alpha_E \rho_E g \cos \theta
\end{aligned} \tag{5.9}$$

5.3.2. Dryout simulation model and constitutive equation

The dryout can be obtained by the breakdown of the liquid film flow along the heated surface, in other word the CHF occur when the liquid film flow rate equal zero. The liquid film flow rate can be given as

$$\frac{\partial W_F}{\partial z} = P_{wet} \left(m_D - m_E - \frac{q_w}{h_{fg}} \right) \tag{5.10}$$

where W_F is the liquid film flow rate, P_{wet} is the perimeter of the liquid film, m_D is the droplets deposition rate, m_E is the droplets entrainment rate, q_w is the wall heat flux and h_{fg} is the latent heat of evaporation.

Equation 5.10 can be applied for the tube channel which has a single liquid film in the flow channel. However, in the case of annulus channel, there are two liquid films flow along the heated surface and the inner surface of the flow channel as show in [Fig.5.1]. Therefore, to simulate the dryout phenomenon in the annulus channel, Eq.5.10 should be applied for two difference liquid films

$$\frac{\partial W_{F,in}}{\partial z} = P_{wet,in} \left(m_{D,in} - m_{E,in} - \frac{q_w}{h_{fg}} \right) \quad (5.11)$$

$$\frac{\partial W_{F,out}}{\partial z} = P_{wet,out} (m_{D,out} - m_{E,out}) \quad (5.12)$$

Equation 5.11 is used to calculate the liquid film flow rate which flow along the heated surface. On the other hand, Eq.5.12 is used to calculate the liquid film flow rate along the inner surface of the flow channel, thus the evaporation factor is not taken into account. The deposition rate, can be obtained by

$$m_{D,k} = k_{D,k} C \quad (5.13)$$

k = in, out

where k_D is the mass transfer coefficient and C is the droplets concentration in the gas core. To calculate the mass transfer coefficient, k_D and the droplets concentration in the gas core, C the correlation of Sugawara [44-46] was used. The mass transfer coefficient was calculated as follow

$$\frac{k_{D,k}}{u_G} = 9.0 \times 10^{-3} \left(\frac{C}{\rho_G} \right)^{-0.5} \text{Re}_G^{-0.2} \text{Sc}^{-2/3} \quad (5.14)$$

and

$$C = \frac{W_E}{\frac{W_E u_E}{\rho_G} + \frac{W_E}{\rho_F}} \quad (5.15)$$

The Reynolds number of gas core can be obtained by

$$\text{Re}_{G,k} = \frac{u_G D_{FG}}{\nu_G} \quad (5.16)$$

where D_{FG} is the hydraulic diameter of the gas core, ν_G is the kinematic viscosity of gas phase. The Schmidt number, Sc can be obtained through the Lewis relation, $Le = Sc/Pr \approx 1$. [44-46]

The entrainment rate can be calculated by using Sugawara [44-46] equation as follow

$$m_{E,k} = 1.07 \left(\frac{\tau_{FG,k} \Delta h_{eq,k}}{\sigma} \right) \left(\frac{u_G \mu_L}{\sigma} \right) \left(\frac{\rho_L}{\rho_G} \right)^{0.4} \quad (5.17)$$

If $\text{Re}_{G,k} \geq 10^5$

$$\Delta h_{eq,k} = k_{s,k} \quad (5.18)$$

If $\text{Re}_{G,k} \leq 10^5$

$$\Delta h_{eq,k} = k_{s,k} [2.136 \log_{10}(\text{Re}_{G,k}) - 9.68] \quad (5.19)$$

where

$$k_{s,k} = 0.57\delta_k + 21.73 \times 10^3 \delta_k^2 - 38.8 \times 10^6 \delta_k^3 + 55.68 \times 10^9 \delta_k^4 \quad (5.20)$$

where the τ_{FG} is the interfacial shear stress, is the hydrodynamic equivalent wave height, μ_L is the dynamic viscosity of liquid phase and σ is the surface tension. The $k_{s,k}$ is the wave roughness and δ_k is the liquid film thickness. The interfacial shear stress τ_{FG} can be obtained by

$$\tau_{FG,k} = A_{FG,k} f_{FG,k} \left(\frac{\rho_G}{2} \right) (u_G - u_{F,k}) |u_G - u_{F,k}| \quad (5.21)$$

Wallis correlation

$$f_{FG,k} = 0.079 \text{Re}_{G,k}^{-0.25} (1 - 300\delta_k / D_{hyd}) \quad (5.22)$$

Other constitutive equations can be obtained as follow

Wall shear stress [52]

$$\tau_{WF,k} = A_{WF,k} f_{WF,k} \left(\frac{\rho_F}{2} \right) u_{F,k} |u_{F,k}| \quad (5.23)$$

$$\text{Re}_{F,k} = \frac{u_{F,k} D_{F,k}}{\nu_F} \quad (5.24)$$

If $\text{Re}_{F,k} \geq 105$

$$f_{WF,k} = 8 \times 10^{-4} + 0.05525 \text{Re}_{F,k}^{-0.237} \quad (5.25)$$

If $\text{Re}_{F,k} \leq 105$

$$f_{WF,k} = 0.079 \text{Re}_{F,k}^{-0.25} \quad (5.26)$$

Droplet shear stress

$$\tau_{EG,k} = A_{EG} K_{EG} \left(\frac{\rho_G}{2} \right) (u_G - u_E) |u_G - u_E| \quad (5.27)$$

$$K_{EG} = \frac{24}{\text{Re}_E} (1 + 0.15 \text{Re}_E^{0.687}) + \frac{0.42}{1 + 4.25 \times 10^4 \text{Re}_E^{-1.16}} \quad (5.28)$$

$$\text{Re}_E = \left(\frac{|u_G - u_E| D_E}{\nu_E} \right) \quad (5.29)$$

5.3.3. Analyzing the enhancement of CHF in single pin experiment

As mentioned in chapter 2, in annulus channel the outer liquid film has an effect on the enhancement of CHF. Due to the effect of wire spacer and spiral flow, the disturbance of the steam flow on the outer liquid film was enhanced. And the result is the enhancement of entrainment rate in the outer liquid film. Since the promotion of entrainment rate at the outer liquid film, the droplets concentration in the gas core become higher which lead to the improvement of deposition rate for the inner liquid film, thus the CHF was enhanced. The entrainment rate in single pin without wire spacer can be obtain from Eq.5.17, thus the entrainment rate in single pin channel with wire spacer can be obtained as follow

$$m_{E,k} = C_1 \times 1.07 \left(\frac{\tau_{FG,k} \Delta h_{eq,k}}{\sigma} \right) \left(\frac{u_G \mu_L}{\sigma} \right) \left(\frac{\rho_L}{\rho_G} \right)^{0.4} \quad (5.30)$$

where C_1 is the entrainment multiple factor. Therefore to clarify the enhancement of CHF in the case of wire spacer, the parametric study for such kind of parameter is obtained.

5.4. Dryout simulation for three-pin bundle experiment

5.4.1. Three fluid model in three-pin bundle channel

The cross section at the center of three-pin bundle flow channel is shown in Fig.5.3. It can be seen that the system can be simplify as the round tube channel with the helical coil wire inserted

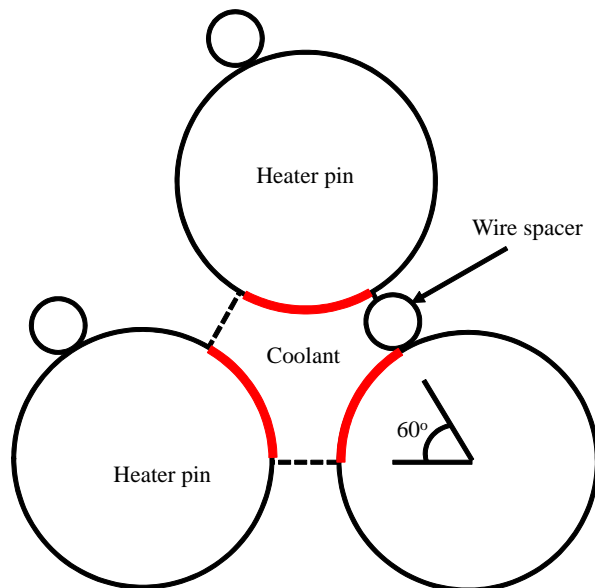


Fig.5.2. Cross section at the center of three-pin rod bundle

The tube diameter equal half of the heater pin diameter and the wire diameter is equal half of the original wire diameter. Therefore, if in the case of annulus channel, the separate liquid films flow were taken into account, in the case of three-pin bundle simulation, only single liquid film was simulated. The three-fluid model method was also used for the case of bundle pin simulation. The constitutive equations for the three-pin bundle simulation are the same with that for single pin simulation. Since the single film flow was taken into account, thus the field equations for the three-pin bundle can be given as follow

Continuity equation

Gas phase

$$\frac{\partial}{\partial z}(\alpha_G \rho_G u_G A) = P_{heat} \frac{q_w}{h_{fg}} \quad (5.31)$$

Liquid phase

$$\frac{\partial}{\partial z}(\alpha_F \rho_F u_F A) = P_{wet} (m_D - m_E) - P_{heat} \frac{q_w}{h_{fg}} \quad (5.32)$$

Droplets phase

$$\frac{\partial}{\partial z}(\alpha_E \rho_E u_E A) = P_{wet} (m_E - m_D) \quad (5.33)$$

where

$$\alpha_F + \alpha_G + \alpha_E = 1 \quad (5.34)$$

Momentum equation

Gas phase

$$\begin{aligned} \frac{\partial}{\partial z} (\alpha_G \rho_G u_G^2) + \alpha_G \frac{\partial P}{\partial z} = & -A_{FG} \tau_{FG} \\ & -A_{EG} \tau_{EG} + \frac{P_{heat}}{A} \frac{q_w}{h_{fg}} u_F - \alpha_G \rho_G g \cos \theta \end{aligned} \quad (5.35)$$

Liquid phase

$$\begin{aligned} \frac{\partial}{\partial z} (\alpha_F \rho_F u_F^2) + \alpha_F \frac{\partial P}{\partial z} = & A_{FG} \tau_{FG} - A_{WF} \tau_{WF} + \frac{P_{wet}}{A} (m_D u_E - m_E u_F) \\ & - \frac{P_{heat}}{A} \frac{q_w}{h_{fg}} u_F - \alpha_F \rho_F g \cos \theta \end{aligned} \quad (5.36)$$

Droplets phase

$$\begin{aligned} \frac{\partial}{\partial z} (\alpha_E \rho_E u_E^2) + \alpha_E \frac{\partial P}{\partial z} = & A_{EG} \tau_{EG} + A_{EF} \tau_{EF} + \frac{P_{wet}}{A} (m_E u_F - m_D u_E) \\ & - \alpha_E \rho_E g \cos \theta \end{aligned} \quad (5.37)$$

5.4.2. Analyzing the enhancement of CHF in three-pin experiment

As presented in chapter 4, the CHF in the case of three-pin bundle experiment was enhanced by the promotion of deposition rate as a result of centrifugal force. Details under the effect of centrifugal force, the droplets tend to move from the gas core to the heated wall which lead to a higher deposition rate and promote the CHF values. According to Eq.5.13, 5.14 and 5.15, the deposition rate can be obtained by multiply the mass transfer coefficient, k_D with the droplet concentration in the gas core, C . Under the effect of centrifugal force, the mass transfer rate was enhanced. Therefore, in order to simulate the enhancement of CHF values in three-pin bundle channel, the parametric study on mass transfer coefficient is needed.

5.5. Results and discussion

5.5.1. Calculation results for single pin channel

The calculation values are the position along the heated surface where CHF occur. The calculation results were obtained by keep the constant values of subcooling enthalpy, mass flux and outlet pressure, then changing the heat flux values. Thus, the CHF position for the difference heat flux values at the same subcooling condition was obtained. Fig.5.3 shows the comparison between the calculation results with the experimental data in the case of without wire spacer. It can be seen that at the same mass flux and pressure condition, the experimental data were close to the calculation results.

The enhancement of CHF values in the case of flow channel with wire spacer was investigated by the parametric study on the hydraulic equivalent wave height. Originally, the hydraulic equivalent wave height is set equal 0.1. In this case, the CHF position in the case flow channel with wire spacer cannot be obtained because of the high heat flux values so that the CHF position is very close to zero. By increasing the hydraulic equivalent wave height values, the CHF in the case of flow channel with wire spacer shifted to the downstream of the flow channel. The calculation was repeated with difference values of hydraulic equivalent wave height values until the calculation results met the experimental data. The results are shown from Fig.5.4 to Fig.5.9 for difference subcooling condition.

It can be seen that, by changing the hydraulic equivalent wave height values, the CHF position was shifted from the upstream to the downstream of the flow channel. It also shows that at the same subcooling, mass flux, pressure and position, the CHF values were higher with the higher hydraulic equivalent wave height values. Moreover, with the hydraulic equivalent wave height lower than 2.0, the CHF slightly shifted from the upstream to the downstream of flow channel. However, with the hydraulic equivalent wave height higher than 2.0, the CHF has a large increase even with the small change in the hydraulic equivalent wave height. Finally, it can be concluded that the CHF was promoted by the rise of hydraulic equivalent

wave height which lead to the higher entrainment rate of the outer liquid film flow and the result is the improvement of deposition rate of inner liquid film flow.

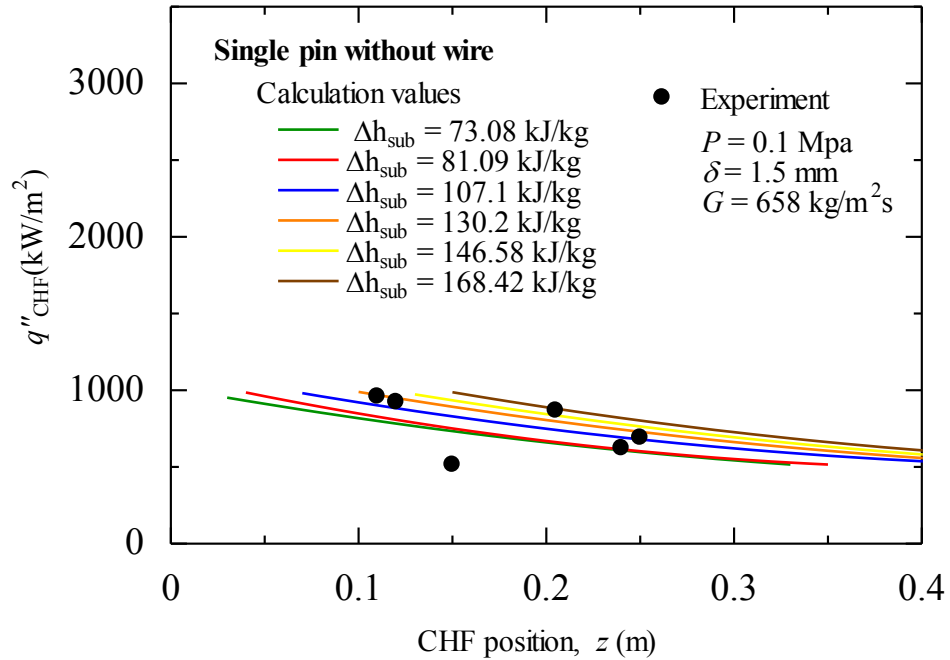


Fig.5.3 Comparison between experimental data and calculation results in case of flow channel without wire spacer

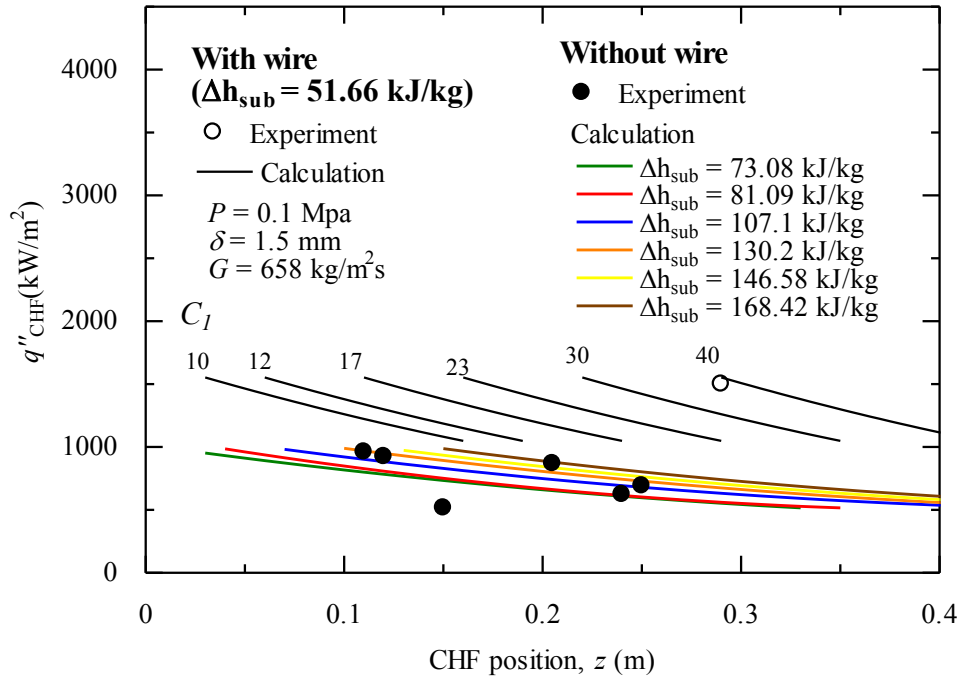


Fig.5.4 CHF position in single pin channel with wire spacer

$(\Delta h_{sub} = 51.66 \text{ kJ/kg})$

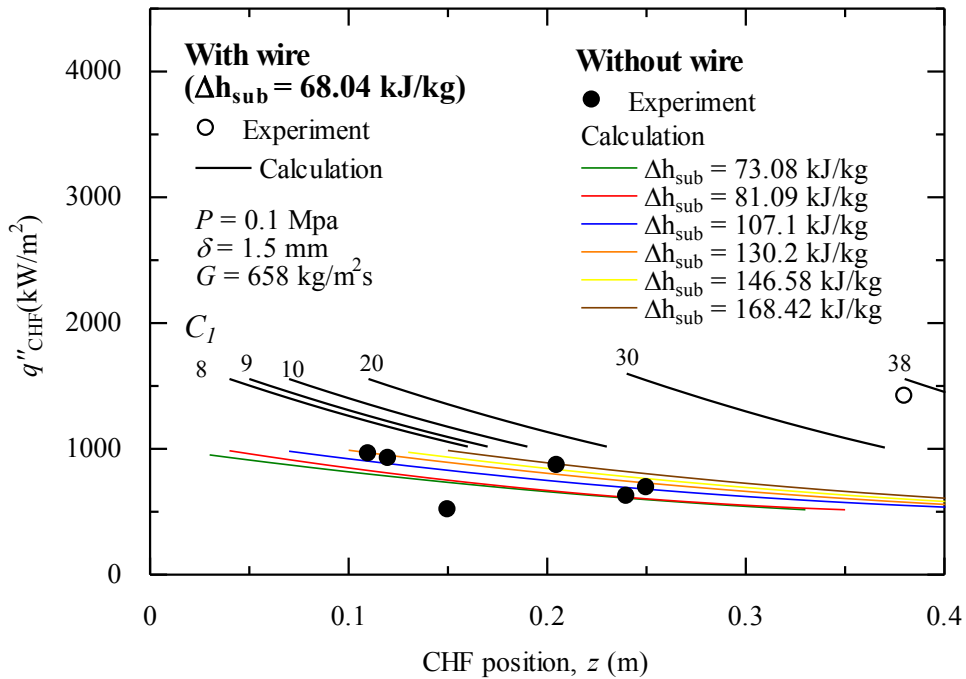


Fig.5.5 CHF position in single pin channel with wire spacer

$(\Delta h_{sub} = 68.04 \text{ kJ/kg})$

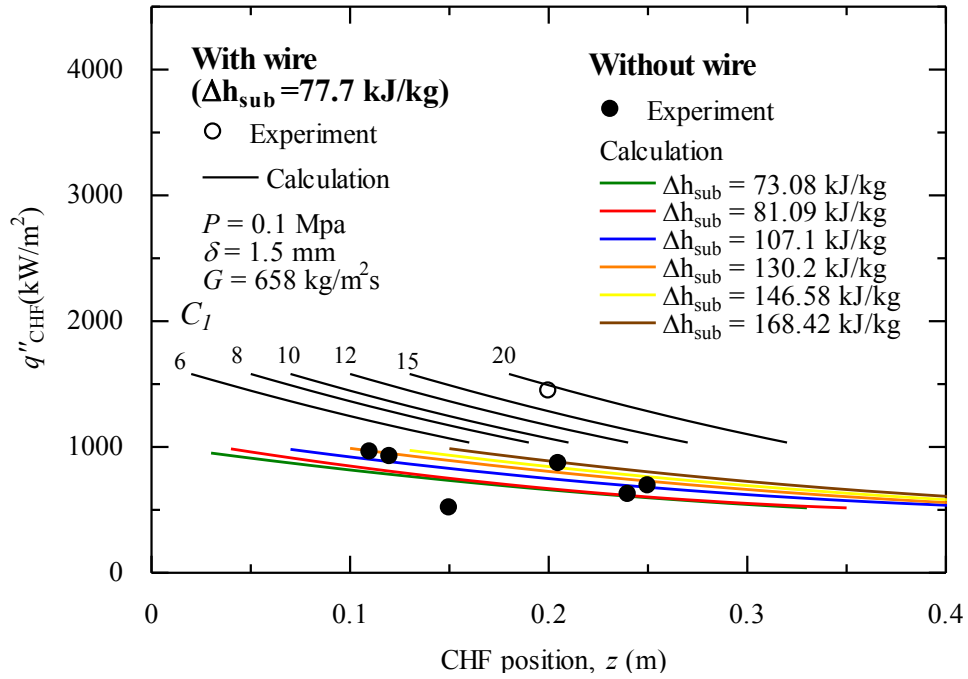


Fig.5.6 CHF position in single pin channel with wire spacer

($\Delta h_{sub} = 77.7$ kJ/kg)

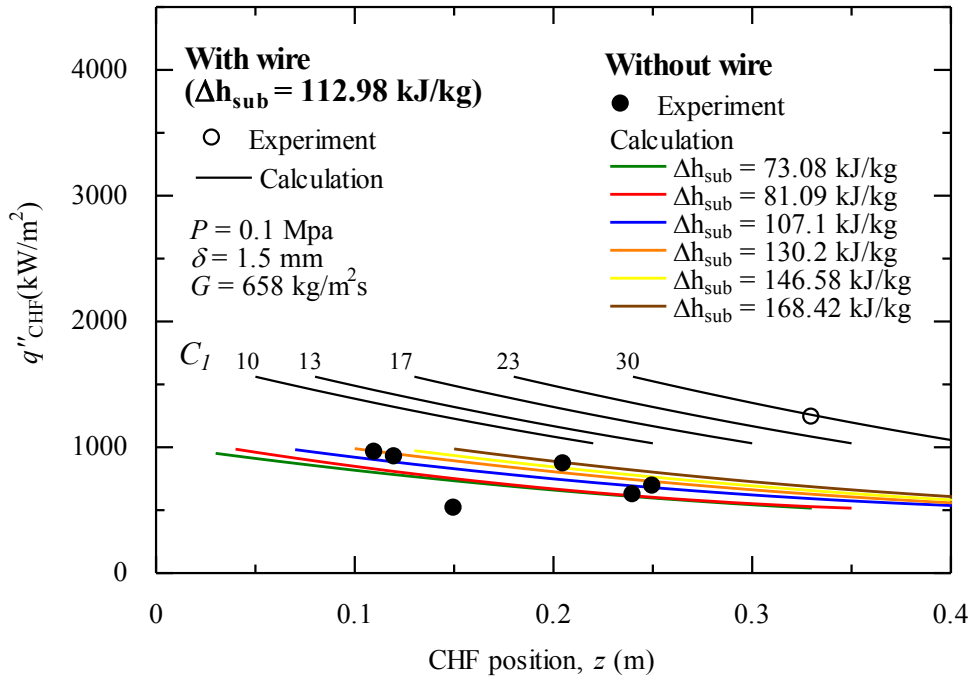


Fig.5.7 CHF position in single pin channel with wire spacer

($\Delta h_{sub} = 112.98$ kJ/kg)

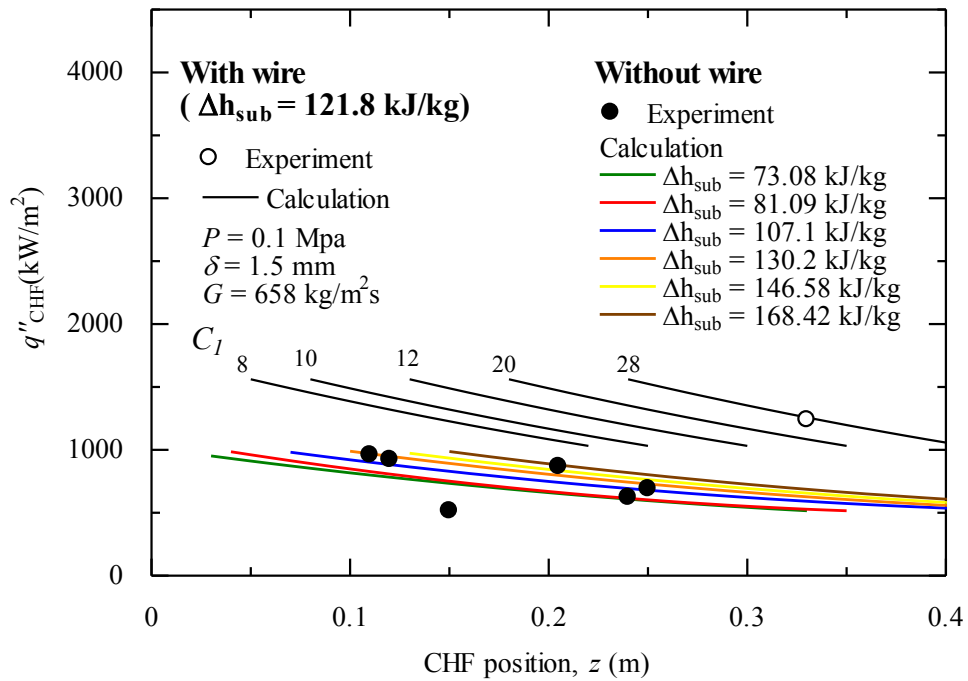


Fig.5.8 CHF position in single pin channel with wire spacer

$(\Delta h_{sub} = 121.8 \text{ kJ/kg})$

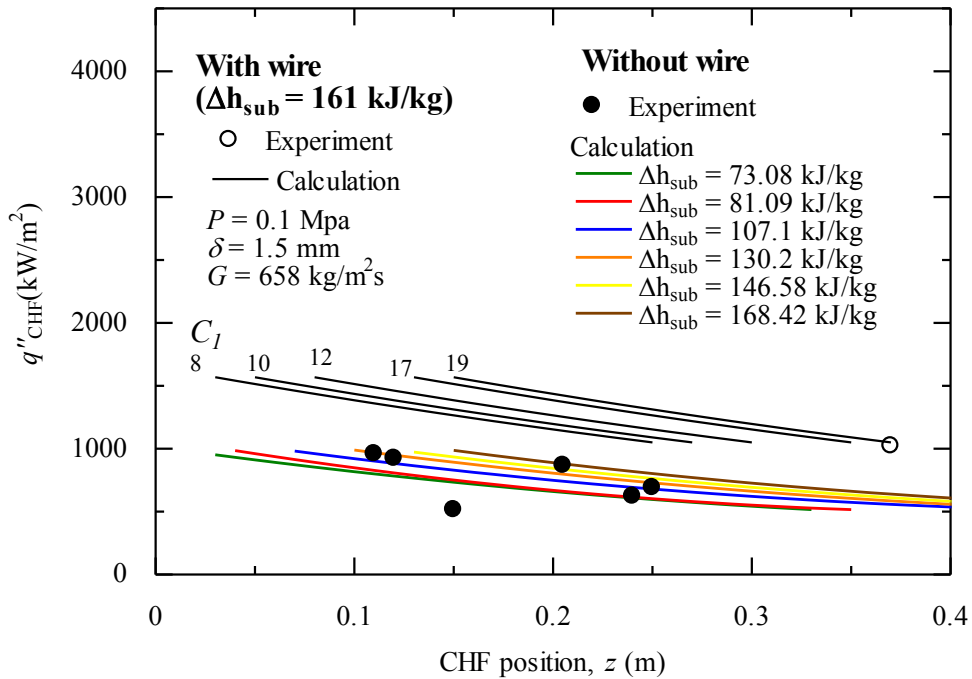


Fig.5.9 CHF position in single pin channel with wire spacer

$$(\Delta h_{\text{sub}} = 161 \text{ kJ/kg})$$

5.5.2. Calculation results for three-pin channel

Fig.5.10 shows the comparison between the calculation results with the experimental data in three-pin bundle without wire spacer. It is clear that the experimental data were close to the calculation results at the same subcooling, mass flux and pressure condition.

As discussed in chapter 4, the enhancement of CHF in case of three-pin bundle with wire spacer base on the improvement of deposition rate under the effect of centrifugal force. In the case of three-pin bundle without wire spacer, the mass transfer coefficient was calculated by Eq.5.14. However, this correlation cannot be applied to calculate for the case of three-pin bundle with wire spacer. Thus the parametric study on mass transfer coefficient is needed to clarify the enhancement of CHF base on the increase of deposition rate. The calculation was repeated with difference values of mass transfer coefficient until the calculation results met the experimental data. The results are shown from Fig.5.11 to Fig.5.16 for difference subcooling condition.

According to the figure from 5.11 to 5.16, at the same subcooling, mass flux, pressure and position, the CHF values became higher by increasing the mass transfer coefficient. Besides, the CHF positions were shifted from the upstream to the

downstream of flow channel by increasing the mass transfer coefficient. Finally, it can be concluded that the mechanism of the enhancement of CHF in three-pin bundle with wire spacer is based on the increase of deposition rate under the effect of centrifugal force.

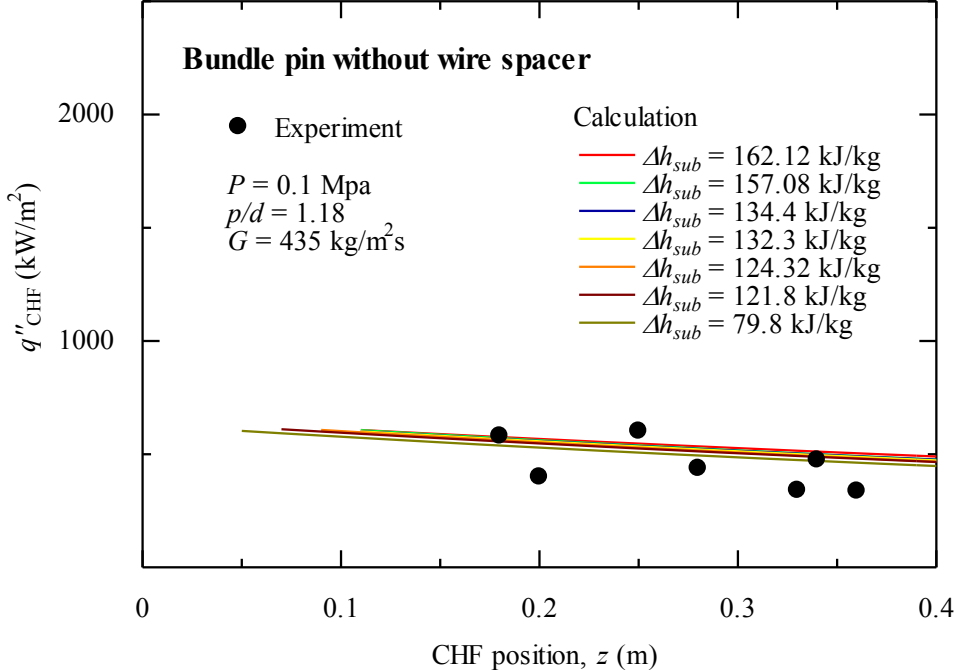


Fig.5.10 Comparison between experimental data and calculation results in case of three-pin bundle without wire spacer

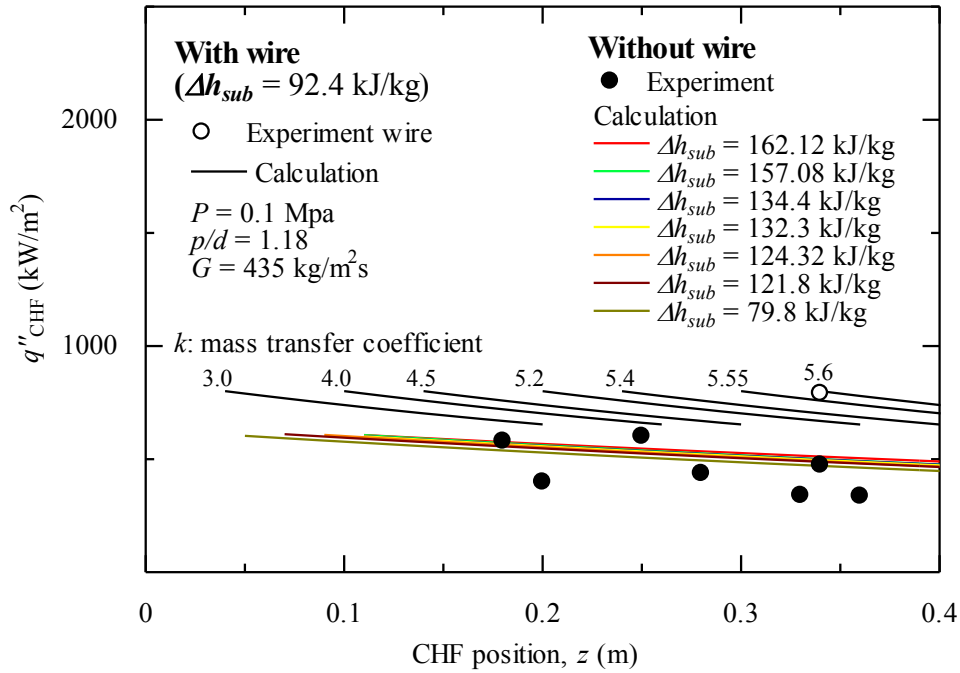


Fig.5.11 CHF position in bundle pin channel with wire spacer

$(\Delta h_{sub} = 92.4 \text{ kJ/kg})$

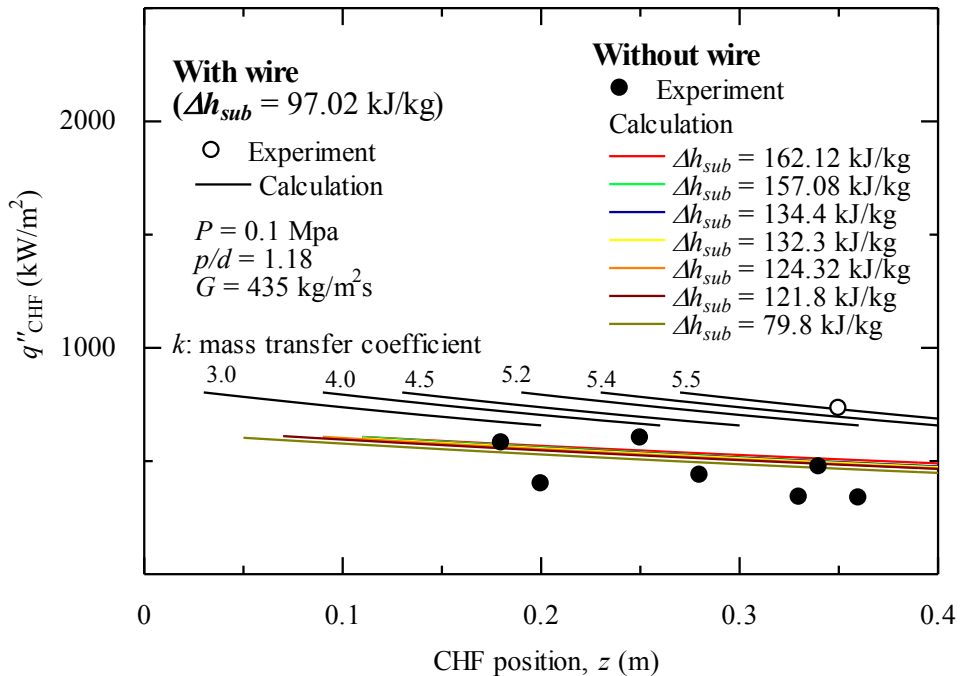


Fig.5.12 CHF position in bundle pin channel with wire spacer

$(\Delta h_{sub} = 97.02 \text{ kJ/kg})$

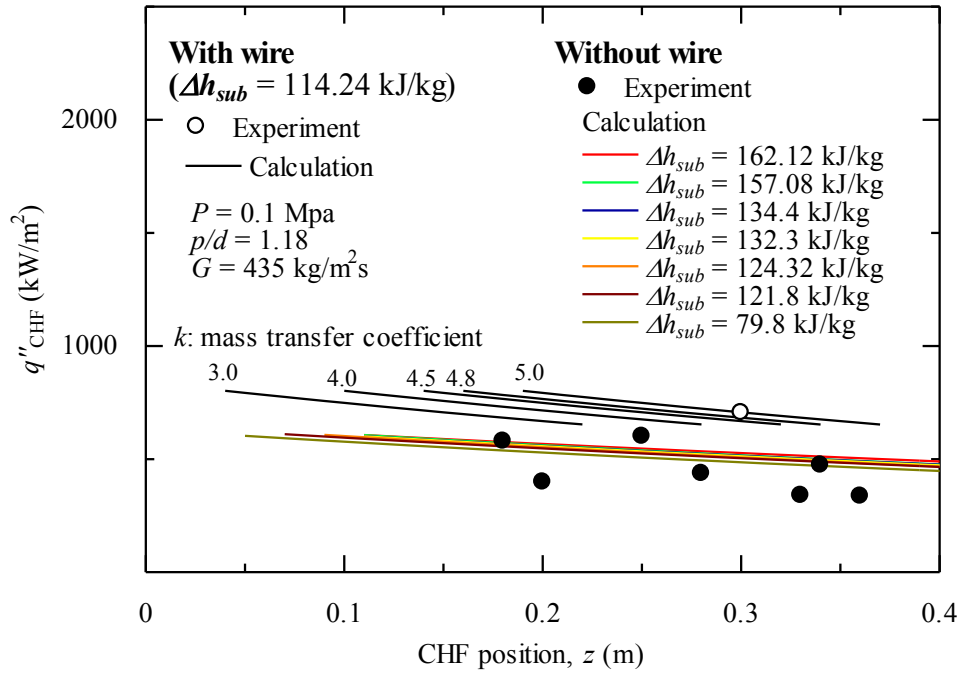


Fig.5.13 CHF position in bundle pin channel with wire spacer
($\Delta h_{sub} = 114.24$ kJ/kg)

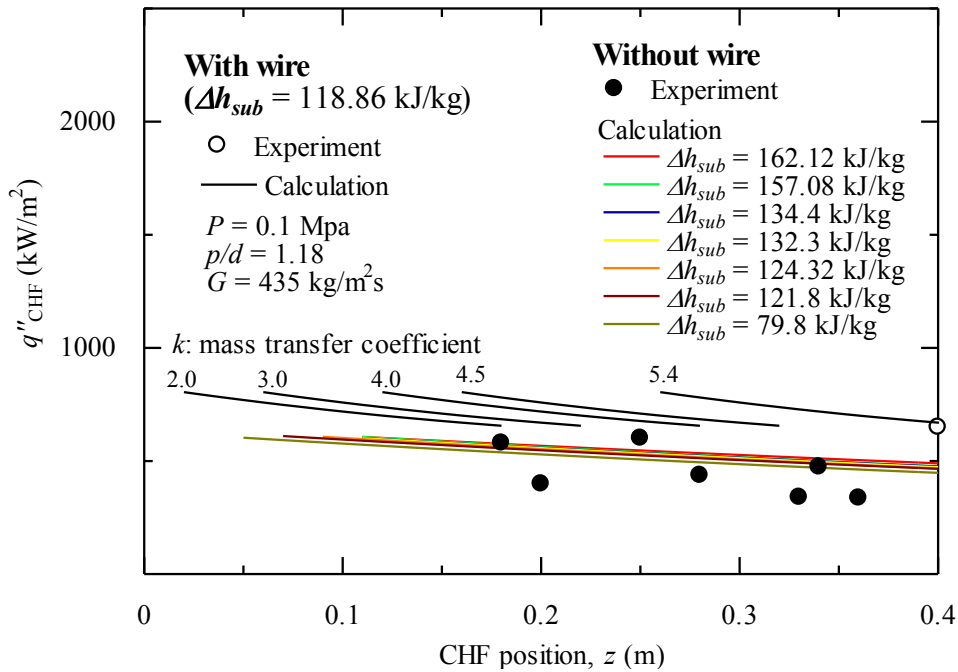


Fig.5.14 CHF position in bundle pin channel with wire spacer
($\Delta h_{sub} = 118.86$ kJ/kg)

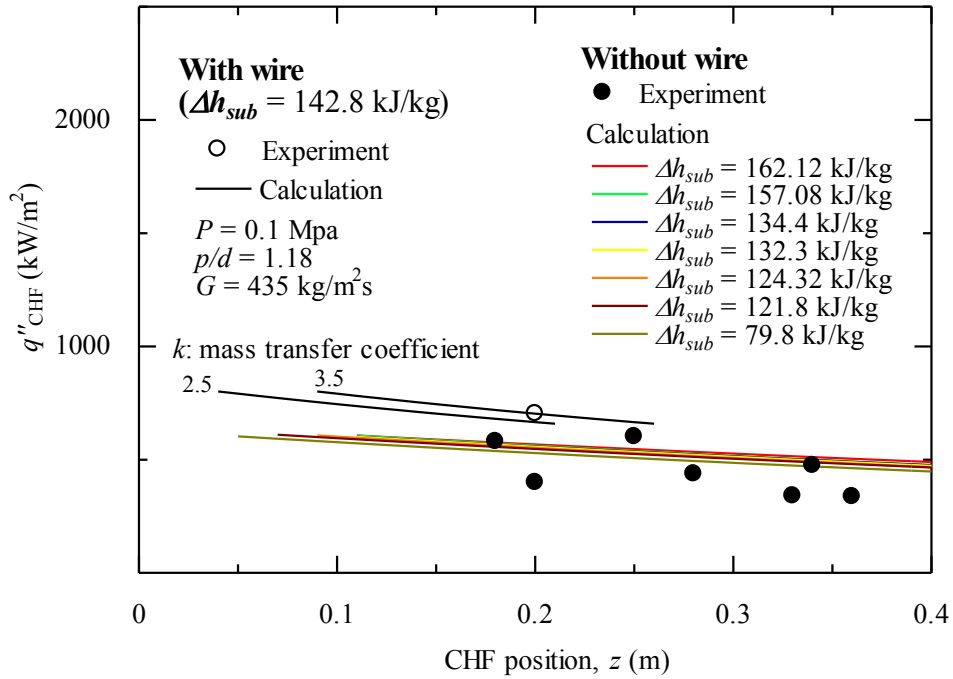


Fig.5.15 CHF position in bundle pin channel with wire spacer
 $(\Delta h_{sub} = 142.8 \text{ kJ/kg})$

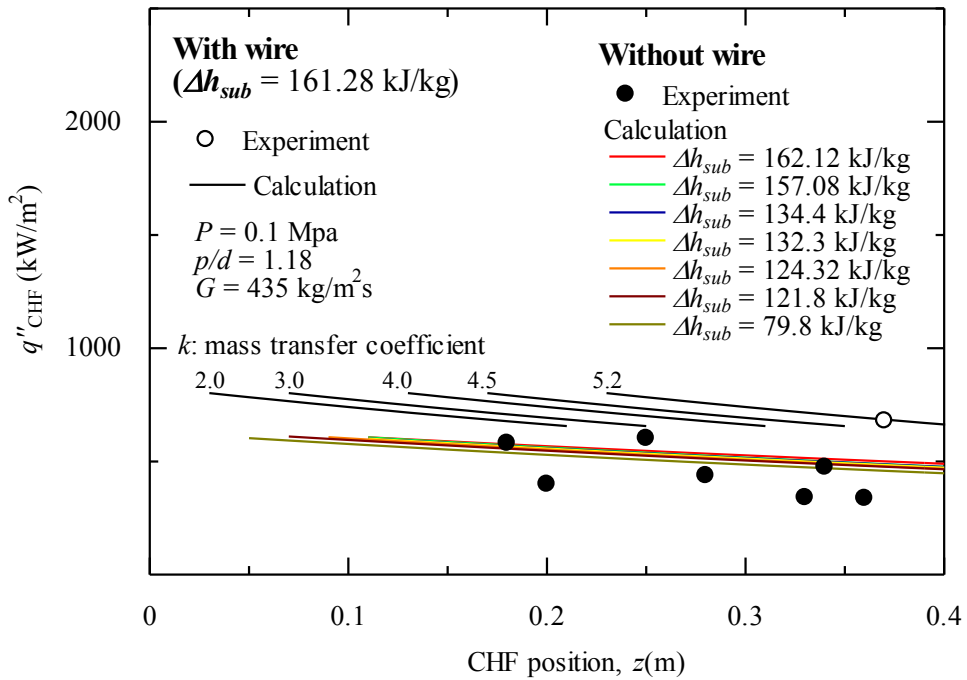


Fig.5.16 CHF position in bundle pin channel with wire spacer

$$(\Delta h_{\text{sub}} = 161.28 \text{ kJ/kg})$$

5.6. Conclusion

The three-fluid model method can be used to simulate the dryout phenomenon in tight lattice core for both of annulus channel and bundle pin channel. In the case of annulus channel, the two separated liquid film flow is simulated. On the other hand, in the case of three-pin bundle, only single liquid film flow is simulated. The parametric studies on hydraulic equivalent wave length and mass transfer coefficient were created to clarify the mechanism of the enhancement of CHF in single pin and three-pin bundle channel. The conclusions are as follow

- (1) The CHF experimental data in single pin channel without wire spacer are agreed well with calculation results under the same mass flux, subcooling and pressure condition.
- (2) The enhancement of CHF in single pin channel with wire spacer is based on the increase of entrainment rate of the outer liquid film which leads to the improvement of deposition rate of the inner liquid film.
- (3) The CHF experimental data in three-pin bundle test section without wire spacer close to the calculation results under the same mass flux, subcooling and pressure condition.
- (4) The enhancement of CHF in three-pin bundle test section with wire spacer is based on the rise of mass transfer coefficient

Chapter 6. Conclusions

The present study can be considered as a fundamental study on CHF behavior in tight lattice core for high conversion boiling water reactor. The conclusions of each chapter in present study can be summarized as follow

Chapter 2

The CHF experimental single pin and bundle pin test section are designed and setup successfully. The new techniques and design have been developed for the single pin and three-pin bundle CHF experiments:

- (1) Teflon tube and Teflon coated wire spacers.
- (2) Tight triangular arrangement of the heater pins.

- (3) Parametric changes of gap size, pitch to diameter ratio and axial pitch of wire spacer.
- (4) Three point junction method for detection of the surface temperature.
- (5) Thin thermocouple for detection of the rapid rise of surface temperature of the heat pins.
- (6) High current electrodes configuration for three-pin bundle.
- (7) Triangular flow channel with small cross section.

Chapter 3

The CHF phenomena for the tight lattice fuel arrangement with the effect of wire spacer were investigated by mean of the experiment for single fuel pin with and without wire spacer and three difference values of gap size of 1.1, 1.5, 2.0 mm. Besides, the effect of wire pitch was made clear by the experiment with two dissimilar wire pitch value of 100 mm and 200 mm. The conclusions are as follows:

- (1) The CHF values increased with the rise of mass flux under the same geometric and quality condition because of the increasing of mass flux lead to the change in heat transfer coefficient of the heater pin.
- (2) The CHF in case of heater pin with circular shape wire was enhanced up to 25% compared with it in case of without wire space under the same flow

condition. Therefore, the coolability or heat removability was enhanced by the existence of the wire spacer and spiral flow.

- (3) With the same flow rate condition, the CHF values can be increased up to 100% with the decrease of gap size. Therefore, the flow channel with smaller gap size a higher coolability compared with the flow channel with larger gap size.
- (4) The change in a pitch of wire, H , with two difference values of 100 mm and 200 mm did not have a large influence on the CHF if the mass flux was kept constant. The experiment data was nearly the same value even with two different cases of wire pitchh.
- (5) The CHF in boiling two-phase flow was mostly caused by liquid film dry-out. Nevertheless, in case of high velocity and high heat flux, the burn-out at high heat flux appeared.
- (6) Directly comparison with the CHF look-up tables of Groveneveld et al. (2007) had a big different with the test results because of the different in geometric condition. In case of the CHF look-up tables Groveneveld et al. (2007) the CHF was performed in a round tube which was different with the CHF in annuli flow as shown in our experiment. The experimental values of single pin without wire spacer agreed well with the predicted method by using the rod-centered approach method of Doerffer et al.(1994). It also

shown the predicted values of CHF in case of channel without wire spacer were lower than the experimental data of channel with wire spacer. That agreed with the experimental results.

Chapter 4

Critical heat flux in boiling water flow in a tight rod bundle was investigated experimentally for a three-pin bundle with and without wire spacers. Two different values of pitch to diameter ratio were chosen: 1.10 and 1.18. The conclusions are as follows:

- (1) The CHF values increased with the increase of the mass flux values under the same quality condition. The effect of mass flux on CHF in tight rod bundle with wire spacer was the same with that in single pin channel.
- (2) The CHF was enhanced by up to 50% with wire spacer compared with it without wire spacer under constant mass flux condition. The enhancement was more significant at the low quality region. Thus, the coolability in tight lattice core could be optimized by using wire spacer.
- (3) Under constant flow rate conditions, the CHF values increased by up to 150% when decrease the pitch to diameter ration from 1.18 to 1.10.

- (4) Under constant mass flux conditions, the tendency of CHF values did not change even with different values of p/d . the CHF decrease around 5% when changing the p/d from 1.18 to 1.10.
- (5) Under the same mass flux condition, the CHF is nearly the same even with difference values of wire pitch.
- (6) The positions of CHF at $p/d = 1.18$ and low mass flux were located in the downstream region of the flow channel. However, when the mass flux was increased, the CHF occurred in the middle of the heater pin. Under constant mass flux condition, CHF occurred at nearly the same position for both of $p/d = 1.10$ and 1.8.
- (7) The CHF experimental data in the case of three-pin bundle without wire spacer were agreed with the prediction method given by Min Lee within $\pm 50\%$ of deviation. On the other hand, the CHF experimental data with wire spacer were higher than the calculated results for bundle without wire spacer at the same quality condition.
- (8) The new correlation of CHF in bundle pin with wire spacer was created by the fitting method. The correlation was shown as a function of mass flux, quality and gap size value. The new correlation can predict the CHF data with the deviation of $\pm 25\%$ which is good enough in the case of boiling two-phase flow phenomena.

Chapter 5

The three-fluid model method can be used to simulate the dryout phenomenon in tight lattice core for both of annulus channel and bundle pin channel. In the case of annulus channel, the two separated liquid film flow is simulated. On the other hand, in the case of three-pin bundle, only single liquid film flow is simulated. The parametric studies on hydraulic equivalent wave length and mass transfer coefficient were created to clarify the mechanism of the enhancement of CHF in single pin and three-pin bundle channel. The conclusions are as follow

- (1) The CHF experimental data in single pin channel without wire spacer are agreed well with calculation results under the same mass flux, subcooling and pressure condition.
- (2) The enhancement of CHF in single pin channel with wire spacer is based on the increase of hydraulic equivalent wave length.
- (3) The CHF experimental data in three-pin bundle test section without wire spacer close to the calculation results under the same mass flux, subcooling and pressure condition.
- (4) The enhancement of CHF in three-pin bundle test section with wire spacer is based on the rise of mass transfer coefficient

Summary

Experiment study

- (1) The CHF of tight lattice core with wire spacer values increases with increasing mass flux in the same geometry and at the same quality condition.
- (2) The CHF values in tight lattice core with wire spacer were higher than that without wire spacer at the same mass flux condition.
- (3) At the same flow rate, the CHF increases with the decreasing gap size or the pitch to diameter ratio.
- (4) The change of wire pitch, H did not have a large influence to the CHF at the same mass flux condition.
- (5) In the tight lattice core, the coolability can be maximized by using the wire spacer.
- (6) The new empirical correlation for CHF in tight lattice core with wire spacer was created and could predict the CHF data within $\pm 25\%$ of deviation.

Analytical study

- (1) The CHF can be estimated by the multi-fluid model.
- (2) The parametric study shows CHF may be enhanced by increase of the droplets entrainment rate in outer liquid film in annuli channel. On the other

hand, by changing the mass transfer coefficient in the three-pin-bundle subchannel, the CHF was increased.

References

1. Ahmad., S.Y. (1973). “Fluid-to-fluid modeling of critical heat flux: a compensated distortion model”. *International Journal Heat and Mass Transfer* 16, 641-662.
2. AP1000 Design Control Document. Chapter 4 Reactor. Revision 14. (n.d.).
3. Bethke., S. (1992). Analysis of critical heat flux in rod bundle (in German). *PhD. Thesis, Technical University Braunschweig*.
4. Bui., T.D., Dhir., V.K. (1985). “Transition boiling heat transfer of a vertical surface”. *Tras. ASME J. Heat Transfer* 107, 756-763.

5. Cheng, X., (2005). "Experimental studies on critical heat flux in vertical tight 37-rod bundles using Freon-12.". *International Journal of Multiphase Flow* 31, 1198-1219.
6. Cheng, X., Erbacher, F.J., and Müller, U. (1997). "Critical heat flux in uniformly heated vertical tubes". *International Journal of Heat Mass Transfer* 40, 2929-2939.
7. Cheng, X., Müller, U. (1998). "Critical Heat Flux and Turbulent Mixing in Hexagonal Tight Rod Bundles". *International Journal of Multiphase Flow* 24 (8), 1245-63.
8. Courtaud, M., Deruaz, R., and D'Aillon, L. G. (1988). "The French Thermal-hydraulic Program Addressing the Requirements of the Future Pressurized Water Reactors". *Nucl. Technol.* 80 (1), 73-82.
9. Dalle., Donne., M. (1991). "CHF-KfK-3 : A critical heat flux correlation for triangular arrays of rod with tight lattices". *Research Karlsruhe, KfK-4826*.
10. Diller, P., Todreas, N., Hejzlar, P. (2009). "Thermal-hydraulic Analysis for Wire-Wrapped PWR Cores". *Nuclear Engineering and Design* 239 (8) , 1461-70.

11. Doerffer, S., Groeneveld, D. C., Cheng, S. C., Rudzinski, K. F. (1994). "A Comparison of Critical Heat Flux in Tubes and Annuli". *Nuclear Engineering and Design* 149 (1-3), 167-75.
12. El-Genk., M. H.-H. (1988). "Experimental studies of critical heat flux for low flow of water in vertical annuli at near atmospheric pressure". *International Journal of Heat and Mass Transfer* 31, 2291-2304.
13. Fighetti., C.F., Reddy., D.G. (1983). "A generalized subchannel CHF correlation for PWR and BWR fuel assemblies. Electric Power Research Institute". *EPRI-NP-2609-Vol.2*.
14. Groeneveld, D. C., Shan, J. Q., Vasić, A. Z., Leung, L. K. H., Durmayaz, A., Yang, J., Cheng, S. C., Tanase, A. (2007). "The 2006 CHF Look-up Table". *Nuclear Engineering and Design* 237 (15-17), 1909-22.
15. Groeneveld., D.C., Cheng, S.C., Doan., T. (1986). "1986 AECL-UO critical heat flux look up table". *Heat Transfer Engng* 7, 46-62.
16. Groeneveld., D.C., Leung., L.K.H., Kirillov., P.L., Bobkov., V.P., Smogalev., I.P., Vinogradov., V.N., Huang., X.C., Royer., E. (1996). "The 1995 look-up table for critical heat flux in tubes". *Nuclear Engineering and Design* 163, 1-23.

17. Guo., Z., El-Genk., M.S. (1992). “An experimental study of saturated pool boiling from downward facing and inclined surfaces”. *International Journal of Heat and Mass Transfer* 35, 2109-2117.
18. Haas., C. e. (2013). “Critical heat flux for flow boiling of water at low pressure in vertical internally heated annuli”. *International Journal of Multiphase Flow* 60, 380-391.
19. Iwamura., T., Okubo., T., Shimada., S., Usui., S., Shirakawa., T., Nakatsuka., T., Kugo., T., Akie., H., Nakano., Y., Wada., S. (1999). “Research on reduced-moderation water reactor (RMWR)”. *JAERI-Research* 99-058.
20. JAEA website. Japan Atomic Energy Agency.
<http://www.jara.go.jp/04/monju/EnglishSite/>. (n.d.).
21. Kamiyama., K., Makoto., S., Konomura., M. (2000). Research on Water-cooled Fast Breeder Reactors. *JNC TN9400* 200-064.
22. Katto., Y. (1983). “Critical heat flux in forced convective flow”. *ASME-JSME Therm. Engng Joint Conf. Proc.* (3), 1-10.
23. Katto., Y. (1990). “A physical approach to critical heat flux of subcooled flow boiling in round tubes”. *International Journal of Heat and Mass Transfer* 33, 611-620.

24. Katto., Y. (1990). "Prediction of critical heat flux of subcooled flow boiling in round tubes". *International Journal of Heat and Mass Transfer* 33, 1921-1928.
25. Katto., Y. (1992). "A prediction model of subcooled water flow boiling CHF for pressure in the range 0.1-20 MPa". *International Journal of Heat and Mass Transfer* 35, 1115-1123.
26. Katto., Y., Ashida., S. (1982). "Critical heat flux in high-pressure regime for forced convection boiling in uniformly heated vertical tube of low length-to-diameter ratio". *Proc. 7th International Heat Transfer Conference* 4, 291-296.
27. Keisuke Okumura et al. (1990). "Conceptual design study of High conversion light water reactor". *JAERI-M 90-096*.
28. Kureta, M., Tamai, H., Ohnuki, A., Sato, T., Liu, W., and Akimoto, H. (2005). "Critical Power Experiment with a Tight-Lattice 37-Rod Bundle". *Journal of Nuclear Science and Technology* 43(2), 198-205.
29. Kureta., M., Akimoto. (2005). "Critical power correlation for axially uniformly heated tight-lattice bundles". *Nuclear Technology* (143), 89-100.

30. Lee., M. (2000). "A critical heat flux approach for square rod bundles using the 1995 Groenveld CHF table and bundle data of heat transfer research facility". *Nuclear Engineering and Design* 197, 357-374.
31. Liu, W., Kureta, M., Ohnuki, A., (2004). "Critical power in 7-rod tight lattice bundle". *JSME Int.J., B* 44 (2), 299-305.
32. Liu., W. K. (2004). "Critical power in 7-rod tight lattice bundle". *JSME International Journal B* 47 (2), 299-305.
33. Liu., W., Kureta., M., Iwamura., T., Akimoto., H. (2003). "Critical power characteristics of tight lattice bundles". *Proc. 11th International Conference on Nuclear Engineering, Tokyo, Japan. ICONE 11- 36099*.
34. Mishima., K., Nishihara., H., Michiyashi., I. (1985). "Boiling burnout and flow instabilities for water flowing in a round tube under atmospheric pressure". *International Journal of Heat and Mass Transfer* 28, 1115-1129.
35. Nakatsuka, T., Tamai, H., Akimoto. (2005). "Subchannel analysis of 37-rod tight-lattice bundle experiments for reduced-moderation water reactor". *Proceedings of International Conference on Nuclear Energy System for Future Generation and Global Sustainability (GLOBAL 2005) , Japan, Paper No. 386*.

36. Nariai., H., Inasaka., F., Shimura., T. (1987). "Critical heat flux of subcooled flow boiling in narrow tube". *ASME-JSME Therm. Engng Joint Conf. Proc.* (5), 455-462.
37. Ninokata, H., Aritomi., T., Anegawa., et al. (1997). "Development of the NASCA code for prediction of transient BT and post BT phenomena in BWR rod bundles". *Proc. 4th Int. Seminar on Subchannel Analysis, Tokyo, Japan,* 231-265.
38. Ohnuki, A., Takase, K., Kureta, M., Yoshida, H., Tamai, H., Liu, W., Nakatsuka, T., Misawa, T., and Akimoto, H. (2005). "Master Plan and Current Status for Feasibility Study on Thermal/Hydraulic Performance of Reduced-Moderation Water Reactor". *Proceedings of International Conference on Nuclear Energy System for Future Generation and Global Sustainability (GLOBAL 2005), Japan.,* Paper No. 091.
39. Okubo., T., Iwamura., T., Takeda., et al. (2003). "Design study on Reduced-Moderation Water Reactor (RMWR) core for plutonium multiple recycling". *Proc. GENES4/ANP2003, Kyoto, Japan,* #1145.
40. Park., K.-A., Bergles., A.E. (1988). "Effects of size of simulated microelectronic chips on boiling and critical heat flux". *Trans.ASME J. Heat Transfer* 110, 728-734.

41. Sidik, P., Takaki, N., and Sekimoto, H. (2006). "Impact of Different Moderator Ratios with Light and Heavy Water Cooled Reactor in Equilibrium States". *Annals of Nuclear Energy* 33 (7), 561.
42. Sidik, P., Takaki, N., and Sekimoto, H. (2008). "Preliminary Study on Feasibility of Large and Small Water Cooled Thorium Breeder Reactor in Equilibrium States". *Progress in Nuclear Energy* 50 (2-6), 320-4.
43. Status report 80 - Reduced-Moderation Water Reactor (RMWR). (n.d.).
44. Sugawara, S. (1990). "Droplet deposition and entrainment modeling based on the three-fluid model". *Nuclear Engineering and Design* 122, 67-84.
45. Sugawara, S., Miyamoto, Y., (1990). "FIDAS: Detailed subchannel analysis code based on the three-fluid and three-field model". *Nuclear Engineering and Design* 120, 147-161.
46. Sugawara, S., Sakai, T., Watanabe, K., Rummens, H.E.C. (1991). "Subchannel analysis by the FIDAS code based on the three-fluid model". *Nuclear Engineering and Design* 132, 253-264.
47. Syeilendra, P. (2013). "Study on Hydrodynamic Model of Fuel Subassembly with Wire-Wrapped Rods for Nuclear Reactors". *Doctoral dissertation, Tokyo Institute of Technology.*

48. Tamai, H., Kureta, M., Liu, W., Sato, T., Ohnuki, A., Akimoto, H. (2007). "Gap Width Effect on Critical Power Based on Tight-Lattice 37-Rod Bundle Experiments". *Journal of Nuclear Science and Technology* 44 (1), 54-63.
49. Tamai., H., Kureta., M., Akimoto., H. (2003). "Pressure drop characteristics in tight-lattice rod bundles for reduced-moderation water reactors". *11th International Conference on Nuclear Engineering, Tokyo, Japan. ICONE11-36098*.
50. Tamai., H., Kureta., M., Ohnuki., A., Sato., T., Akimoto., H. (2006). "Pressure drop Experiments using Tight-Lattice 37-Rod Bundles". *Journal of Nuclear Science and Technology* 43 (6), 699-706.
51. Uchikawa, S., Okubo, T., Kugo, T., Akie, H., Takeda, R., Nakano, Y., Ohnuki, A., and Iwamura, T. (2006). "Conceptual Design of Innovative Water Reactor for Flexible Fuel Cycle (FLWR) and Its Recycle Characteristics". *Journal of Nuclear Science and Technology* 44 (3), 277-84.
52. Wallis., G., B., McGrrraw-Hill. (1969). "One-dimensional two-phase flow".
53. Wasim, R, and Kwang, Y. K. (2008). "Effects of Wire-Spacer Shape in LMR on Thermal-hydraulic Performance". *Nuclear Engineering and Design* 238 (10), 2678-83.

54. Yagov., V.V., Puzin., V.A. (1984). "Critical heat flux in forced-convection boiling of refrigerant-12 under conditions of local heat sources". *Heat Transfer Sov. Res.* 16(4), 47-52.
55. Yamamoto., Y., Hiraiwa., K., Morooka., S., Abe., N. (2003). "Critical power performance of tight lattice bundles". *Proc. 11th International Conference on Nuclear Engineering, Tokyo, Japan. ICONE 11- 36283.*
56. Yoshida., H., Ose., Y., Kureta., M., et al. (2005). "Investigation of water-vapor two-phase flow characteristics in a tight-lattice core by large-scale numerical simulation, (IV) large-scale analysis of water-vapor two-phase flow in rod bundles with TPFIT code using earth simulator". *Nippon Genshiryoku Gakkai-Shi (4)*, 106-114 (in Japanese).

List of Achievements

International Journal

- 1) Tri Dan LE, Minoru Takahashi,” Improvement of Critical Heat Flux Performance by Wire Spacer,” *Journal of Energy and Power Engineering*, Vol. 9, (2015) pp.844-851.
- 2) Tri Dan LE, Minoru TAKAHASHI, “Enhancement of Critical Heat Flux in Tight Rod Bundle With Wire Spacer,” *Journal of Energy and Power Engineering*, Vol. 10, No. 2 (2016) (in print)

International Conferences

- 1) Tri Dan LE, Minoru TAKAHASHI, “Experiment of Heat Transfer Coefficient and Critical Heat Flux in Single Pin and Triangular Pin Array with Wire Wrap Spacer,” *The 4th International Symposium on Innovative Nuclear Energy Systems, November 6-8th, 2013, Tokyo, Japan.*
- 2) Tri Dan LE, Noriaki INABA, Minoru TAKAHASHI, “Investigation of Critical Heat Flux in Single Fuel Pin With and Without Wire Spacer,” *The 22nd International Conference on Nuclear Engineering, July 7th -11th, 2014, Prague, Czech Republic. ICONE22-30892.*

- 3) Tri Dan LE, Noriaki INABA, Minoru TAKAHASHI, “Experiment of Critical Heat Flux for Single Fuel Pin With and Without Wire Spacer,”*The 10th International Topical Meeting on Nuclear Thermal Hydraulic, Operation and Safety, December 14th -18th , 2014, Okinawa, Japan. NUTHOS10-1012.*
- 4) Tri Dan LE, Noriaki INABA, Minoru TAKAHASHI,“Critical Heat Flux Behavior of Heater Pin With and Without Wire spacer in Boiling Two-Phase Flow,”*The 23nd International Conference on Nuclear Engineering, May 17th - 21st , 2015, Chiba, Japan. ICONE23-1728.*
- 5) Tri Dan LE, Noriaki INABA, Minoru TAKAHASHI, “Experimental Study on Critical Heat Flux Behavior in Single Fuel Pin With and Without Wire Spacer,”*The 11st National Conference on Nuclear Science and Technology, August 05th -07th , 2015, Danang, Vietnam.*
- 6) Sho Tanabe, Dan Tri Le, Masatoshi Kondo, Minoru Takahashi, “Experimental Study on Critical Heat Flux In Three Pin Bundle with Wire Spacer for Boiling Water Reactor,” *The 24th International Conference on Nuclear Engineering, July 26th -30th , 2016, Charlotte, North Carolina, USA, ICONE24-60997. (to be presented)*

Domestic conferences

- 1) Tri Dan LE, Noriaki INABA, Minoru TAKAHASHI, “Critical Heat Flux in Single Fuel Pin with and without Wire Spacer,” *2014 Annual Spring Meeting of AESJ, March 24th -16th , 2014, Tokyo, Japan. M22*
- 2) Tri Dan LE, Noriaki INABA., Minoru TAKAHASHI, “Critical Heat Flux in Single Fuel Pin with and without Wire Spacer 2nd Report Effect of Pitch to Diameter Ratio (P/D),” *2014 Annual Fall Meeting of AESJ, September 8th - 10th , 2014, Kyoto, Japan. K36*
- 3) Tri Dan LE, Noriaki INABA, Minoru TAKAHASHI, “Critical Heat Flux in Triangular Pin Bundle with and without Wire Spacer.,”*2015 Annual Spring Meeting of AESJ, March 20th – 22nd , 2015, Ibaraki, Japan. I41.*
- 4) Tri Dan Le, Sho Tanabe, Minoru Takahashi, Masatoshi Kondo “Critical Heat Flux in Tight Lattice Three-Pin Bundle with and without Wire Spacer” *2016 Annual Meeting of AESJ, March 26th – 28th , 2016, Tohoku, Japan, 3C01.* (to be presented)